Durham University

Durham E-Theses

Musculo-Skeletal Stress Markers in Bioarchaeology: Indicators of Activity Levels or Human Variation? A re-analysis and Interpretation.

Henderson, Charlotte

How to cite:

Henderson, Charlotte (2009) *Musculo-Skeletal Stress Markers in Bioarchaeology: Indicators of Activity Levels or Human Variation? A re-analysis and Interpretation.*, Durham theses, Durham University. Available at Durham E-Theses Online: http://etheses.dur.ac.uk/1953/

Use policy

The full-text may be used and/or reproduced, and given to third parties in any format or medium, without prior permission or charge, for personal research or study, educational, or not-for-profit purposes provided that:

- a full bibliographic reference is made to the original source
- a link is made to the metadata record in Durham E-Theses
- the full-text is not changed in any way

The full-text must not be sold in any format or medium without the formal permission of the copyright holders.

Please consult the full Durham E-Theses policy for further details.

Academic Support Office, The Palatine Centre, Durham University, Stockton Road, Durham, DH1 3LE
e-mail: e-theses.admin@durham.ac.uk Tel: +44 0191 334 6107
http://etheses.dur.ac.uk

Chapter 6. Materials and Methods

6.1 Introduction

Current recording methods for MSM do not take into account anatomical characteristics of these sites, they are not quantitative, and they do not mirror clinical descriptions of enthesopathies. These failings have been discussed in the previous chapters. These chapters have also provided groundwork for creating a new recording method that does reflect these factors, stores the data digitally and can be analysed quantitatively. The aim is that it should be objective. The approach used to create this method and a discussion of the method itself will follow. An important factor discussed in Chapter 5, is the relationship between disease processes and enthesopathy formation. For this reason stringent controls will be used to remove cases of disease related-enthesopathy formation (called "bone formers") from the sample. These cases will also be compared with the remaining sample to determine if enthesopathies caused by disease differ from those (more likely to be) caused by musculoskeletal stress.

Trials of various methods were undertaken to determine the best methods to use and these will be discussed in this chapter, prior to a discussion of the final method. It should be remembered that the aim is to develop a recording method based on the discussions in the previous chapters. However, clinical evidence does not provide clear differences between enthesopathy appearance depending on their aetiology: traumatic or caused by disease. This is a major limitation. It was decided upon that bone formers should be recorded in the same manner as the other skeletons to determine if the new recording method found differences in enthesopathy expression. Further hypotheses to be tested using the new methodology were:

1) Enthesopathies form in individuals whose entheses are too small to effectively dissipate forces localised at the enthesis.
2) Individuals with enthesopathies are larger than those without

27 JUL 2009

3) That the size of the enthesis correlates with the size of the bone in the locality of the enthesis, *e.g.* the x and y dimensions of the common extensor origin should correlate with the width of the epicondyle of the humerus

4) Bone formers have more appendicular enthesopathies than non-bone formers

5) Roughness parameters, as used in materials science, can be applied to entheses to record their surface topology quantitatively and to differentiate those with enthesopathies and those without.

a.) If roughness parameters can be applied, then is there a relationship between surface roughness and size of entheses.

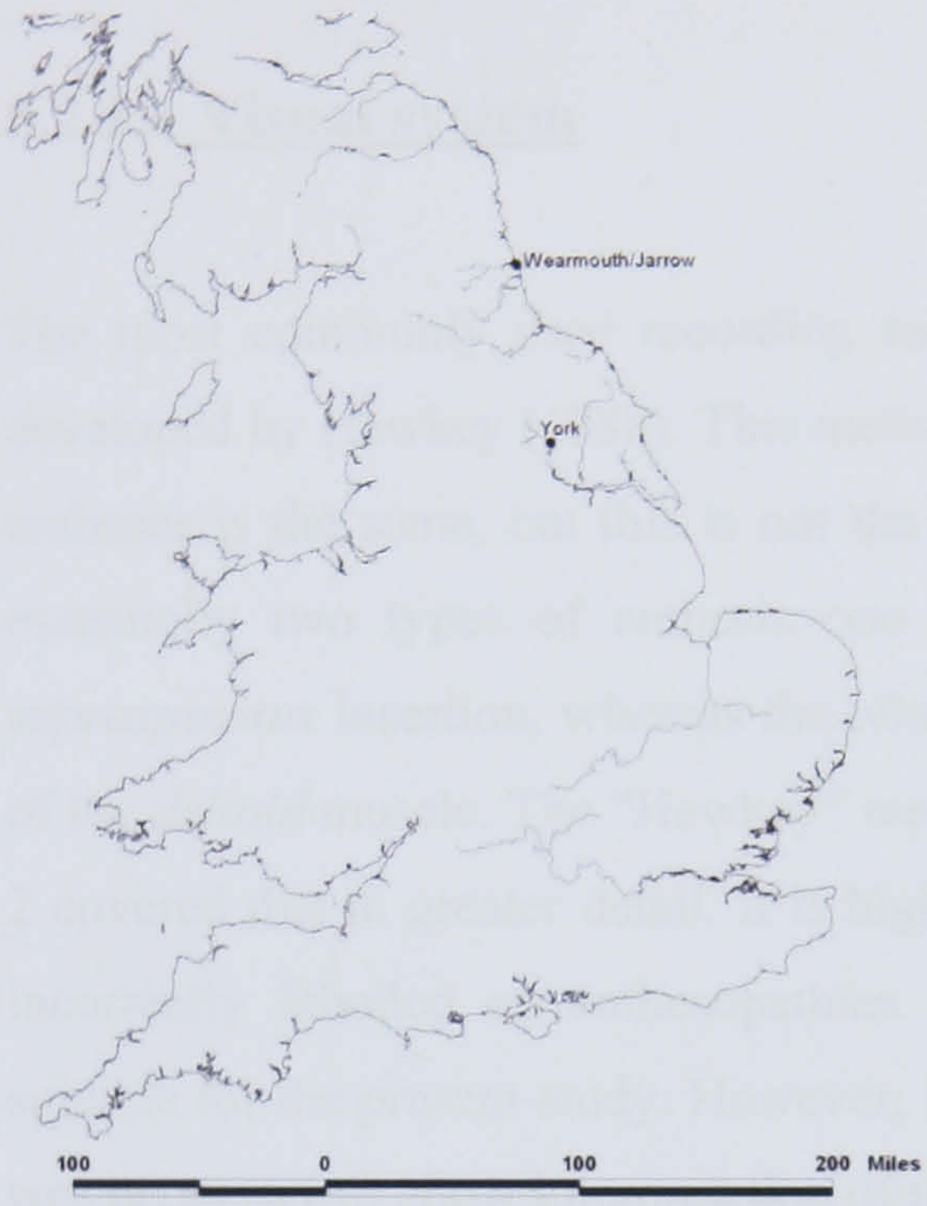
6.2 Pilot Study: Materials and Methods

Numerous pilot studies were set up to determine the best method of digitally recording the surface topology of the enthesis, without creating huge datasets or requiring expensive equipment. This author is of the opinion that the recording of enthesopathies in skeletal assemblages is of equal importance as other anomalies and pathological signs. It was, therefore, thought that any unnecessary cost or time involved in recording entheses would mean that the methodology could never be adopted by the majority of bioarchaeologists. Three-dimensional methods have been used, recently (Zumwalt 2004), but require equipment which is not available to all bioarchaeologists. Furthermore, it is necessary when comparing samples to have comparable data points. In the same way that, when comparing the size of the bone specific landmarks are used to measure each bone, such "landmarks" are required when comparing three-dimensional data (Bookstein 1991; von Cramon-Taubadel, *et al.* 2007). Entheses do not have landmarks and so comparison using three-dimensional methods would rely on controversial techniques (O'Higgens pers. comm.). This was a further reason for using two-dimensional analysis.

6.2.1 Pilot Study: Materials

The pilot studies, including visual inspection and measurement. were undertaken on human skeletal remains from Jarrow and Monkwearmouth. Both sites are from the medieval period (spanning the late 7th century AD to 14th century AD) of Northeast England (Figure 6.0, note also the location of York the provenance of the main study material). Jarrow (founded in c. 681 AD) is located just south of the Tyne and Monkwearmouth (founded c. 673 AD) near modern Sunderland at the mouth of the Wear; both are important early monastic sites (Cramp 2005). Other, unmarked disarticulated bone was also used to increase the sample size. All of this material is curated in the Department of Archaeology, Durham University, England. These skeletal remains were chosen, not because of their archaeological provenance, but purely as testing material to test the different methods and intra- and inter-observer error. This material included both male and female skeletal remains of varying ages, all with fused humeral, radial and ulnar epiphyses, indicating the end of growth of these bones. The age and sex distribution of this material is unimportant for the reasons stated above.

Figure 6.0 Map of the sites used adapted from Dobson (2005)



Only three bones were recorded from each individual; the humerus, radius and ulna. The upper limb was chosen because it is normally more commonly associated with occupation in both clinical (Chapter 4) and bioarchaeological literature (Chapter 3). Three entheses were used for the full recording method; the *supraspinatus,* common extensor origin and the *biceps brachii*. These sites were chosen partly because of the quantity of literature on injuries and enthesopathies at these sites, and because they are all fibrocartilaginous entheses. Fibrocartilaginous entheses were chosen because of their normally smooth imprint, making it easy to determine when the site is abnormal. Fibrocartilaginous entheses are also the best studied and there is considerable literature on the normal appearance, development, histology and biochemistry of these sites (as discussed in Chapter 3).

6.2.2 Pilot Study. Methods: recording of entheses

The aim of the pilot studies were to develop a reproducible visual recording system and quantitative recording system and to determine whether measuring the size of

entheses was worthwhile in the full-scale study. Sample sizes for these pilots were small, but gave a good indication of whether the method was useable.

6.2.2.1 Visual system

The most commonly used recording technique, as discussed in Chapter 2, is that developed by Hawkey (1988). This method assumes that the normal appearance of all entheses is the same, but this is not the case (as discussed in Chapter 3). There are essentially two types of enthesis one with a normally smooth surface, *e.g.* the *supraspinatus* insertion, whereas the other type is normally rugged, *e.g.* the insertion of the *deltoid* muscle. The "Hawkey" method does not take this into account; Chapter 2 covered this in greater detail. It is highly probable that normal entheses have been incorrectly labelled as enthesopathies. Consequently, this method did not seem suitable for the present study. However, it was decided that a visual recording system was necessary to allow interpretation of the quantitative data. Two approaches seemed to be the most useful. One was the complete recording of every detail of the surface and the other was to record only the presence or absence of enthesopathies, without further detail. The latter method is simple and quick, but it was decided that this did not allow for the differentiation between lytic lesions and bone spurs (and other enthesopathies, as described in Chapter 7). Recording such different enthesopathies as one single entity seemed to be removing a vital part of the data because so little is currently known about enthesopathies. For this reason an attempt was made to record as much data as possible.

To do this all the changes found at the three primary entheses (*supraspinatus*, common extensor origin, and *biceps brachii*) were noted down from all the trial bones (an example of the *supraspinatus* is demonstrated in Figure 6.1). This was used to determine the range of abnormalities found. This was then used to create a recording form (Table 6.1). In the final method (Table 6.2) the other entheses were recorded in a similar manner, but with less detail and with no metrical data. Damaged entheses were consigned to the "absent" category if this damage covered a large surface area.

Figure 6.1 Flowchart of method.

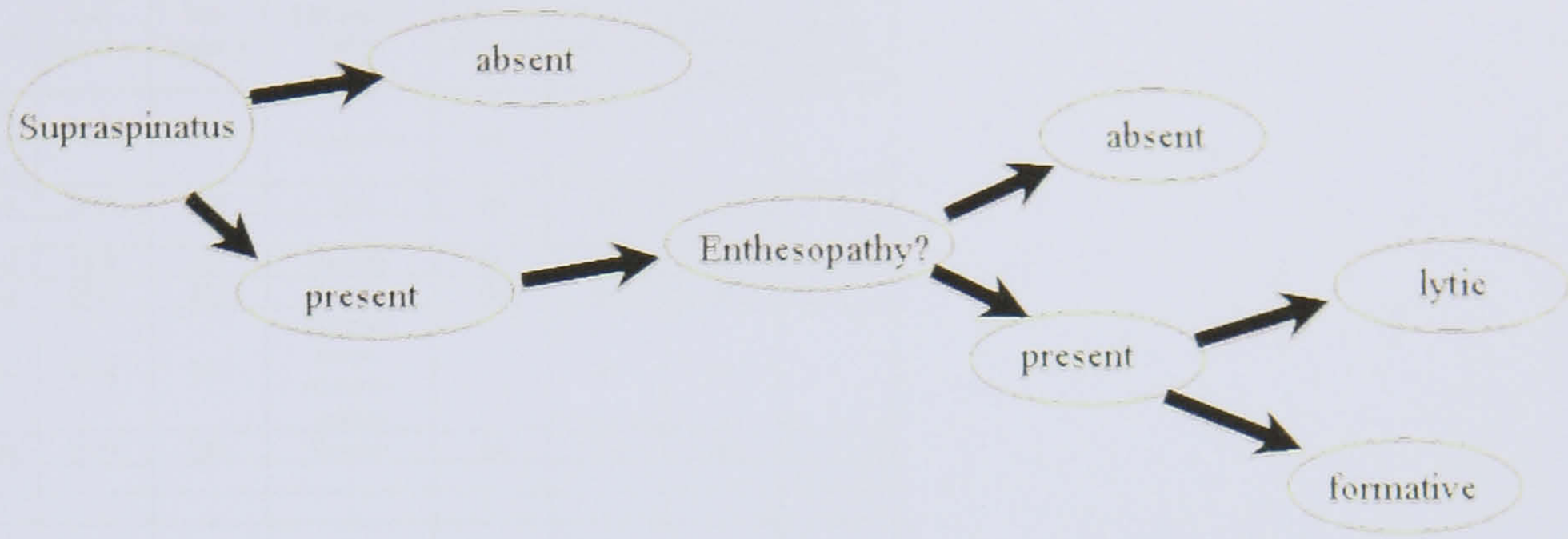


Table 6.1 The visual recording of the right *supraspinatus* insertion demonstrating typical responses (from the Fishergate House recording form, see Appendix IV).

Left Supraspinatus:	Left Supra: x	Left Supra: y	Left Supra: surface	Left Supra normal?	Left Supra: OD	Left Supra: exostosis size	Left Supra: photos
Present, partially damaged	-	-	No smooth	no	no	no	-
Present	14.8	10.19	Yes	no	no	no	-
Present	13.47	6.27	Smooth	Yes	no	no	-
Present	17.83	8.23	Smooth	Yes	no	no	-
Present	22.52	8.25	Marginal lumps, otherwise smooth	?	no	no	-
Present	20.03	9.68	Unevan	no	Yes	no	-
-	-	-	-	-	-	-	-
-	-	-	-	-	-	-	-
-	-	-	-	-	-	-	-
Present	15.58	10.23	Marginal lumps, otherwise smooth	no	Possibly	-	-
Present	16.88	9.98	Smooth	Yes	no	None	-
Present	15.37	17.35	unevan	no	Yes	no	-
Present	14	10.94	Smooth	Yes	no	no	-
Eroded	-	-	-	-	-	-	-
-	-	-	-	-	-	-	-
-	-	-	-	-	-	-	-
-	-	-	-	-	-	-	-
Eroded	-	-	-	-	-	-	-
Present	17.46	7.34	Smooth	Yes	no	Tiny	no
Present	18.2	10.44	Damaged	?	?	no	no
Present	16.01	6.08	unevan	no	no	Multiple tiny lumpy new bone marginally	no
Missing	-	-	-	-	-	-	-
-	-	-	-	-	-	-	-
Present	16.43	10.26	Smooth	Yes	no	no	no
Present	20.08	6.43	Smooth	Yes	no	no	no
-	-	-	-	-	-	-	-
Present	14.87	7.91	Smooth	Yes	no	no	no
-	-	-	-	-	-	-	-
Np	-	-	-	-	-	-	-
-	-	-	-	--	-	-	-
-	-	-	-	-	-	-	-
Partially present	19.42	9.53	-	-	-	-	-
-	-	-	-	-	-	-	-
Present	16.44	6.54	Smooth, but woven bone between humeral head and insertion	?	no	no	no
Present	20.52	7.19	Smooth, but some damage	Yes	?may be pm damage	no	no
Present	15.03	8.54	Smooth, but slight marginal exostoses on anterior	no	no	no	no
-	-	-	-	-	-	-	-
Present	17.29	7.38	Smooth	Yes	no	no	no
Present	16.72	7.32	Smooth	Yes	no	no	no
Present	15.6	10.2	Smooth	no	Yes	no	no

Table 6.2 Other entheses recorded along with recording methodology and example of data (based on the right side, this was also applied to the left side). From Fishergate data, see Appendix IV.

Left Subscapularis	Left Subscapularis normal?
Present	No
Present	No
Present	No
Present	Yes, but marginal erosive lesion on articular side
Present	No
Present	No
-	-
Np	-
-	-
Present	No (OD)
Present	No (rounded exostosis)
Present	N (OD and exostosis)
Present	(nppled, but less so than R)
Present	No (?rupture)
-	-
Np	-
-	-
Present	No, possible OD
Present	No (?rupture)
Present	No (?rupture)
Present	No (?rupture on head side, along with same shape as right side)
Present	No (area of large holes)
-	-
Present	No, no smooth surface
Present	Yes
-	-
Present	No (woven bone
-	-
Present	Unevan, lumps and lytic lesions (OD)
-	-
-	-
Present	Yes
-	-
Present	No, completely mered with humeral head with no smooth surface
Present, but damaged	?
Present	Lumps of woven bone
-	-
Present	Yes
Np	-
Present	No, lots of large holes, with trabecuale visible

To test this recording method for intra-observer error. the same bones were recorded twice by this author using the same method. It was found that in 94 percent of cases the responses were identical. This method was also tested for inter-observer error which was not statistically significant.

6.2.2.2. Measurement

Measurement of bones is widely employed to provide quantitative data used when describing individuals in the past (Brickley and McKinley 2004; Buikstra and Ubelaker 1994). Such descriptions are used to calculate stature and the biomechanics, *e.g.* the bending moment of the lower limb (platycnemia and platymeria). It is not currently known whether there is a relationship between bone size and enthesis size or between either of these and enthesopathy formation. One hypothesis is that enthesopathies form in individuals whose entheses are too small to dissipate the forces effectively. Therefore the aim of taking measurements was two-fold. Firstly, the hypothesis that enthesopathies would be more common in small entheses because of the lack of surface area for the distribution of load. The second aim was to test the hypothesis that the size of the enthesis correlates with the size of the bone in the locality of the enthesis.

Bones were measured following Bass (1995) and Buikstra and Ubelaker (1994) (Table 6.3. Measurements made and indices calculated). Indices used to gauge the "robusticity" of the bones were calculated from some of these measurements. The indices used were:

- Robusticity index of the humerus - (humerus minimum circumference x 100)/Humerus maximum length (Bass 1995);
- Humerus head index - vertical head height/transverse head height
- Radiohumeral index – (radius maximum length x 100)/humerus maximum length (Bass 1995);
- Radius diameter index - (A-P diameter x 100)/M-L diameter

- Modified calliper index – (ulna least circumference x 100)/ulna maximum length

Table 6.3 Measurements made and indices calculated, with definitions and equipment used.

Measurement		
Humerus: maximum length	Maxumum length of a humerus Bass (1995) p. 152	Osteometric board
Humerus: minimum circumference	Circumference of the humerus at the level of the nutrient foramen, or just below the deltoid tuberosity if the nutrient foramen is located elsewhere (*ibid*.)	Tape measure
Humerus: vertical head diameter	Diameter of the humeral head taken proximo-distally at the midpoint (Buikstra and Ubelaker (1994) p. 80)	Sliding caliper
humerus: transverse head diameter	Diameter of the humeral head taken perpendicular to the vertical head diameter	Sliding caliper
humerus: condylar width	distance between the most medially and most laterally points of the distal condyle of the humerus	Sliding caliper
humerus: epicondylar width	distance between the most medially and most laterally points of the distal humerus (Buikstra and Ubelaker 1994 p. 80)	Osteometric board
Common extensor origin (CEO): x	Length of the common extensor origin measured from the posterior side to the edge of the lateral condyle	Sliding caliper
CEO: y	Length of the common extensor origin measured from the anconeus origin to the shaft proximally to the common extensor origin.	Sliding caliper
Supraspinatus (Supra): x	Length of the supraspinatus insertion measured from the bicipital groove to the infraspinatus insertion	Sliding caliper
Supra: y	Length of the supraspinatus insertion measured from the humeral head to the shaft	Sliding caliper
Radius maximum length	greatest length from proximal head to distal styloid process of radius (Buikstra and Ubelaker 1994 p. 80)	Osteometric board
Radius antero-posterior (A-P) diameter	distance between antero-posterior aspect of the radius at the pronator teres insertion	Sliding caliper
Radius medio-lateral (M-L) diameter	distance between medio-lateral aspect of the radius at the pronator teres insertion	Sliding caliper
Ulna maximum length	Distance between from proximal end of olecranon process to distal most point of the styloid process	Osteometric board
Ulna circumference	Minimum circumference near the distal end of the ulna	Tape measure
Biceps brachii x	90 degrees to y at midpoint	Sliding caliper
Biceps brachii y	Proximal-distal ends of enthesis (smooth parts only) measured at the midpoint of x	Sliding caliper
Indices		
Humerus: Robusticity	Minimum circumference x 100 divided by the maximum length, as defined by Bass 1995, p.152	
Humeral head index	Vertical head diameter/transverse head diameter	
Radial shaft index	(A-P diameter x 100)/M-L diameter	
Radio-humeral index	(radius max length x100)/humerus max length	
Modified calliper index	(Ulna least circumference x 100)/Ulna max leangth	

These measurements were made on the trial bones. Intra- and inter-observer error was calculated for the measurements of the entheses. Intra-observer error was assessed by two-sample t-tests of length and breadth of the *supraspinatus* and common extensor entheses on two separate days using the same measuring equipment. At a 95 percent confidence interval these t-tests indicated that there was no significant difference between the sample means, indicating that the measurements were repeatable. Because the majority of these measurements are in common usage it was decided to apply them to the final data set. The results of intra- and inter-observer error analysis on the final data set are presented below.

6.3 Intra-observer error

6.3.1 Intra-observer error: Measurement data

Intra-observer error tests were performed using the non-parametric Mann-Whitney U test. This was used in preference to the Student's t-test because of the small sample size. Table 6.4 demonstrates that there were no statistically significant differences in measurements of the humerus.

Table 6.4. Measurements of the humerus: intraobserver error. N=8

	Maximum Length	Minimum Circumference	Vertical head	Supraspinatus x	Supraspinatus y
Mann-Whitney U	8.000	15.500	22.000	14.000	16.000
Z	-1.559	-.330	-.320	-.641	-.320
Exact Sig. [2*(1-tailed Sig.)]	.149(a)	.755(a)	.805(a)	.589(a)	.818(a)

a Not corrected for ties.

b Grouping Variable: Observation

6.3.2 Inter-observer error: Measurement data

Two observers who had never used the recording methodology described in Chapter 6 recorded the dimensions of ten humeri and also the curvature of the entheses of the y-axis of the common extensor origin. Time constraints only allowed the following measurements to be recorded fully by one observer:

Humerus: vertical head diameter

Humerus: transverse head diameter

Humerus: condylar width

Supraspinatus: x

Supraspinatus: y

Non-parametric tests presented inTable 6.5 were used to determine whether there were any statistically significant differences between the observers at $\alpha = 0.05$. No statistically significant differences were found between the observers.

Table 6.5 Measurements of the humerus: interobserver error. N = 10.

	Vertical head	Transverse Head	Condylar width	Supraspinatus x	Supraspinatus y
Mann-Whitney U	30.000	18.000	38.000	16.000	27.000
Z	-.889	-1.302	-.178	-1.389	-.116
Exact Sig. [2*(1-tailed Sig.)]	.408(a)	.220(a)	.897(a)	.189(a)	.955(a)

a Not corrected for ties.

b Grouping Variable: Observer

6.4 Methods to Record Enthesis Shape

6.4.1 Assessment of curvature

The shape of the enthesis determines the surface area of the attachment site. This cannot be measured using sliding callipers because they cannot compensate for buckling of the surface. Ideally, as discussed above, three-dimensional analyses of the

surfaces, as undertaken on sheep entheses (Zumwalt 2004), provide the greatest information. However, there are problems with this approach: it can be prohibitively expensive making it difficult for all research groups to afford. It also requires the data points to correspond from individual to individual, which can require complex mathematical procedures to correct (Bookstein 1996/1997). Consequently, a two dimensional approach was chosen and only two regions of the enthesis analysed – the x and y axes (which are the same as those used for measuring). This method has the advantage that the intersection of the x- and y-axes occurs at the midpoint, by definition this should make this point identical on all individuals. The end point of these lines is also determined by this midpoint, and it should be comparable from individual to individual. This simple method should, therefore, mean that many of the problems encountered in geometric morphometry which require size and shape scaling can be avoided.

The aim, therefore, was to digitise a line representing, in two-dimensions, the curvature of the surface (Figure 6.2). Detail is lost, but if the x- or y-axis does intersect an anomaly, then the anomaly is recorded. If the anomaly is not intersected, then it is still recorded visually. Once a digital representation is created, quantitative analysis can be applied (see below).

Figure 6.2 Two-dimensional representation of three-dimensional surface (F13 common extensor origin axis x).

6.4.2 Laser line

The initial technique attempted to draw a line across the enthesis surface using a laser beam. The laser beam was slowly moved across the surface along a stable axis, whilst a camera on a long exposure setting (*circa* 2 minutes) was used to capture the image of the line (Figure 6.3). However, the light levels had to be kept low to balance the exposure of the bone (*i.e.* to avoid over-exposure) and for the red laser light to be visible. This made it difficult to line-up the x- and y-axes. It was also difficult to determine the delimitations of the enthesis on the final photograph. Most importantly, the closeness of the bone to the camera varied depending on the size of the bone, thus making the resolution of the profile variable. Attempts were made to correct for this, but the darkness of the images meant that the method proved not to be reproducible.

Figure 6.3 Laser beam method.



6.4.3 Casting

Casts using FIMO, a polymer clay, were taken of the surfaces, with the aim of being able to draw lines across the surfaces in the x- and y-axes to be photographed and thereby digitised (Figure 6.4). However, it proved impossible to determine where the surface began and ended on the fired casts (as with the laser line) and was therefore non-reproducible. In less well preserved bones, parts of the enthesis were found to attach themselves to the FIMO and vice versa, so conservation issues also ruled out this approach.

Figure 6.4 Cast of enthesis. JA67LW with arrows indicating ends of enthesis.



6.4.4 Profile Gauge

The final method attempted was to use a profile gauge. This is a metal device often used to shape tiles to fit in awkward spaces. It has movable prongs of 0.8 mm in width. This device placed on the surface of the enthesis in the x and then the y dimensions was used to draw the shape of the enthesis onto paper. It was found that a propelling pencil (0.5 mm lead) was the best method of transferring the curves from the profile gauge to the paper. The *supraspinatus* enthesis was tested for intra-observer error (tested for differences in roughness parameters, discussed below), which was found to be minimal. This method was repeated to test for inter-observer error, but only on the *supraspinatus* y-axis (which was perceived by the author as the hardest to line up). This data demonstrated that, at 95 percent confidence interval there was no statistically significant difference between the two samples (Section 6.7).

The repeatability, simplicity and low cost of this technique make it ideal for the shape analysis of entheses. However, digitising the data is time-consuming. Ideally the data would be digitised as it is collected, which would make this technique quick and

simple to use, thereby making it of use to anybody wishing to digitally record these entheses.

6.5 Surface Roughness: Quantitative Analysis

The pages of curves were scanned in and each curve cut to the ends of each line using Corel Photo-Paint11. The "Auto Equalize" function was then used to make the line stand out more clearly against the background. Then the colour mode was changed to black and white. This was performed as follows: "Black and White" was selected from "Color mode", conversion was set to "Line Art" and the "Threshold" set to "128" (where different threshold settings were necessary, the file name was changed to "..bw[threshold number].bmp". The image was then scrutinised for extraneous marks, which were removed where appropriate. The image was then converted to "Grayscale (8-bit)" and saved as a ".bmp" file to allow analysis in the Matlab routine (Appendix II). Prior to this analysis the curves were flipped and rotated so that the left and right sides could be pooled (See Figures 6.5 and 6.6; Table 6.6).

Figure 6.5 Page prior to curve digitisation.

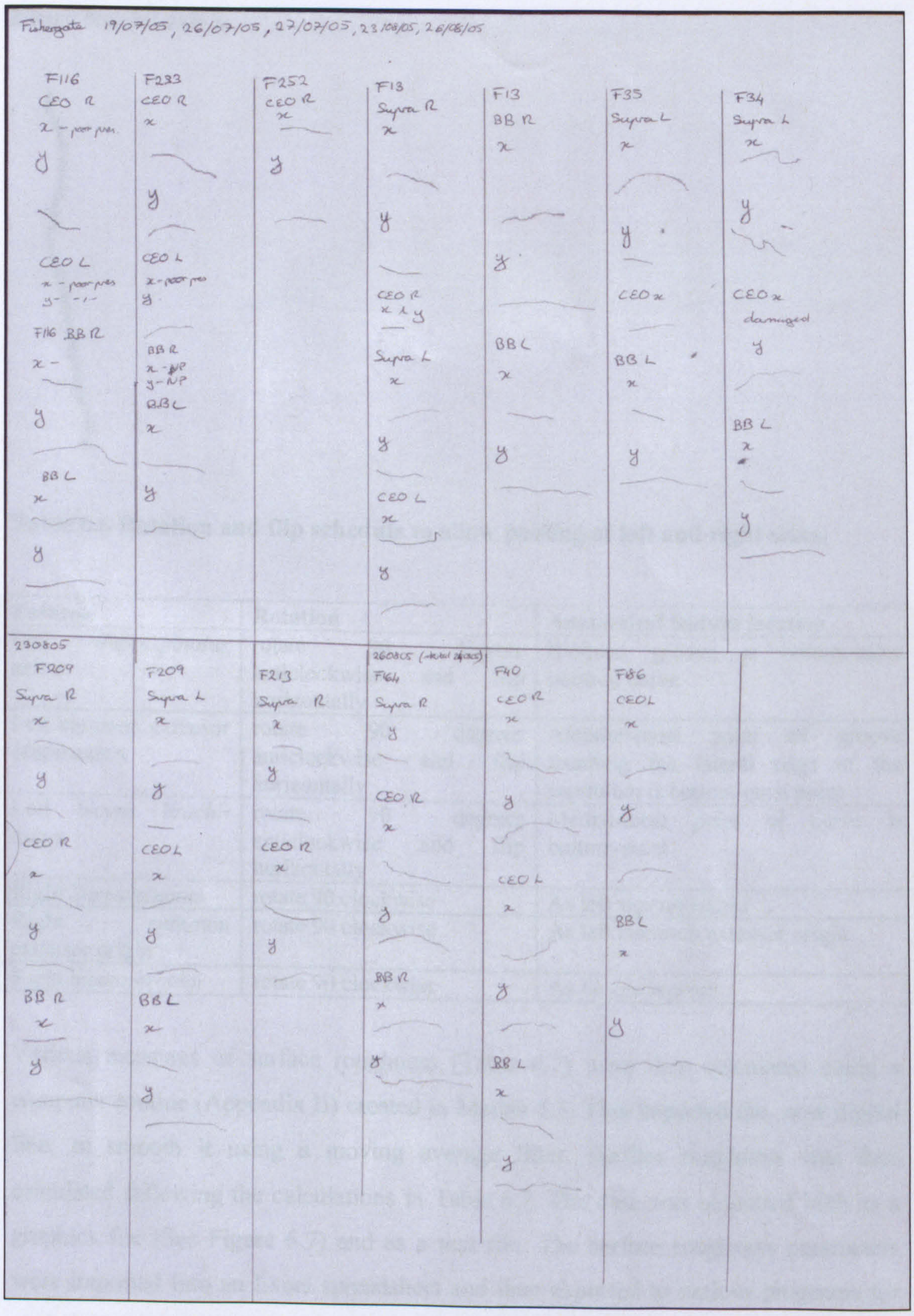


Figure 6.6 End result of edits to graphical data prior to analysis for F13 left *biceps brachii* axis x.



Table 6.6 Rotation and flip schedule to allow pooling of left and right sides.

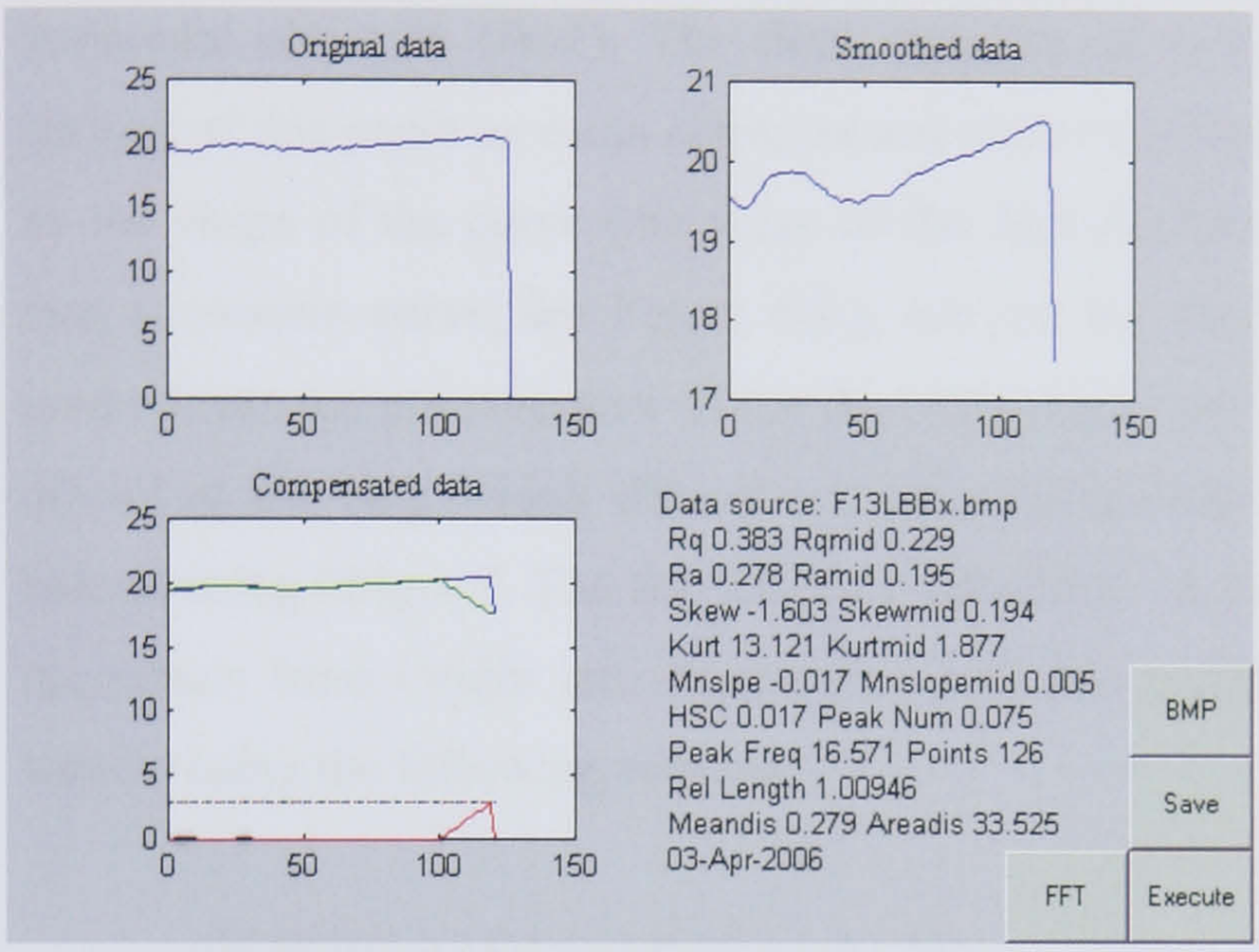
Enthesis	Rotation	Anatomical feature location
Left *Supraspinatus* axis x	rotate 90 degrees anticlockwise and flip horizontally	Bicipital groove at bottom-most point of curve
Left common extensor origin axis x	rotate 90 degrees anticlockwise and flip horizontally	Anterior-most point of groove touching the lateral edge of the capitulum is bottom-most point
Left *biceps brachii* axis x	rotate 90 degrees anticlockwise and flip horizontally	Medial-most point of curve is bottom-most
Right *Supraspinatus*	rotate 90 clockwise	As left *supraspinatus*
Right common extensor origin	rotate 90 clockwise	As left common extensor origin
Right *biceps brachii*	rotate 90 clockwise	As *biceps brachii*

Various measures of surface roughness (Table 6.7) were then calculated using a computer routine (Appendix II) created in Matlab 5.3. This imported the, now digital line, to smooth it using a moving average filter. Surface roughness was then calculated following the calculations in Table 6.7. The data was outputted both as a graphics file (See Figure 6.7) and as a text file. The surface roughness parameters were imported into an Excel spreadsheet and then exported to various programs for statistical analysis. If this study were to include a larger sample size or more entheses, then a database would be required for data management and analysis.

Table 6.7 Summary of roughness parameters used, based on (Gadelmawla, *et al.* 2002) The Matlab routine used to calculate these are in Appendix II.

Parameter	Calculation
Root mean square roughness (**Rq**)	Standard deviation of the distribution of surface heights. $Rq = \sqrt{\frac{1}{n}\sum_{i=1}^{n} y_i^{\,2}}$
Arithmetic average height (**Ra**)	The average absolute deviation of the roughness irregularities from the mean line over a sampling length. It provides no information about the wavelength and is not sensitive to small changes in profile. $Ra = \frac{1}{n}\sum_{i=1}^{n} \lvert y_i \rvert$
Mean slope (**Mnslope**)	Mean absolute profile slope over the assessment length (in this case pixels). $\Delta_a = \frac{1}{n-1}\sum_{i=1}^{n-1} \frac{\delta_{yi}}{\delta_{xi}}$
High spot count (**HSC**)	Number of high regions of the profile above the mean line (or a parallel line to it) per unit length (in this case measured in points, representing pixels) along the assessment length.
Peak number (**Peaknum**)	number of peak turning points per unit length (pixels)
Peak frequency (**Peakfreq**)	mean peak to peak distance (based on the peak number)
Relative length (**Rellength**)	Calculated by a summation of the lengths of the individual parts of the profile divided by the assessment length (pixels). $l_o = \frac{1}{L}\sum_{i=1}^{n} l_i$
Mean displacement (**Meandis**)	Mean of the displacement (the displacement is represented by the red line in the output file) it is represented by the black line in the output file (see Figure 6.7).
Area displacement (**Areadis**)	Area under the red line, *i.e.* the sum of each point along the red line (see Figure 6.7).
Rq of Fast Fourier Transform of curve (**FFTRq**)	The curve, smoothed with a high pass filter at 0.1Hz (in Origin 7), creating a curve to which the Rq roughness parameter is applied (in Excel).

Figure 6.7 Graphics output of Matlab routine for F13 left *biceps brachii* axis x (roughness parameter name followed by "mid" indicates the roughness parameter for the middle two-thirds of the surface)



6.6 Strengths and Limitations of Roughness Parameters

Roughness parameters, *i.e.* measures of the variation in surface smoothness, are widely used in materials science to categorise surfaces and in manufacturing to determine whether materials or products are suitable for their proposed application (Scarr 1967). Scaling up from this, some of these same mathematical principles can be used in wear analysis of dentition and, moving away from bioarchaeology, flint tools (Astruc, *et al.* 2003) and geological applications. Such parameters can be applied in two- or three-dimensions. The surfaces of the entheses were all three-dimensional, but for this project, as discussed elsewhere, a two-dimensional approach was taken.

The parameters used in this study fall into four main categories: measures of amplitude, measures of spacing, measures combining both amplitude and measures of space, and measures of the deviation of the curve from a fitted line ($y = mx+c$). These are all defined in Table 6.10. Descriptors of amplitude (Rq and Ra) measure the vertical variations in surface roughness in relation to a mean line, *i.e.* the height variation in relation to the mean line (Gadelmawla, *et al.* 2002). These are the most

commonly used measures of surface topography, but they are affected by the slope of the curve (see Figure 6.8). Spacing parameters (HSC, Peak number, Peak frequency) measure horizontal variations, *e.g.* the number of peaks in the sampling length, whereas hybrid parameters (mean slope and relative length) combine both vertical and horizontal elements (*ibid.*). The final category of parameters was defined by the authors of this paper as mean displacement and area displacement. These are affected by the shape of the curve (the value of the area displacement is higher in a convex than a concave curve, see Figure 6.8.), not just the frequency of the curve. A final method was the measurement of the Rq of the high pass Fourier transform filter (cut off set at 0.1 Hz), which filtered out frequencies below 0.1 Hz of the curve (see below) using Origin 7. The Rq was then calculated on the high pass filter by pasting the values from Origin into Microsoft Excel (but excluding the two first and last values) using the following formula:

=SQRT((1/124)*SUMSQ(A1:A124))

So the square root of (the sum of squares of rows A1 to A124 divided by 124), where 124 is the number of rows. The actual number of rows varied, and the numbers were changed accordingly.

Test data (Figure 6.8) were created by drawing lines, to test how the roughness parameters functioned under various conditions. Note that on the file output mid-section roughness has been calculated. This was not used in the final analysis. Skewness and kurtosis of the curves were also calculated because they can provide useful additional descriptions of the Rq and Ra data. These were tested in the final analysis on some enthesis axes. They were not used on all of the data because the other ten parameters were assumed to be sufficient to record surface variation.

Figure 6.8 Test images (1 to 6) showing roughness parameters. Note the variation in roughness parameter values with the surface shape.

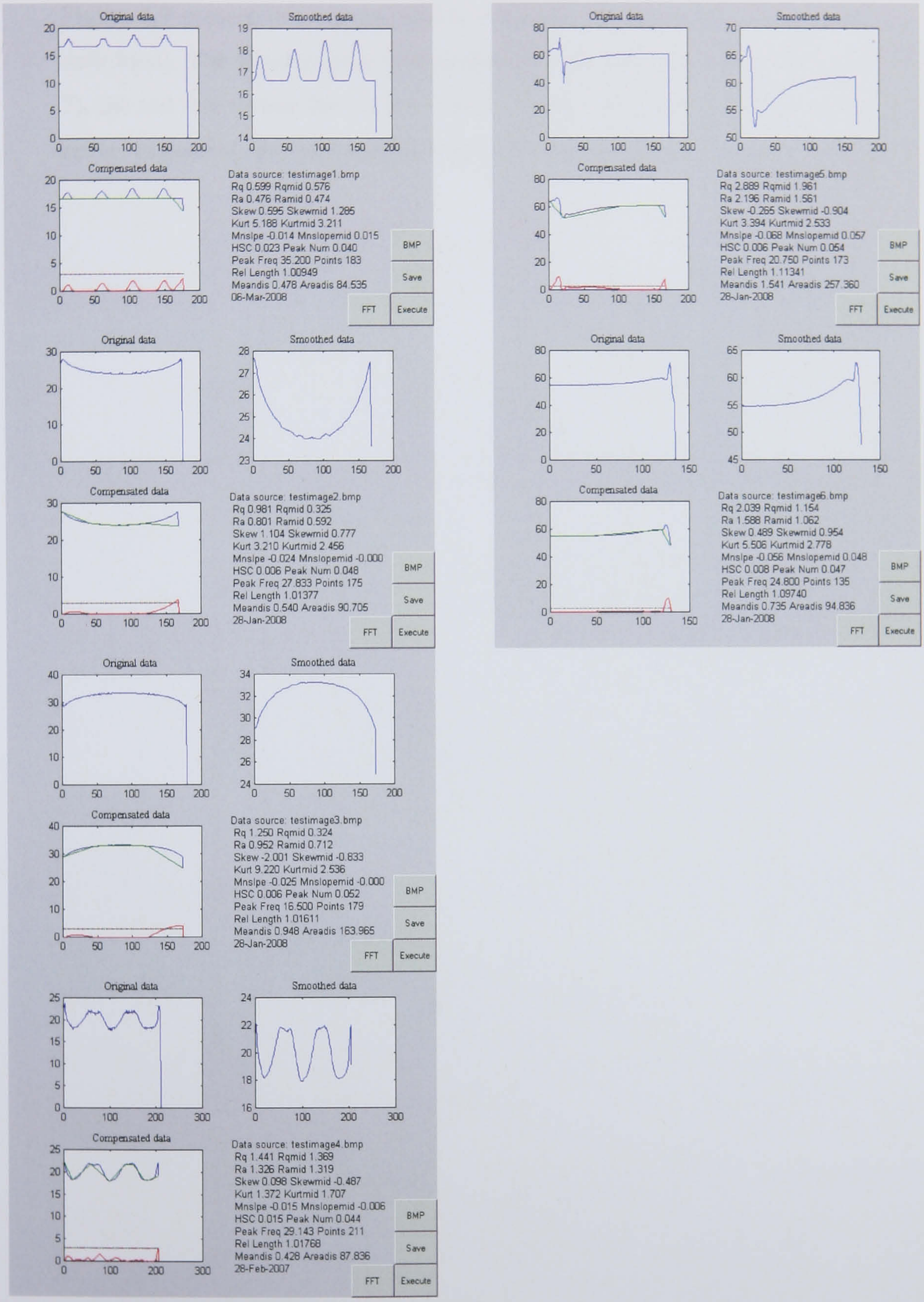
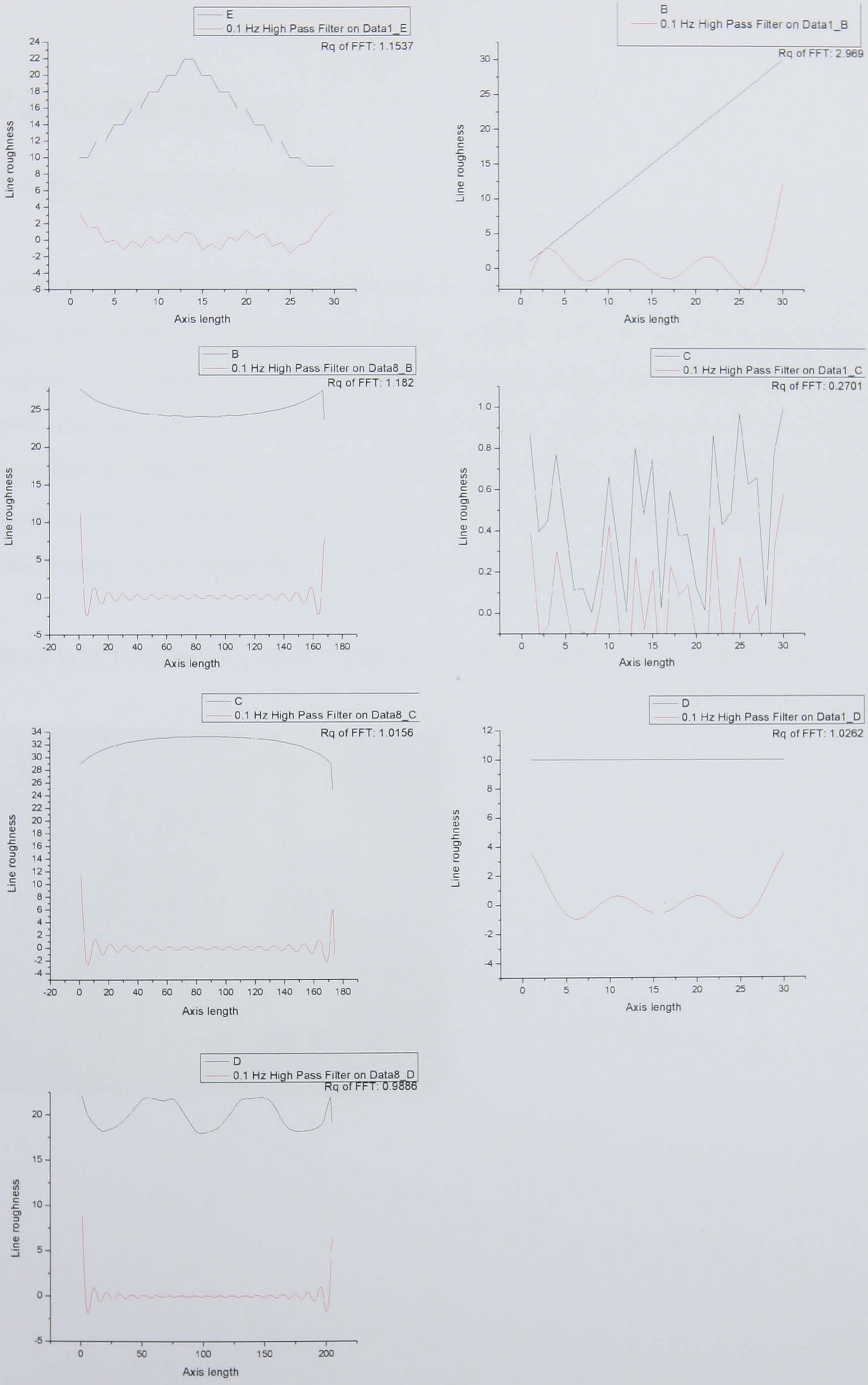


Figure 6.9 present test curves used to calculate the Rq of FFT (see Table 6.7 for a definition). The Black (upper line) represents a hypothetical curve (created in Origin 7), the red line (lower line) is the result if the 0.1 Hz high pass filter on the original curve. In general, this indicates that Rq of FFT is lower if the original curve is rough.

Figure 6.9 Test images for Rq of FFT. Where lines B, C, D, and E are the test image lines presented in Figure 6.8. The second line is a high pass filter applied to the line with its Rq value presented below.



In summary, these roughness parameters quantify various features of the curves. This should make them ideal for quantifying two-dimensional curves of entheses.

6.7 Intra-observer error

6.7.1 Roughness parameters

Roughness parameters were compared for the y dimension of the common extensor origin (see Figure 6.10). The profile of the common extensor origin y dimension was assessed on 8 humeri twice, using the same profile gauge but on separate days. The drawn curves were assessed as described above. The values of the roughness parameters on the different days are presented in Table 6.8. The parameters were compared using a Mann-Whitney U test (Table 6.9). No significant differences were found for any of the roughness parameters (at $\alpha = 0.05$).

Figure 6.10 Common extensor origin axis y. Line indicates location of y axis.

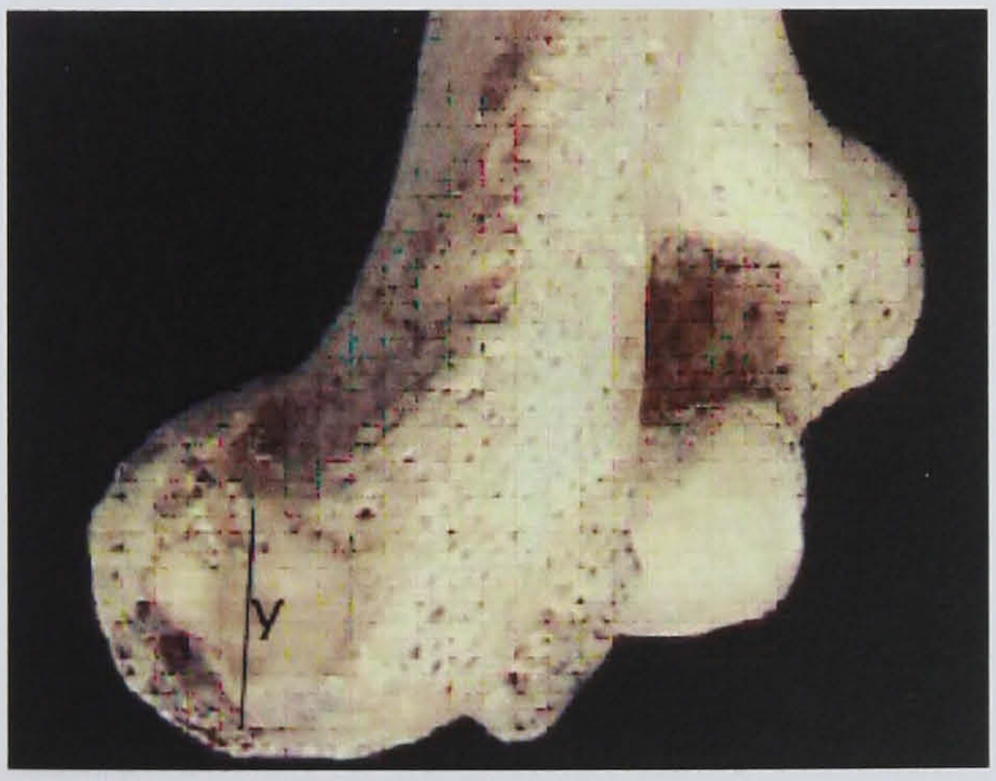


Table 6.8. Roughness parameter values for the common extensor origin y recorded on two separate occasions. N = 8.

Skeleton	Side	Occ-asion	Rq	Ra	Mn-slope	HSC	Peak-num	Peak-freq	Rell	Mn-Dis	Area-dis
Ja70GX	left	1st	1.08	0.74	0.00	0.00	0.08	14.83	1.00	0.33	61.56
Ja67KD	left	1st	0.66	0.45	0.01	0.02	0.07	15.86	1.00	0.17	22.90
ja67ky	left	1st	1.09	0.69	-0.01	0.02	0.07	15.57	1.00	0.29	35.33
Ja67MD	right	1st	0.26	0.19	0.00	0.03	0.07	15.13	0.99	0.98	13.10
ja67nk	right	1st	0.95	0.76	0.01	0.02	0.06	16.00	1.00	0.22	28.05
ja67nn	left	1st	1.31	1.02	0.00	0.01	0.07	17.78	1.00	0.23	37.72
ja70aak161	left	1st	0.56	0.40	0.01	0.02	0.06	16.86	1.00	0.15	20.75
Ja70XU	left	1st	0.34	0.25	0.00	0.01	0.06	19.86	0.99	0.08	11.72
Ja70GX	left	2nd	1.29	0.93	0.00	0.01	0.07	14.89	1.01	0.34	56.31
Ja67KD	left	2nd	0.72	0.53	-0.02	0.01	0.07	15.33	1.00	0.26	39.48
ja67ky	left	2nd	0.88	0.57	0.00	0.01	0.07	16.17	1.00	0.24	28.45
Ja67MD	right	2nd	0.52	0.40	0.01	0.01	0.06	18.33	1.00	0.13	23.26
ja67nk	right	2nd	0.41	0.29	-0.01	0.01	0.06	18.00	1.00	0.20	28.35
ja67nn	left	2nd	2.06	1.31	-0.02	0.01	0.06	19.86	1.01	0.63	92.95
ja70aak161	left	2nd	0.90	0.55	-0.02	0.02	0.08	14.11	1.00	0.20	26.88
Ja70XU	left	2nd	0.59	0.43	0.00	0.03	0.06	19.00	1.00	0.26	38.13

Table 6.9 Intraobserver error test of roughness parameters: non-parametric test. N=8.

	Rq	Ra	Mnslope	HSC	Peaknum	Peakfreq	Rell	MnDis	Areadis
Mann-Whitney U	30.000	29.000	13.500	25.000	30.000	27.500	24.000	28.000	17.000
Z	-.210	-.315	-1.952	-.737	-.211	-.473	-.840	-.420	-1.575
Exact Sig. [2*(1-tailed Sig.)]	.878(a)	.798(a)	.050(a)	.505(a)	.878(a)	.645(a)	.442(a)	.721(a)	.130(a)

a Not corrected for ties.

b Grouping Variable: Recording

6.8 Interobserver error

6.8.1 Roughness parameters

The majority of roughness parameters for the common extensor origin dimension y demonstrated no statistically different values between observers using Mann-Whitney U tests (Tables 6.10 and 6.11). This indicated that this method is robust and can be

widely used.

Table 6.10 Descriptive statistics of parametric roughness parameters divided into observer 1 (Obs 1) and observer 2 (Obs 2).

Obs		N	Minimum	Maximum	Mean	Std. Deviation
1	Rq	8	.477	1.026	.68538	.169176
	Ra	8	.311	.774	.48963	.142557
	Skew	8	-2.712	-1.315	-1.86488	.464225
	Kurt	8	5.046	14.784	7.32713	3.283570
	Mnslope	8	-.015	-.002	-.00775	.004652
	HSC	8	.006	.020	.01013	.005027
	Peaknum	8	.053	.078	.06750	.008468
	PeakFreq	8	15.200	19.833	17.35663	1.686899
	Points	8	120	157	134.88	13.389
	Rellength	8	1.00397	1.01925	1.0103313	.00490479
	Meandis	8	.175	.394	.27913	.097464
	Areadis	8	22.725	51.557	36.95488	10.922258
	Valid N (listwise)	8				
2	Rq	8	.451	1.449	.95350	.393170
	Ra	8	.221	1.088	.63488	.333905
	Skew	8	-6.318	-.219	-3.10588	2.173913
	Kurt	8	5.674	59.395	23.08800	22.685006
	Mnslope	8	-.052	-.014	-.02763	.012282
	HSC	8	.006	.037	.01463	.010364
	Peaknum	8	.057	.076	.06888	.006058
	PeakFreq	8	15.125	21.750	17.65625	2.340862
	Points	8	124	185	150.75	21.711
	Rellength	8	1.01235	1.03016	1.0224275	.00736164
	Meandis	8	.090	.526	.27988	.134023
	Areadis	8	13.726	91.983	43.74550	26.174779
	Valid N (listwise)	8				

Table 6.11 Non-parametric tests for inter-observer error of roughness parameters. N = 8.

	Rq	Ra	Mnslope	HSC	Peaknum	PeakFreq	Meandis	Areadis
Mann-Whitney U	22.000	26.000	15.000	24.000	28.500	31.000	30.000	30.000
Z	-1.050	-.630	-1.789	-.854	-.369	-.105	-.210	-.210
Exact Sig. [2*(1-tailed Sig.)]	.328(a)	.574(a)	.083(a)	.442(a)	.721(a)	.959(a)	.878(a)	.878(a)

a Not corrected for ties.

b Grouping Variable: Obs

6.9 Main Study: Materials

Skeletal material from the late medieval site of Fishergate House, York (England), curated in the Department of Archaeology, Durham University, was used. The exact dates for the skeletons are as yet unknown, but the majority are thought to date to the late medieval period (mid-14th to mid-15th century AD) (Holst 2005). The skeletal report on this site has been published (Holst 2005) and it is thought that these individuals represent a group of society used to manual labour. This is represented by the presence of Schmorl's nodes, DJD, patterns of trauma and lack of size difference between right and left upper limbs (Holst 2005). From previous research (Henderson 2002) on these skeletons, it was known that there are a large number of enthesopathies. It was decided that these skeletons were ideal for testing a new system for recording enthesopathies, based on their prevalence in this skeletal assemblage.

Only adult, male skeletons (n=43) were used to avoid the effects of development and hormones (sexual dimorphism) on entheses. Although a skeletal report has been published for this site, it was only used to determine the sex of the skeletons used in the present study. The skeletons were placed in two age categories: young adult and adult. Young adults were designated based on the visibility of epiphyseal fusion lines of late fusing epiphyses. Adults were those with fully fused late fusing epiphyses. It was decided that further subdivision of age was not appropriate for three reasons. Firstly, adult ageing is primarily based on degeneration of the skeleton, but enthesopathies are also a sign of degeneration and this would lead to circular arguments. Secondly, it was decided that the age categories would be too small for statistical analysis. Thirdly because this is a test sample to determine whether this new recording technique is viable, it was decided that the hypotheses to be tested did not require this subdivision. The influence of age was, therefore, not studied. The only scientific method to assess the effect of age would be to use a known age-at-death skeletal collection, but this was not the aim of this research. However, it age has recently been found to be the primary influence on enthesopathy formation and this must be remembered throughout Chapters 7, 8 and 9.

6.10 Main Study: Methods

This section will focus on the recording form used and the analysis of the data collected. The methods used for measurement, visual inspection and entheseal curvature assessment have been described above. Below is a schematic process flow chart indicating the method for digital data collection and surface roughness calculation (Figure 6.11).

Figure 6.11 Final process flow.



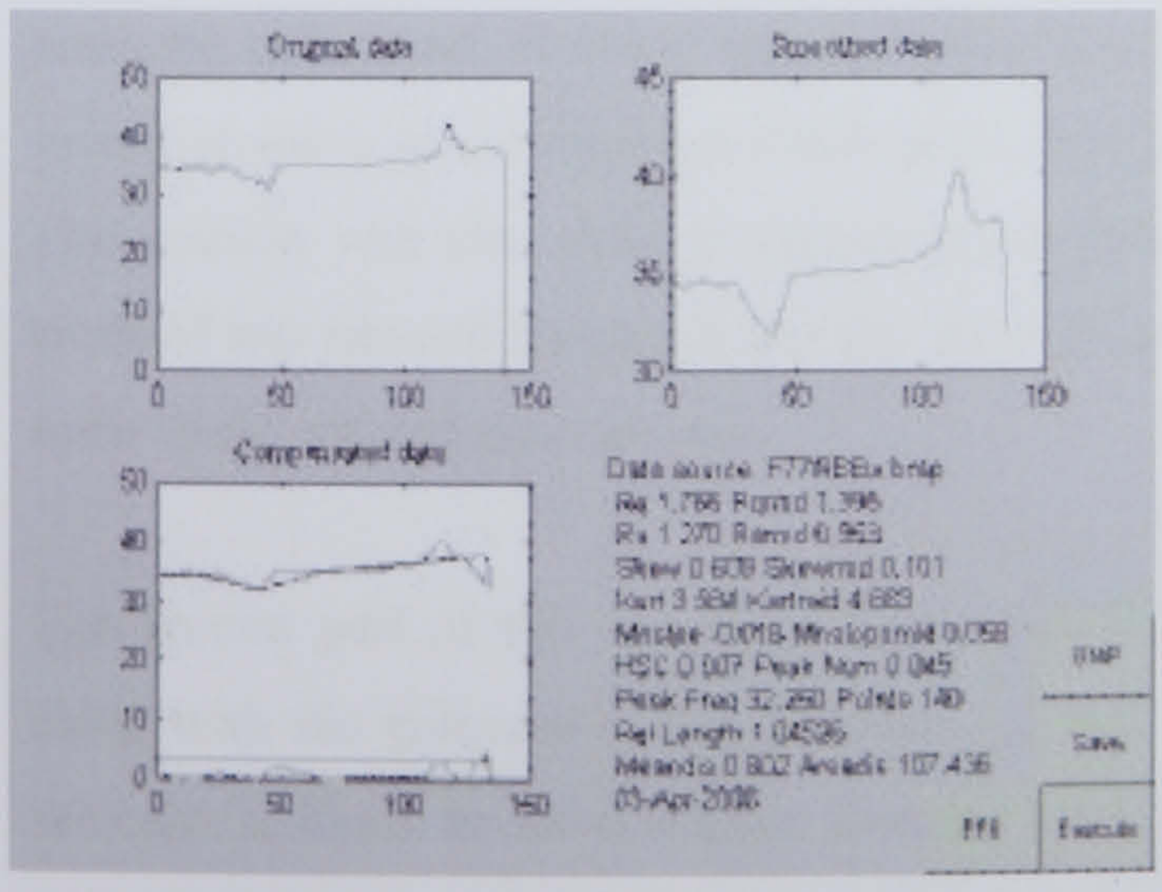
To record the enthesis roughness a profile gauge was placed against the surface to be measured in either the x or y axis.



Radius demonstrating use of the profile gauge in axis x on the *biceps brachii* insertion



F77 biceps brachii axis x



STAGE 1

The skeletons used for this research are male skeletons from Fishergate House, York, England. These skeletons tend to have well-marked entheses. Three entheses on the upper limb were recorded for this study: *supraspinatus,* common extensor origin, and *biceps brachii.* In addition to the method described below, the presence of abnormalities was also recorded.

STAGE 2

The line from the profile gauge representing the topography of the enthesis is transferred to paper and digitised.

STAGE 3

This line is then "scanned" using a routine written for Matlab, which calculates the roughness parameters described in Table 6.10.

6.10.1 Main Study: Recording Form

The recording form was created in an Excel spreadsheet and data were entered into this directly. The recording form was divided into three sections. The first section catalogues the age of the skeleton, the presence of enthesopathies and degenerative changes in the axial skeleton and lower limb. It also catalogues the presence of fractures, which may cause secondary enthesopathy formation. This section was also used to catalogue the presence of pathological changes which may indicate the presence of a bone forming disease. Specifically, these were changes around the sacroiliac joint, spinal ligament ossification, and foot and hand phalangeal anomalies. This section was also used to record photographs taken. Digital photographs were taken of any unusual change at any site for further analysis later and to visually record some of the written descriptions.

The second part of the recording form records the measurements of the humerus, along with the entheses of the humerus (as listed above). It also notes whether the skeleton is likely to have a bone forming disease based on the first section of the recording form. Section three records the measurements of the radius and ulna, as well

as the entheses of these bones (as listed above). These divisions were created using different worksheets in the main spreadsheet. See Appendix IV for all of the data, Appendix V presents the roughness values for each enthesis.

6.10.2 Disease Identification:

Chapter 5, the literature review of bone forming diseases, was used to create general diagnostic criteria for probable bone formers. The definition of bone former used in this research: 1) the presence of unilateral or bilateral sacroiliac enthesopathy along with spinal ankylosis or 2) unilateral or bilateral sacroiliac enthesopathy with multiple spinal ligament ossification on 2 or more vertebrae. Cases of unilateral or bilateral sacroiliac joint enthesopathy with only one ligament (or joint capsule) are questionably bone formers, and should be counted as bone formers if there is enthesopathy presence at multiple appendicular sites or there are distal phalanx changes of either the hand or foot (see Table 6.12). It was decided that it would be a mistake to under-diagnose bone formers because their enthesopathies may differ in size or shape from those with other causes and affect the final classification of entheses. Skeletons not preserved well enough for disease presence to be determined were classified as undiagnosable and were not used in the final analysis.

Table 6.12 General diagnostic criteria for bone forming diseases used in this study. Note that although changes to phalanges and carpals were recorded, these could not be used in the diagnostic criteria because of poor sample size due to preservation.

Must fulfill the following criteria	General signs	Description
1) The combination of these changes (as found typically in the seronegative spondyloarthropathies)	Spinal enthesopathy formation	Occurring at any enthesis
	Sacroiliac joint lesions	Comprises: ankylosis, erosion of joint surface, adjacent ligament ossification
2) Signs of fluorosis	Abnormal bone density and osteosclerosis	(as found in fluorosis)
3) Signs of ochronosis	Blackened cartilage	(as found in ochronosis)
4) Signs of acromegaly	Cranial hypertrophy	(as found in acromegaly)
5) Signs of leprosy (see also phalangeal deformity)	Rhino-maxillary destruction	(as found in leprosy)

6.10.3 Main Study: Analyses performed

To test whether bone formers have more appendicular enthesopathies than non-bone formers; the frequency of enthesopathies in each recorded enthesis was determined for the normal and bone former groups. Normality tests (Shapiro-Wilk) were used and a Student's T-test was then used to determine whether the mean frequency of enthesopathies was greater in the bone forming group. This was also performed to determine if individuals with fractures had a greater frequency of enthesopathies because the trauma causing bone fracture (such as a fall) may lead to enthesis or soft tissue damage.

To test whether the size of the enthesis correlates with the size of the bone, the data were first pooled by side (to increase sample size) and tested for normality using the Shapiro-Wilk normality test (SPSS). The measurements and indices of the humerus were tested for correlation, along with the measurements of the entheses of the humerus. This was repeated with the radius. It was expected that the enthesis size should correlate with local bone size for developmental reasons. The *supraspinatus* enthesis was expected to correlate with the size of the head of the humerus. The size of the common extensor origin was expected to correlate with the measurements of the condyle and epicondyle of the humerus. Finally, the *biceps brachii* insertion was expected to correlate with the medio-lateral diameter of the shaft, upon which it sits.

The differences in size were tested between normal entheses, entheses with abnormalities and the entheses of bone formers to determine if they were statistically significantly different in size. This is expected because the size of an enthesis affects its ability to dissipate stress. This was also undertaken to determine whether separating the bone formers into their own group was justified. The data were divided into normal (no enthesopathy at the enthesis being studied), bone former (separated even in cases where no enthesopathy at the enthesis under study was present) and enthesopathy (non-bone former, but enthesopathy present at enthesis being studied). These data were separated by left and right, but right and left were pooled not by skeleton number, but by appearance of enthesis. This was performed for all three

entheses (common extensor origin, *supraspinatus*, and *biceps brachii*) measured. Normality tests (Shapiro-Wilk) were performed. Those deemed by the normality test to be normal were compared using the Student's T-test.

T-tests (or Wilcoxon signed rank for non-normal data) were performed to compare roughness parameters and size between left and right sides for all entheses recorded (this was performed separately for each enthesis). If no statistically significant differences at $\alpha = 0.05$ were found, then the data were pooled. The same tests were performed on all entheses comparing normal entheses with abnormal ones. The latter were then divided into groups based on whether the line bisected the anomaly or not. Unfortunately, sample sizes were too small to further subdivide the data depending on whether the anomaly was a bone spur, a lytic lesion, or abnormal unevenness of the surface.

Discriminant function analysis was used on the three measured entheses divided into axis x and y to test the ability of the roughness parameters to distinguish between normal individuals, those with enthesopathies and bone formers. Several tests were performed with different categories of the data (Table 6.13). If sample sizes were too small, then not all tests were performed. SPSS 14 was used to determine which of the roughness parameters either alone or used together best distinguished between the groups. The results will be presented in chapter 7 and discussed in chapter 8.

Table 6.13 Tests performed and categories, along with their definitions, used.

Test	**Categories**		
1	1=normal	2=abnormal (enthesopathy present, but not a bone former)	3=bone former
2	1=normal	2=abnormal (enthesopathy present, but not a bone former)	
3	1a=no enthesopathy, or enthesopathy not intersected by profile gauge	4=enthesopathy intersected by profile gauge	

4	1=normal	21=abnormal, but enthesopathy not intersected by profile gauge	22= abnormal, but enthesopathy intersected by profile gauge	31= bone former, but either no enthesopathy, or enthesopathy not intersected by profile gauge	33=bone former with an enthesopathy intersected by profile gauge

6.11 Summary

The aim of this chapter was to present a new method for recording entheses, which takes into account the normal anatomy and the aetiology of enthesopathies. It was important for this method to be simple, cheap, repeatable and quantitative. It was also decided that digitisation was important for storage of the data for future use and reanalysis. It was decided that the bones and entheses should be measured to record the size and the relationship between the size of the enthesis and the size of the individuals. Trials to digitally record surface curvature of entheses have been described along with the method finally used. The method for quantitative analysis has been discussed. It is important to note that because the curvature of the entheses is stored digitally other methods for quantifying this curvature can be employed. Finally, the statistical analyses performed on the final data set were presented.

Chapter 7. Results

7.1 Introduction

The previous Chapter 6 demonstrated that the new method for recording and quantifying enthesis size and shape had low levels of both inter- and intra-observer error. The current chapter presents the results of the main study, using the skeletal material from Fishergate House, York, England. The aim is to determine whether the hypotheses presented in Chapter 6 are substantiated. This chapter is divided into the skeletal analysis which describes the age distribution of the sample, types and locations of enthesopathies, the presence of DJD, crude fracture prevalence and their relationship to enthesopathy presence, and finally, enthesopathy presence in bone formers. This provides a background to the sample and presents the possibilities of non-activity related aetiologies of enthesopathies in this sample. The second part of this Chapter presents the data on enthesopathies used to test the hypotheses. This section is divided into the visual recording of appendicular enthesopathies and their metric analysis. The following sections explore the relationship between enthesopathies and size and between size and roughness of the enthesis. Finally, the application of the roughness parameters to record and describe entheses and the ability of the roughness parameters to correctly classify the entheses will be presented. Discussion and interpretation of these results will be presented in Chapter 8. Unless otherwise stated, all statistical tests were performed using SPSS 14 with a 95 percent confidence interval selected for the calculation of statistical significance.

7.2 Skeletal analysis

The age distribution did not permit the analysis of enthesis morphology and enthesopathy formation by age. Age assessment of the sample, using the methods described in Chapter 6, indicated that there were 34 mature males, but only two young males: seven were of indeterminate age (total number of males was 43). The sample size differences would bias any results derived from this division. The reasons for this

were discussed in Chapter 6. However, studying the sample by age is necessary in most studies because of the increased incidence of enthesopathies in older individuals (Benjamin *et al.* 2006). In a study of the relationship between physical stress and enthesopathy formation, this would be a serious concern and strict ageing criteria would be necessary. However, the aim of this study was to create a more systematic recording system and a quantitative method for interpretation of entheses type, so this is not of primary importance in the present study. For this reason age groups were pooled.

The main purpose of this study was in the recording of enthesopathy presence. The results of the visual method for recording enthesopathies, based on their presence and absence, are presented in Table 7.1. This data is of particular interest because the most commonly affected enthesis is the *subscapularis*. Clinical research (Levitz and Iannotti 1995) indicated that the most commonly affected enthesis should be the *Supraspinatus*, which is most commonly affected in rotator cuff tears. This will be discussed in Chapter 8. Table 7.2 and Figures 7.1 to 7.9 provide an insight into the types of enthesopathies found in these entheses. The category "Other" was used for abnormalities which did not fit into either main category. This included entheses with rippled surfaces, and in one case an entheses with the appearance of "an unfused epiphysis" (found in skeleton F13, *brachialis* insertion, left side).

Table 7.0 Percentage of enthesopathies present, based on visual recording.

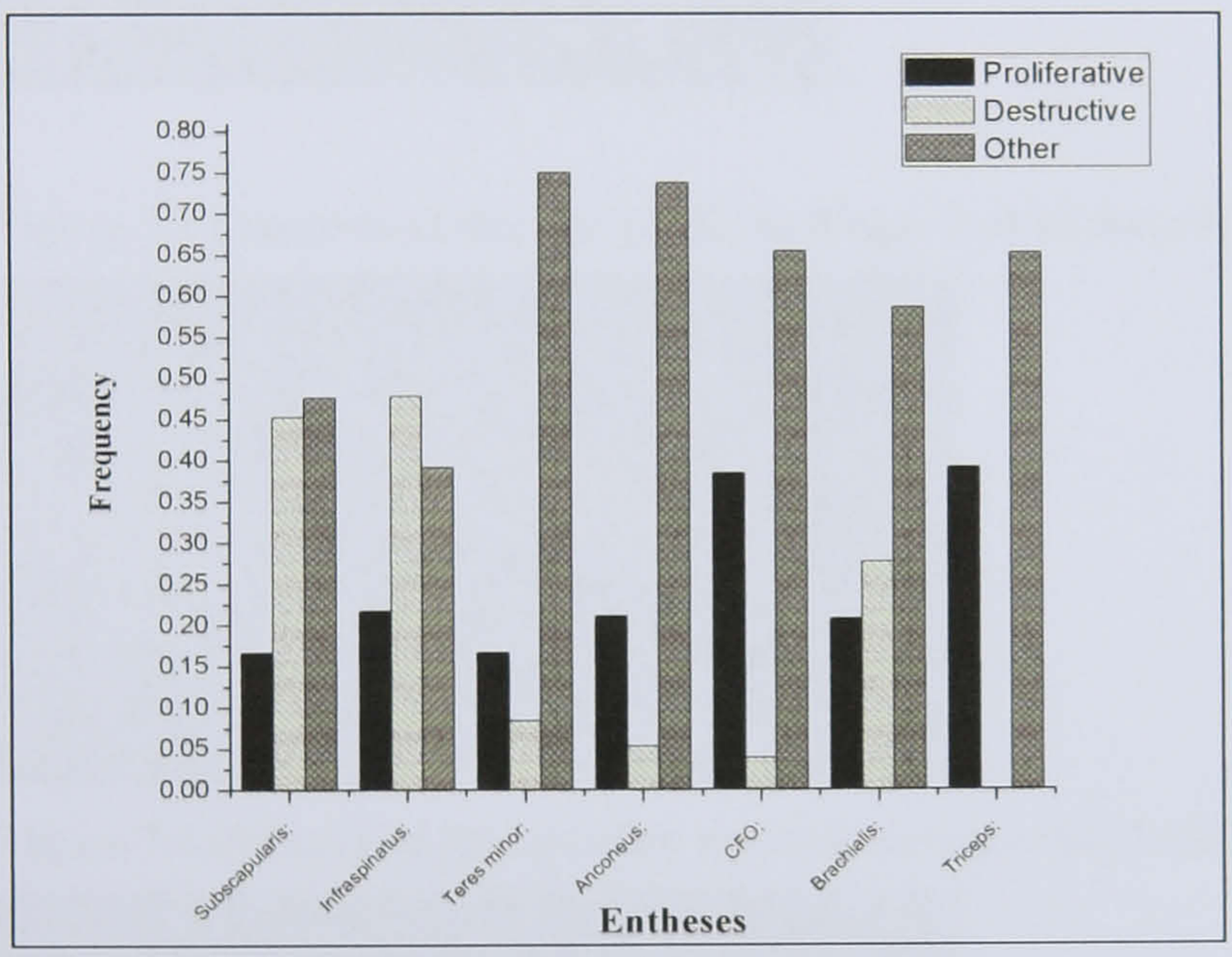
	Number of enthesopathies	**Number of bones with entheses present**	**Percentage with enthesopathies (%)**
Supraspinatus	14	40	35.0%
Common extensor origin	36	54	66.7%
Subscapularis	35	46	76.1%
Infraspinatus	22	42	52.4%
Teres minor	14	38	36.8%
Anconeus	18	54	33.3%
Common flexor origin	25	58	43.1%
Biceps brachii	34	52	65.4%
Brachialis	26	63	41.3%

Triceps brachii	23	60	38.3%

Table 7.1 Types of enthesopathy found.

	Supraspinatus	**Common extensor origin**	***Biceps brachii***
No. of entheses present	42	58	54
Proliferative lesions	4	30	16
Destructive lesions	6	3	5
Other	5	7	14

Figure 7.1 Types of enthesopathy found in the other entheses under study.



Figures 7.2 - 7.9 Types of enthesopathy found.

Figure 7.2. Proliferative bone and the margin of the common extensor origin on F73, right side.



Figure 7.3 Exostosis at the margin of the *biceps brachii* insertion (F73, left).



Figure 7.4 Porosity of the common extensor origin enthesis (F219, right).



Figure 7.5 Lytic lesion at the margin of common extensor origin (F70, left).



Figure 7.6 Almost circular depression with well-rounded margins in the centre of the common extensor origin (F67, right).



Figure 7.7 *Biceps brachii* insertion (F303, left) with pitting and woven new bone formation



Figure 7.8 *Brachialis* (F13 left) enthesis with appearance similar to that of an unfused epiphysis.



Figure 7.9 Loss of normal, smooth enthesis surface.



7.2.1 Degenerative Joint Disease

The skeletons were also studied for the presence of DJD (Table 7.3), to compare degenerative joint changes with enthesopathy presence. Degenerative joint changes have been linked with occupation (for example Holst 2005; Lai and Lovell 1992) and age (Jurmain 1999), both discussed in Chapter 2. Therefore, they may prove useful for the interpretation of enthesopathy formation in these skeletons. Table 7.3 demonstrates that the crude prevalence of DJD in this population. It should be noted that no cases of eburnation were found, only osteophyte formation and pitting. It is interesting to note that the left and right sides are almost equally affected by DJD (Holst 2005). This symmetry is worth noting for the discussion of pooling enthesis roughness data for the left and right sides (Section 7.3.1).

Table 7.2 Degenerative joint disease, manifested by lipping, porosity, or osteophytosis.

Joint	n		DJD		DJD:		Total frequency per number of joints present
	N present left	N present right	Left	Right	Left	Right	
Shoulder	34/43	34/43	8	8	24%	24%	24%
Elbow	35/43	35/43	3	3	9%	9%	9%
Wrist/hand	40/43	37/43	9	8	23%	22%	22%
Hip	37/43	38/43	6	7	16%	18%	17%
Knee	37/43	38/43	8	7	22%	18%	20%
Ankle/foot	34/43	32/43	23	23	68%	72%	70%

7.2.2 Fractures

Fractures may be related to secondary enthesopathy formation caused by soft tissue rupture during the fracture event; joint damage and bone malalignment may also affect the stress at the enthesis. Fractures recorded in this study were those occurring in the upper limb and ribs. Rib entheses were not studied and, consequently, rib presence was not recorded. Rib fractures were recorded, however because they could be caused by falling (Dandy and Edwards 1999), in which case it is possible that the upper limb was used to break the fall. This could in turn cause soft tissue or enthesis damage (as discussed in Chapter 4). Due to the recording method, fracture frequencies are crude. Few fractures were found in the population (Table 7.4). In some entheses, enthesopathies were found three times as frequently in the fractured compared to the non-fracture groups (Table 7.5). Statistical analysis was not performed because the true prevalence rates were not calculated, only the frequencies for the total number of skeletons.

Table 7.3 Fractures: left and right sides pooled (crude frequencies presented).

Location	N of skeletons with fractures present	Frequency by no. skeletons (43) (%)
Arm	3	7%
Ribs	14	28%
Other	6	14%

Table 7.4 Enthesopathy frequency in skeletons with neither upper limb (arm and hand) nor rib fractures; in skeletons with upper limb fractures; and in skeletons with rib fractures. (abbreviations: Supra=*supraspinatus*; CEO=common extensor origin; Subs=*subscapularis*; Infra=*infraspinatus*; Teres=*teres major*; CFO=common flexor origin; BB=*biceps brachii*; Brachial=*brachialis*; and Triceps=*triceps brachii*)

	No Fractures	Upper limb	Ribs
Supra	0.18	0.33	0.41
CEO	0.60	0.80	0.47
Subs	0.79	1.00	0.88
Infra	0.50	0.71	0.47
Teres	0.20	0.60	0.29
Anconeus	0.11	0.29	0.33
CFO	0.24	0.29	0.44
BB	0.53	1.00	0.64
Brachial	0.26	0.33	0.40
Triceps	0.41	0.11	0.29

7.2.3 Disease

Twenty-six skeletons were found to be normal, *i.e.* not fulfilling the criteria for bone-forming diseases. Eleven were found to have possible bone forming diseases, *i.e.* a combination of sacroiliac joint changes and spinal enthesopathies. No cases of leprosy, ochronosis, acromegaly, or fluorosis were found. Some skeletons exhibited changes in the small bones of the hands and feet, which were recorded but not used to classify the skeletons (see Appendix I). Four skeletons (F213, F92, F70, and F139)

were too poorly preserved to observe either the sacroiliac joints or the spine and were excluded from the study.

Tables 7.5 and 7.6 present the frequency of enthesopathies seen in each group. Four of the "bone formers" were diagnosed with DISH or possible seronegative spondyloarthropathy by Holst (2005). The other skeletons had combinations of spinal ligament and sacroiliac joint ossification, but no definite disease could be diagnosed. One of the primary hypotheses was that bone formers would have a greater number of appendicular enthesopathies than other skeletons. Table 7.7 demonstrates that the frequency of enthesopathies was consistently higher in the "bone formers". As can be seen in this figure, fewer enthesopathies occurred in the "normal" category than in the "bone formers". Chi-square tests demonstrated that there was a significantly higher frequency ($p<0.001$) of enthesopathies in the "bone formers" (Figure 7.10). Therefore this hypothesis was corroborated. Table 7.8 presents the significance for each enthesis. It should be noted that small sample sizes caused by poor preservation, particularly in the rotator cuff, may have biased the results.

Table 7.6 Axial and lower limb enthesopathies in skeletons with no signs of bone-forming disease (non-bone formers) and skeletons with possible bone-forming disease (bone formers). Four skeletons whose preservation did not allow for diagnosis were excluded.

n=left and right sides pooled	Enthesopathies associated with			
	Sacroiliac joint	Spine	Knee	Ankle
Non-boneformers	8/47	7/21	9/20	15/20
Boneformers	22/22	11/11	7/10	9/9
N B by definition boneformers must have a combination of sacroiliac and spinal enthesopathy				

Table 7.7 Frequency of enthesopathies seen (left and right sides pooled). Number of enthesopathies found over number of entheses observable.

Enthesis	Non-bone formers (26 skeletons) frequency affected (%)	Bone formers (11 skeletons) frequency affected (%)
Supraspinatus	9/34 (26%)	5/6 (83%)
Common extensor origin	22/39 (56%)	14/15 (93%)
Subscapularis	26/35 (74%)	8/11 (73%)
Infraspinatus	17/36 (47%)	5/6 (83%)
Teres minor	10/32 (31%)	4/6 (67%)
Anconeus	10/40 (25%)	8/14 (57%)
Common flexor origin	12/41 (29%)	13/17 (76%)
Biceps brachii	23/39 (59%)	11/13 (85%)
Triceps brachii	11/41 (27%)	12/19 (63%)
Brachialis	13/44 (30%)	13/19 (68%)

Chi-square tests conducted on the data in Table 7.7 demonstrated that there was a significantly higher frequency ($p<0.001$) of enthesopathies in the "bone formers" (see Table 7.8). This is also presented in Figure 7.10.

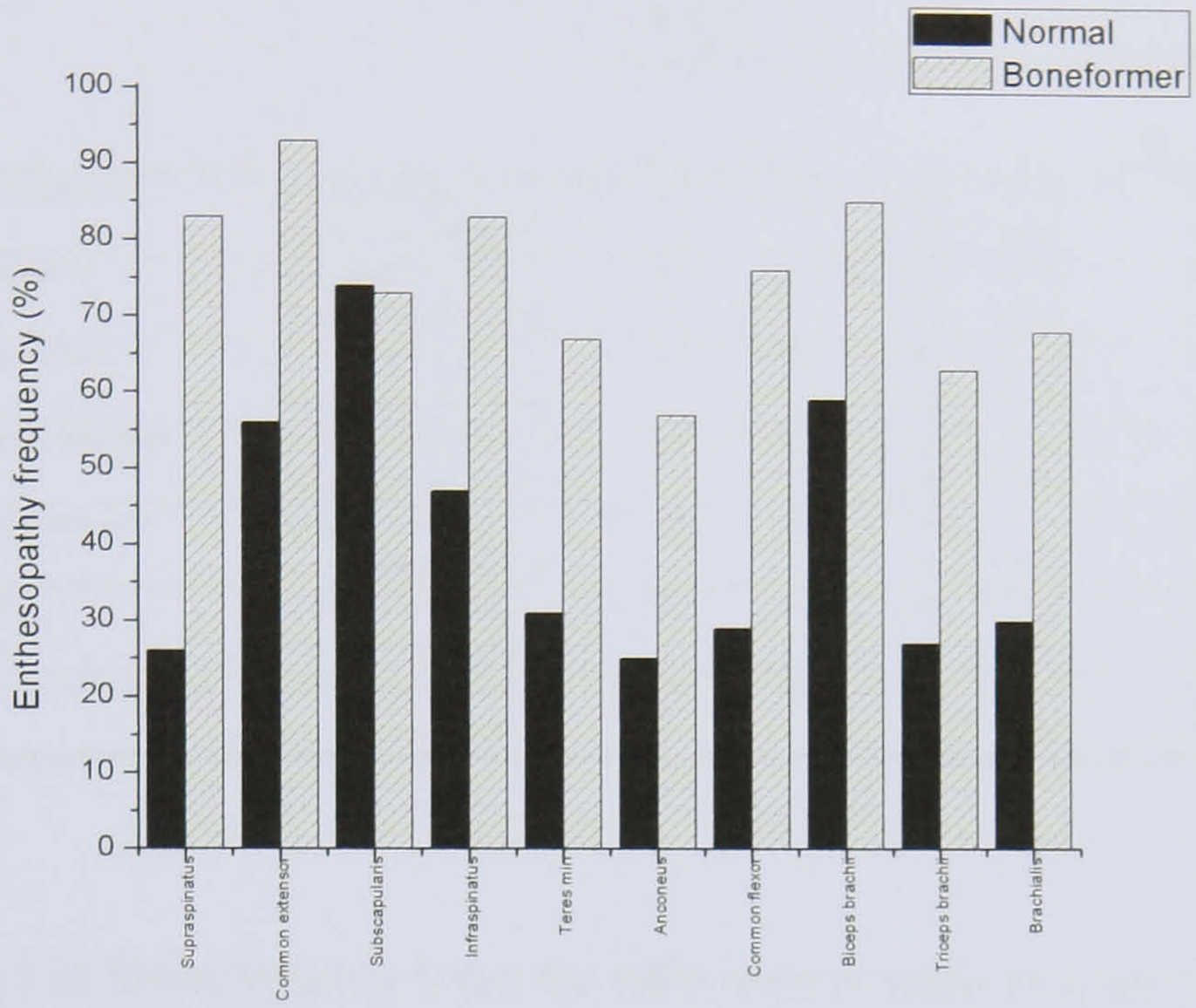
Table 7.8 Chi-square tests comparing the frequency of enthesopathies at different entheses between "bone formers" and "normal" skeletons.

Enthesis	Significant difference in frequency	Comment (df=1)
Subscapularis	-	Frequency of enthesopathies higher in the non-bone formers (see graph above). $p=0.9182$, $Chi^2=0.011$ n=46,
Supraspinatus	X	$p=0.0071$, $Chi^2=7.248$, n=40
Infraspinatus	-	$p=0.1146$, $Chi^2= 2.489$, n=42
Teres minor	-	$p=0.3570$, $Chi^2=0.848$, n=38
Common extensor origin	X	$p=0.0099$, $Chi^2=6.646$ n=54
Anconeus	X	$p=0.0281$, $Chi^2=4.821$, n=54
Common flexor origin	X	$p=0.0010$, $Chi^2=10.918$, n=58
Triceps brachii	X	$p=0.0071$, $Chi^2=7.249$, n=60
Brachialis	X	$p=0.0040$, $Chi^2=8.274$, n=63
Biceps brachii	-	$p=0.0092$, $Chi^2=2.832$, n=42

X = statistically significant ($p<0.05$)

- = not significant ($p<0.05$)

Figure 7.10 Graph of enthesopathy frequency, with left and right sides pooled, divided into "bone formers" (i.e. those with possible disease presence) and non-bone formers (= normal). Undiagnosable (those with spine and or sacroiliac joint absent) were excluded.



7.3 Measurements

7.3.1 Left/Right Side Comparison of Bone Measurements

The Student's T-test and Mann-Whitney's U (for non-normally distributed data) demonstrated that there were no significant differences in size between the left and right sides of the skeletons' upper arm (Tables 7.9 and 7.10), as well as lower arm bones (Tables 7.11 and 7.12). This was also found by Holst (1995). This lack of asymmetry (also found in the data on DJD), may indicate that these individuals were not undertaking occupations with high degrees of limb specificity, *e.g.* writing (as discussed in Chapter 2). The results of these tests indicated that left and right sides could be pooled to increase the sample size. If this were a study of the relationship between enthesopathy presence and activity, then this approach would be questionable. However, for the purposes of this study, it should not affect the results.

Table 7.9 Comparison of means of left and right sides of humeri.

Independent Samples Test

		Levene's Test for Equality of Variances		t-test for Equality of Means				
		F	Sig.	t	df	Sig. (2-tailed)	Mean Difference	Std. Error Difference
Humerus: max length	Equal variances assumed	.022	.881	-.476	46	.637	-2.79	5 862
	Equal variances not assumed			-.476	44.852	.636	-2.79	5.856
Humerus: min circ	Equal variances assumed	.133	.716	-2.564	62	.013	-2.67	1.040
	Equal variances not assumed			-2.583	61.210	.012	-2.67	1.032
Humerus: vert head	Equal variances assumed	.493	.486	-1.398	45	.169	-1.25	895
	Equal variances not assumed			-1.386	42.049	.173	-1.25	.903
humerus: transverse head	Equal variances assumed	.148	.702	-.964	42	.341	-.66	.688
	Equal variances not assumed			-.968	42.000	.339	-.66	.685
humerus: condylar width	Equal variances assumed	.254	.616	-.019	61	.985	-.01	.738
	Equal variances not assumed			-.019	58.671	.985	-.01	.742
Robusticity	Equal variances assumed	.513	.478	-1 344	44	.186	-.4628	.34446
	Equal variances not assumed			-1.333	41.189	.190	-.4628	.34713
Vertical head /transverse head	Equal variances assumed	.001	982	-.448	41	.657	-.0054	.01206
	Equal variances not assumed			-.448	40.263	.656	-.0054	.01206

Table 7.10 Mann-Whitney U test for differences in mean between left and right sides of the epicondylar width of the humerus.

Test Statistics [a]

	humerus: epicondylar width
Mann-Whitney U	472.500
Wilcoxon W	1033.500
Z	-.730
Asymp. Sig. (2-tailed)	.465

[a]. Grouping Variable: side: left=1, right=2

Table 7.11 Comparison of means of left and right sides of radii and ulnae from Fishergate House, York.

Independent Samples Test

		Levene's Test for Equality of Variances		t-test for Equality of Means				
		F	Sig.	t	df	Sig. (2-tailed)	Mean Difference	Std. Error Difference
A-P diameter	Equal variances assumed	.000	.997	-.311	60	757	-.15	.469
	Equal variances not assumed			-.311	59.910	.757	-.15	.469
M-L diameter	Equal variances assumed	.150	.700	-2.432	59	.018	-.99	.408
	Equal variances not assumed			-2.440	58.938	.018	-.99	.407
Biceps: x	Equal variances assumed	.010	.922	.400	54	.691	.41	1.026
	Equal variances not assumed			.400	53.922	.691	.41	1.026
Biceps: y	Equal variances assumed	.334	.566	1.633	52	.108	1.42	.871
	Equal variances not assumed			1.626	50.149	.110	1.42	.874
Ulna: max length	Equal variances assumed	1.833	.186	.284	31	.778	1.27	4.458
	Equal variances not assumed			.296	29.046	.770	1.27	4.280
Ulna: least circumference	Equal variances assumed	.868	.357	-1.012	44	.317	-.78	.773
	Equal variances not assumed			-1.012	39.100	.318	-.78	.773

Table 7.12 Mann-Whitney U test of left and right sides of the lower arm.

Test Statistics [a]

	A-P diameter	Biceps: y
Mann-Whitney U	417.500	282.000
Wilcoxon W	882.500	633.000
Z	-.880	-1.420
Asymp. Sig. (2-tailed)	.379	.156

[a]. Grouping Variable: side: left=1, right=2

7.3.2 Comparison of measurements between normal and abnormal entheses

Student's T-tests were used to compare the size of bones and entheses in individuals without enthesopathies (normal), with enthesopathies (abnormal) and bone formers. For the latter, all bone formers were included whether an enthesopathy was present or not. This was performed to test whether bone formers were in general different to the "normal" population. The "with enthesopathy" category included all those with enthesopathies, independent of whether the axis measured intersected the anomaly. This was performed to test the hypothesis that enthesopathy presence was more common in smaller entheses because of their inability to efficiently distribute loading. However, a preliminary study of the *subscapularis* insertion from disarticulated bone

(that was used to create the method) indicated that the opposite was true (Chapter 6). Therefore, the hypotheses tested were:

Normal < With enthesopathies (abnormal)
Normal < Bone formers
With enthesopathies < Bone formers

The results of this demonstrated that in the majority of cases (as can be seen in Tables 7.13-7.16) normal bones were smaller than those of individuals with a bone-forming disease. This may represent developmental or environmental differences and will be discussed further in Chapter 8.

Table 7.14 presents the data from the Student's t-tests demonstrating that the vertical head and transverse diameters of the head of the humerus and the epicondylar width were statistically significantly (at $\alpha = 0.05$) smaller in bone formers compared to normal individuals. Abnormal data were not compared in this manner because not all entheses had abnormalities and this may skew results; consequently, the data were subdivided by enthesis. In general, statistically significant (at $\alpha = 0.06$) differences in measurement of the bones existed between the normal and abnormal entheses and between the normal and bone formers. Fewer differences were present between the abnormal entheses and the bone formers. The measurements of the axes of the entheses generally demonstrated size differences between the groups classified. This will be discussed in Chapter 8.

Table 7.13 Comparison of means for size of humerus between normal individuals and individuals with bone-forming disease.

Independent Samples Test

		t-test for Equality of Means			
		t	df	Sig. (2-tailed) (p-value divided by 2 for unidirectional analysis)	Mean Difference
Humerus: max length	Equal variances assumed	-1.408	45	.083	-10 06
	Equal variances not assumed	-1.910	25.659	.034	-10.06
Humerus: min circ	Equal variances assumed	-.593	58	.278	-.76
	Equal variances not assumed	-.747	39.474	.230	-.76
Humerus: vert head	Equal variances assumed	-2.013	42	.025	-2.20
	Equal variances not assumed	-2.074	12.937	.029	-2.20
humerus: transverse head	Equal variances assumed	-2.810	39	.004	-2.22
	Equal variances not assumed	-3.625	20.796	.001	-2.22
humerus: condylar width	Equal variances assumed	-1 488	58	.071	-1.26
	Equal variances not assumed	-1.627	32.029	.057	-1.26
humerus: epicondylar width	Equal variances assumed	-2.021	58	.024	-2.31
	Equal variances not assumed	-2.126	26.327	.022	-2.31
Robusticity	Equal variances assumed	1.019	43	.157	.4511
	Equal variances not assumed	1.467	24.729	.078	.4511
Vertical head /transverse head	Equal variances assumed	-.339	38	.368	-.0053
	Equal variances not assumed	-.292	9.274	.388	-.0053

Table 7.14 Sides pooled: *Supraspinatus* Student's t-test comparison of mean size between different classifications of entheses.

Measurement	normal <enthesopathy	normal < bone former	abnormal < bone former
Humerus: max length	Yes	Yes	No
Humerus: min circ	No	No	No
Humerus: vert head	Yes	Yes	No
humerus: transverse head	Yes	Yes	No
humerus: condylar width	Yes	Yes	No
humerus: epicondylar width	Yes	Yes	No
Supra: x	Yes	Yes	Yes
Supra: y	No	No	No
Robusticity	No	No	No
Verthead/transhead	Yes	No	No

Table 7.15 Sides Pooled: Common Extensor Origin: Student's t-test comparison of mean size between different classifications of entheses.

Measurement	normal <enthesopathy	normal < bone former	abnormal < bone former
Humerus: max length	No	Yes	No
Humerus: min circ	No	No	No
Humerus: vert head	No	Yes	No
humerus: transverse head	No	Yes	Yes
humerus: condylar width	No	No	No
humerus: epicondylar width	No	Yes	No
CEO: x	Yes	Yes	No
CEO: y	Yes	Yes	No
Robusticity	No	No	No
Verthead/transhead	No	No	No

Table 7.16 Sides Pooled: *Biceps brachii*: Student's t-test comparison of mean size between different classifications of entheses.

Measurement	normal <enthesopathy	normal < bone former	abnormal < bone former
Radius maximum length	Yes	No	No
Radius A-P diameter	No	No	No
Radius M-L diameter	No	No	No
Radial shaft index	No	No	No
Radio-humeral index	No	No	No
Modified calliper index	No	No	No
Ulna max length	No	No	No
Ulna circumference	No	No	No
***Biceps brachii* x**	Yes	Yes	Yes
***Biceps brachii* y**	Yes	Yes	Yes

7.3.3 Test of correlation between bone measurements and enthesis measurements

The test of the correlation between bone measurements and enthesis measurements was, in part, intended to determine whether enthesis development and bone development were connected, as discussed in Chapter 6. Normality tests were performed (Appendix III) and Pearson correlation coefficients were used if the data were normal to test for linear correlation between these measurements. Spearman's rho was used for non-parametric data. Table 7.18 demonstrated that the *supraspinatus* axes x and y did not statistically significantly correlate with expected structures.

Instead, the *supraspinatus* axis x correlated with condylar width whilst *supraspinatus* axis y correlated with minimum circumference. Both axes correlated with robusticity. The common extensor origin axes correlated with all measurements of the humerus, but not the indices. This was unexpected. The *biceps brachii* axis x demonstrated a statistically significant linear correlation with the medio-lateral diameter of the radius, but no other correlations were found for either axis. Tables 7.17-7.20 demonstrate that there is correlation between the size of entheses (as measured in this study) and the size of the long bones to which they attach.

Table 7.17 Humerus All (excluding undiagnosed skeletons), with left and right sides pooled (X = Bonferroni adjusted 0.05 α = 0.042).

Table 7.18 As above but Spearman's rho for *Supraspinatus* y.

			Humerus: max length	Humerus: min circ	Humerus: vert head	humerus: transverse head	humerus: condylar width	humerus: epicondylar width	Supra: x	Robusticity	Head index: vertical head /transverse head
Spear-man's rho	Supra: y	Correlation Coeffici ent	-0.068	.419(**)	0.071	0.225	0.241	0.166	-0.201	.483(**)	-0.228
		Sig. (2-tailed)	0.686	0.008	0.669	0.188	0.144	0.307	0.226	0.002	0.18
		N	38	39	39	36	38	40	38	37	36
	** Correlation is significant at the 0.01 level (2-tailed).										
	* Correlation is significant at the 0.05 level (2-tailed).										

Table 7.19 Radius: All (including undiagnosed skeletons), with left and right sides pooled. Pearson correlation coefficients.

Correlations

		Radius: max length	M-L diameter	Biceps: x	Ulna: max length	Ulna: least circumference	Radio-Humeral index
Biceps: x	**Pearson Correlation**	0.096	.322(*)	1	-0.012	0.186	-0.186
	Sig. (2-tailed)	0.573	0.016		0.951	0.256	0.307
	N	37	55	56	27	39	32

* Correlation is significant at the 0.05 level (2-tailed); ** Correlation is significant at the 0.01 level (2-tailed).

Table 7.20 Radius: All (including undiagnosed skeletons), with left and right sides pooled. Spearman's rho.

Correlations

			Radius: max length	A-P diameter	M-L diameter	Biceps: x	Biceps: y	Ulna: max length	Ulna: least circumference	Radio-Humeral index
Spearman's rho	**Biceps: x**	**Correlation Coefficient**	0.143	0.156	.363(**)	1	.529(**)	0.056	0.166	-0.135
		Sig. (2-tailed)	0.398	0.255	0.006	.	0	0.781	0.314	0.461
		N	37	55	55	56	54	27	39	32
	Biceps: y	**Correlation Coefficient**	0.324	0.111	0.172	.529(**)	1	0.002	0.185	-0.062
		Sig. (2-tailed)	0.054	0.428	0.218	0	.	0.994	0.274	0.739
		N	36	53	53	54	54	26	37	31

** Correlation is significant at the 0.01 level (2-tailed).

* Correlation is significant at the 0.05 level (2-tailed).

7.4 Roughness parameters

7.4.1 Comparison of quantitative analysis of enthesis surface roughness between left and right sides

The comparison of the values of roughness parameters between left and right sides of

each enthesis axis was performed to determine whether the left and right side roughness parameters could be pooled. Tests of normality were conducted using Shapiro-Wilk. Means of left and right sides were compared, from un-paired samples, consequently, normally distributed data were tested using Student`s t-test, non-parametric data were tested using Wilcoxon rank sum. No statistically significant (α = 0.05) differences were found between left and right sides. This conforms to the lack of difference in size between the left and right sides of these skeletons. These findings will be discussed in Chapter 8.

Table 7.21 Statistical test of difference between left and right sides for the roughness parameters. Statistical significance at α = 0.05. X indicates that no statistically (95 percent confidence level) significant differences were found.

Roughness parameters	***Supra-spinatus* X**	***Supra-spinatus* Y**	**Common Extensor Origin X**	**Common Extensor Origin Y**	***Biceps brachii* X**	***Biceps brachii* Y**
Rq	X	X	X	X	X	X
Ra	X	X	X	X	X	X
Mnslope	X	X	X	X	X	X
HSC	X	X	X	X	X	X
Peaknum	X	X	X	X	X	X
Peakfreq	X	X	X	X	X	X
Rellength	X	X	X	X	X	X
Meandis	X	X	X	X	X	X
Areadis	X	X	X	X	X	X
FFTRq	X	X	X	X	X	X

7.4.2 Test of correlation between enthesis measurements and roughness parameters

Left and right side data were pooled based on the results from the tests described above. The enthesis measurements were then tested for correlation between their size and the values of the roughness parameters. This was performed because the size of an enthesis should affect its ability to dissipate stress and it was hypothesised that the roughness of the enthesis would also measure the amount of available surface for stress dissipation. Parametric data (as determined by normality tests, see Appendix III) were tested for linear correlations using Pearson`s correlation coefficient, whereas nonparametric data were tested with Spearman`s rho. The results of this analysis are presented in Table 7.22. This analysis demonstrated that the majority of roughness

parameters do not correlate with the size of the enthesis (Table 7.22). However, where statistically significances (at α =0.05) were found, then the data were plotted and a linear fit performed (using the software program Origin 7). This was used to determine if outliers were affecting the data (Figures 7.11-7.23). If outliers were visible, then these were removed and the data were re-tested for correlation (using the tests described above).

Table 7.22 Pearson correlation coefficients used to test whether the enthesis dimensions correlation with the roughness parameters. (p.c.c= Pearson correlation coefficient). NB: Axis does not intersect anomaly = all normal entheses along with abnormal and bone formers whose curve did not intersect an enthesopathy.

Enthesis and axis	Correlations	Comments
Supraspinatus X: all	None	
Supraspinatus X: axis does not intersect anomaly	None	
Supraspinatus X: axis intersects anomaly	None	
Supraspinatus Y: all	None	
Supraspinatus Y: axis does not intersect anomaly	None	
Supraspinatus Y: axis intersects anomaly	None	
CEO X: all	Peak number (p.c.c = -0.459, p = 0.001, n = 46)	
CEO X: axis does not intersect anomaly	Peak number (p.c.c = -0.500, p = 0.025, n = 20)	
CEO X: axis intersects anomaly	Peak number (p.c.c = -0.455, p = 0.020, n = 26)	
CEO Y: all	Rq of FFT (p.c.c. = 0.432, p = 0.002, n = 48)	
CEO Y: axis does not intersect anomaly	Peak frequency (p.c.c. = 0.382, p = 0.031, n = 32), Peak number (p.c.c. = -0. 537, p = 0.002, n = 32), Rq of FFT (p.c.c. = 0.394, p = 0.026, n = 32), HSC (rho = -0.578, p = 0.01, n = 32)	All plots demonstrate linear significance, except for the comparison with HSC, which is probably affected by outliers (Figure 7.15)
CEO Y: axis intersects anomaly	none	
Biceps brachii X: all	Peak number (p.c.c. = -0.279, p = 0.043, n = 53), HSC (rho = -0.377, p = 0.005, n=53), area displacement (rho = 0.491, p = 0.000, n = 53)	HSC linear fit is not statistically significant

Enthesis and axis	Correlations	Comments
Biceps brachii X: axis does not intersect anomaly (category 1a)	HSC (p.c.c. = -0.646, p = 0.005, n = 17), Peak number, (p.c.c = -0.621, p = 0.008, n = 17), Area displacement (p.c.c = 0.593, p = 0.012, n = 17)	With the removal of outliers F233 left and F147 left, then the correlation with area displacement is no longer significant
Biceps brachii X: axis intersects anomaly (category 4)	Mean slope (p.c.c. = -0.345, p = 0.039, n = 36), Area displacement (rho = 0.415, p = 0.012, n = 36)	Neither correlation is significant with the outliers removed
Biceps brachii Y: normal	None	
Biceps brachii Y: axis does not intersect anomaly	None	
Biceps brachii Y: axis intersects anomaly	None	

Figure 7.11 Linear fit demonstrating correlation between common extensor axis x (mm^2) and peak number.

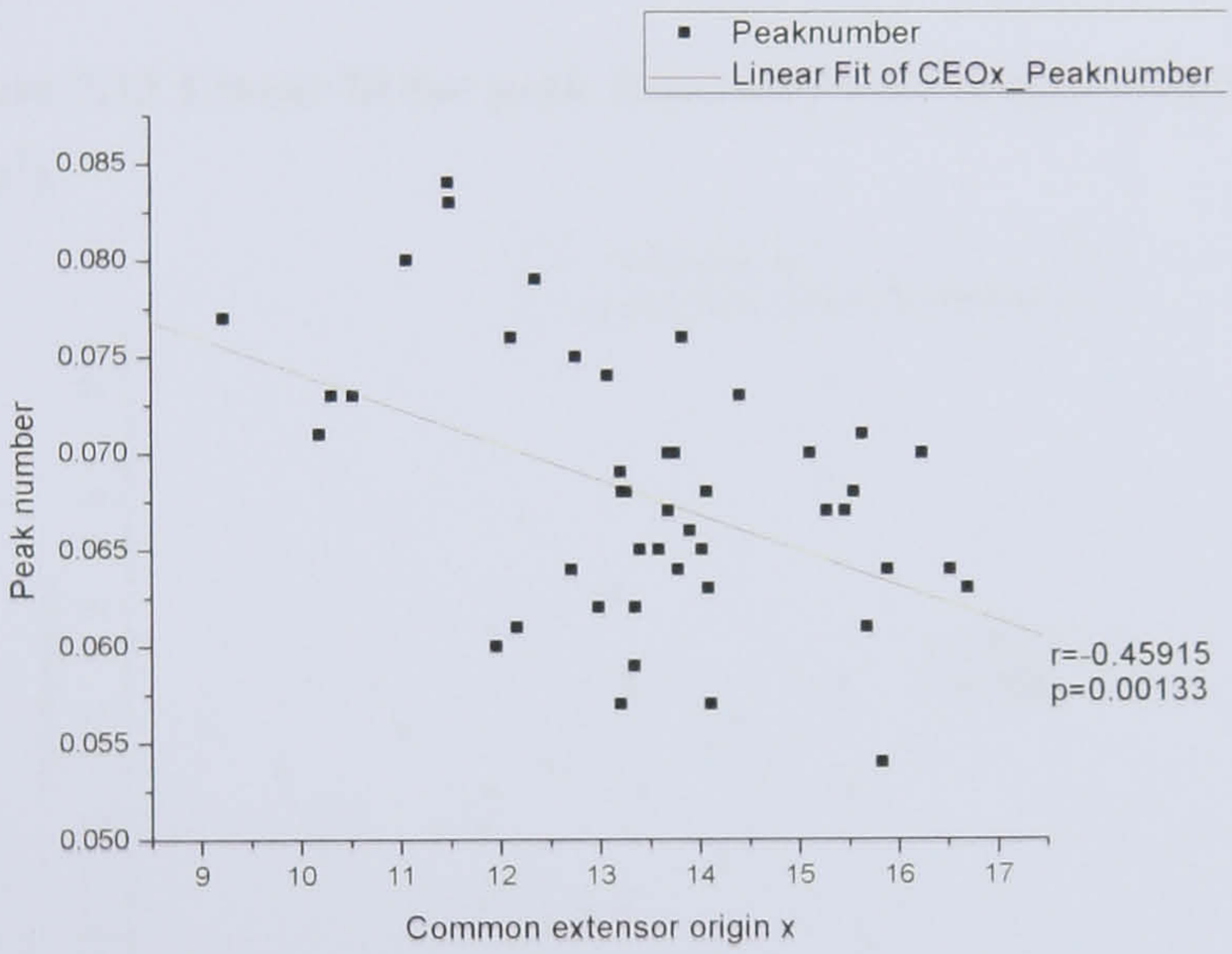


Figure 7.12 Linear fit for Rq of FFT over length of common extensor origin axis y (mm^2).

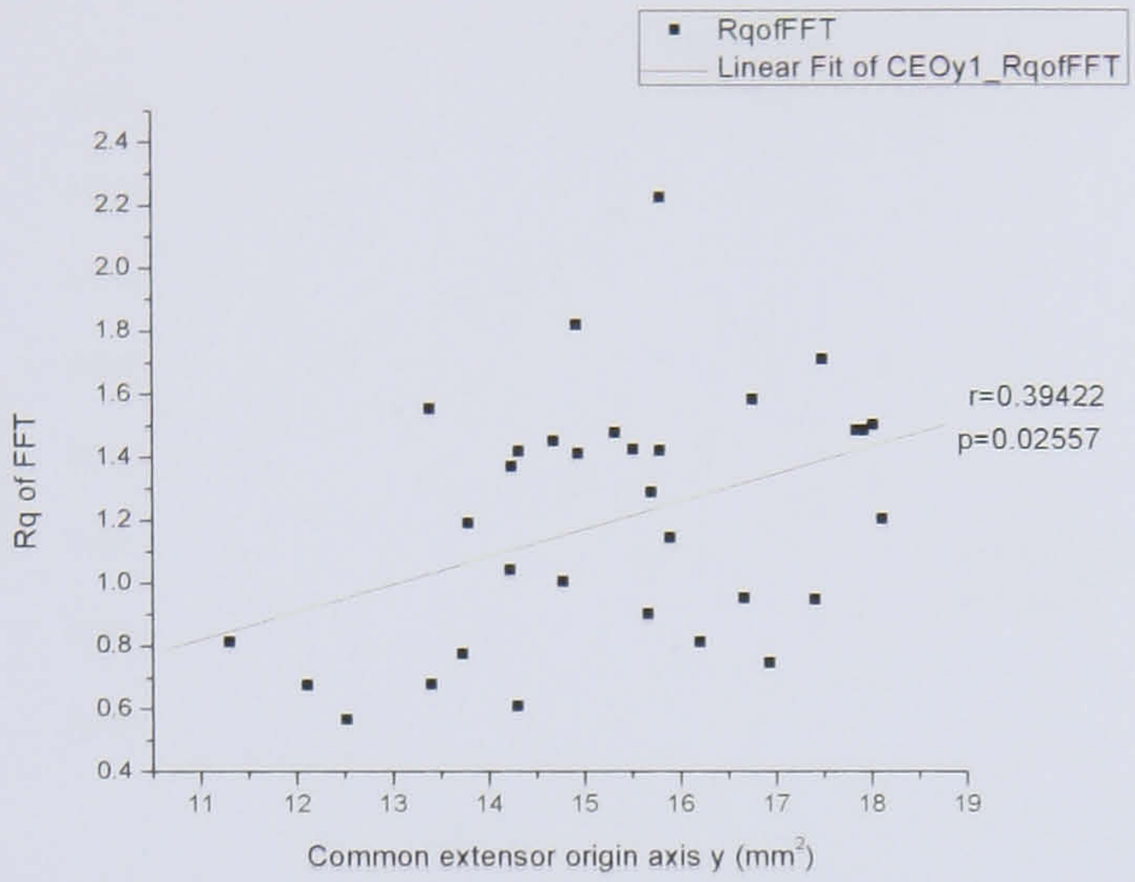


Figure 7.13 Linear fit for peak frequency over length of common extensor origin axis y (mm^2).

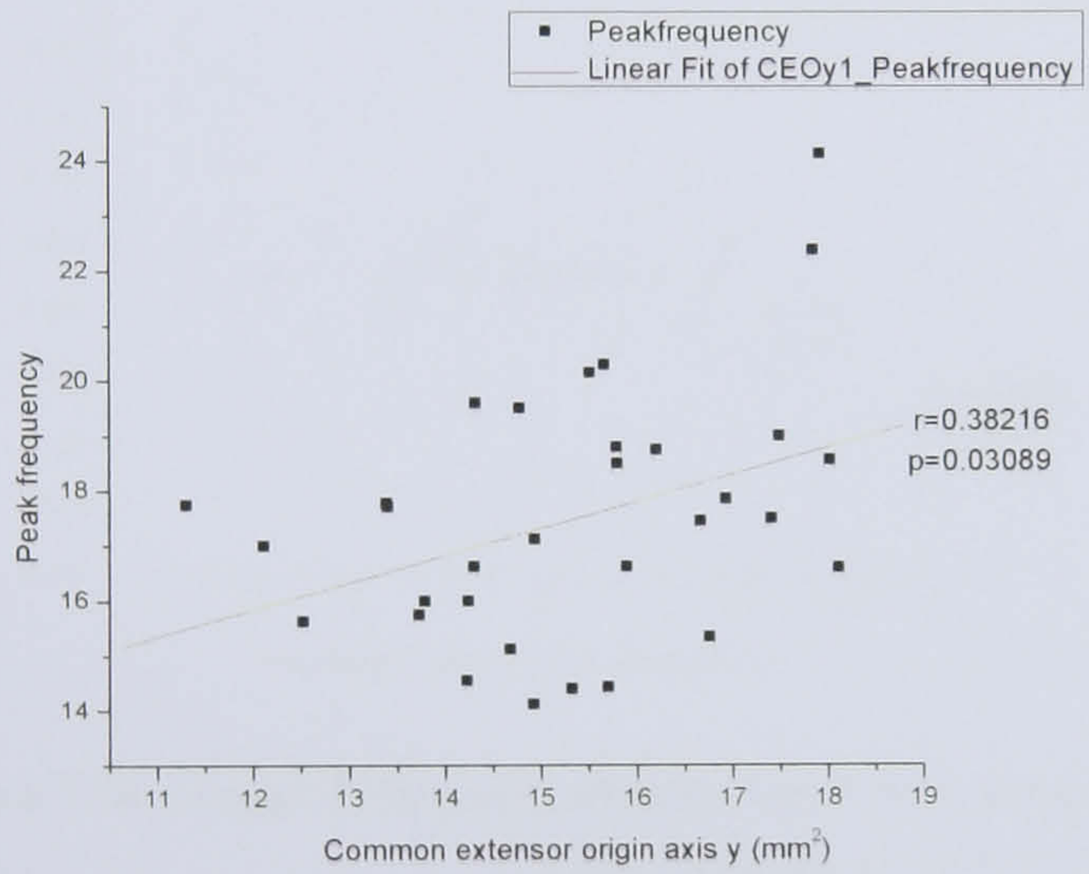


Figure 7.14 Linear fit for peak number over length of common extensor origin axis y (mm^2).

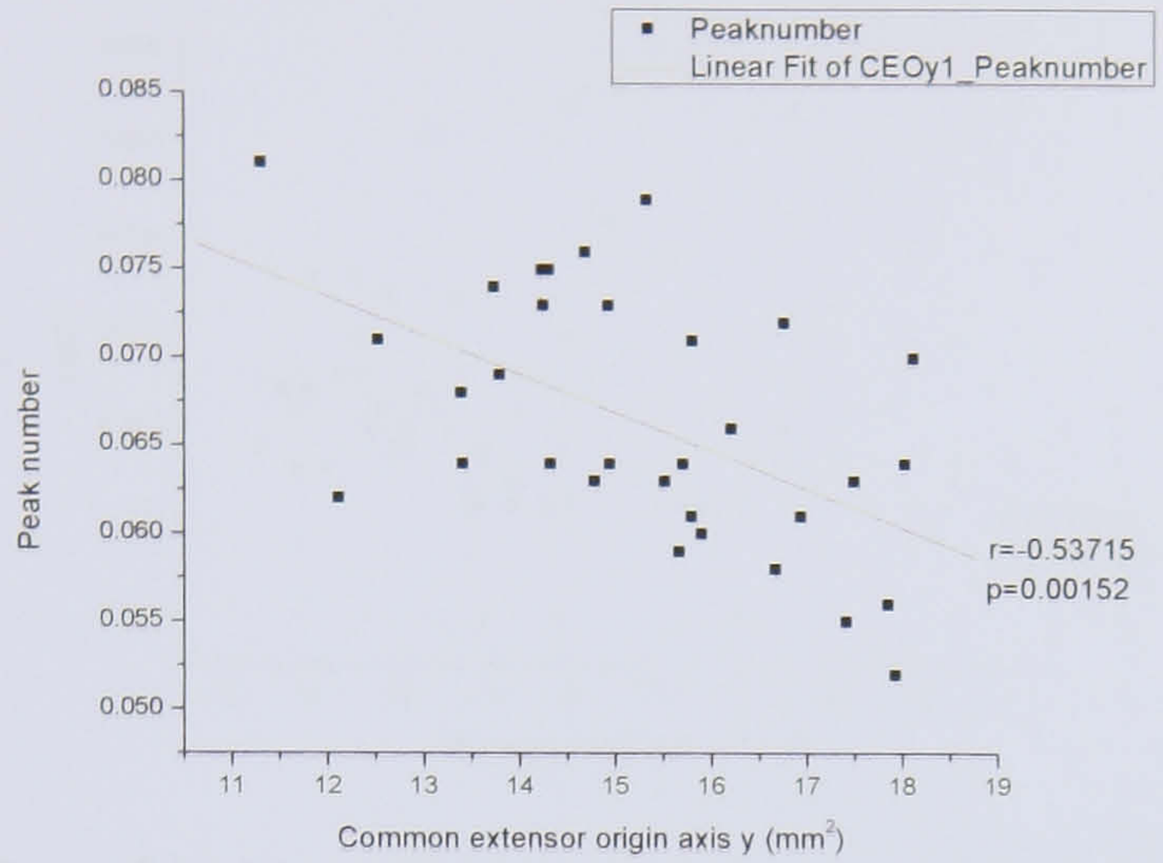


Figure 7.15 Linear fit for HSC over length of common extensor origin axis y (mm^2).

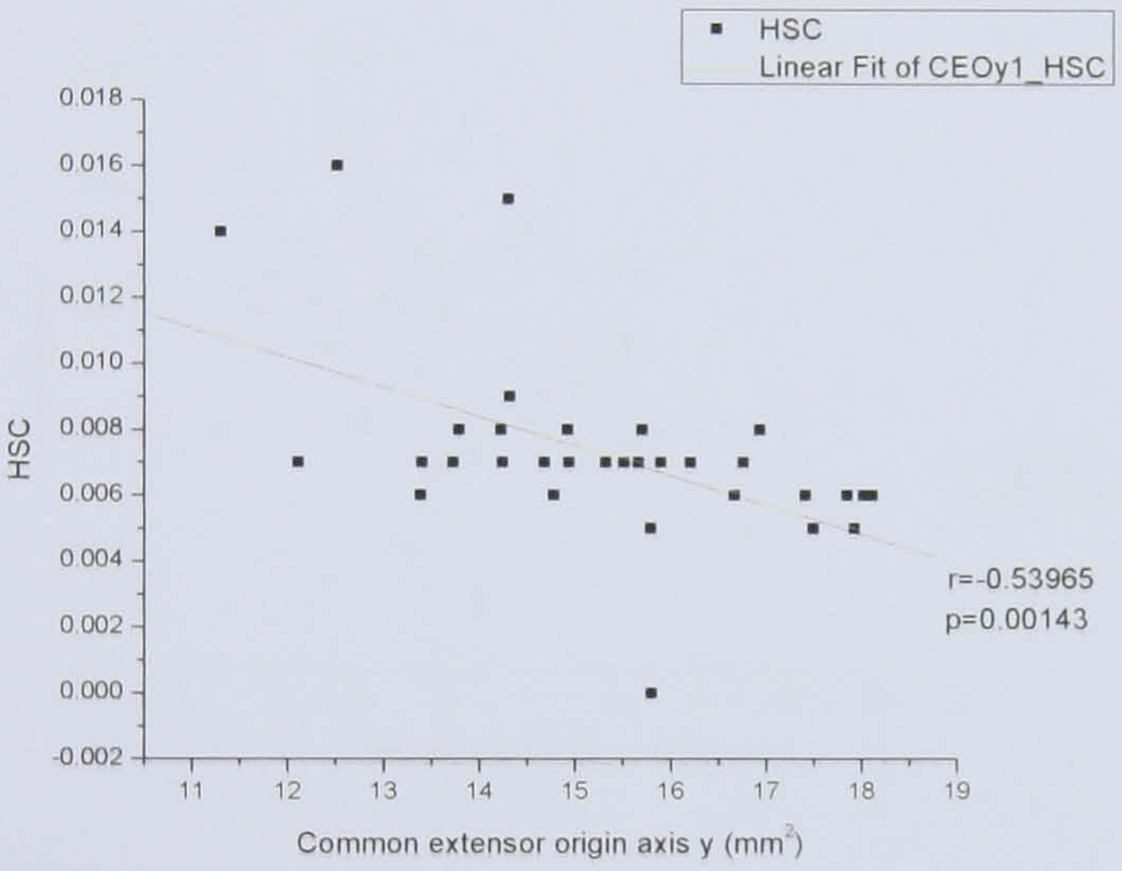


Figure 7.16 Linear fit for area displacement over length of *Biceps brachii* axis x (mm^2).

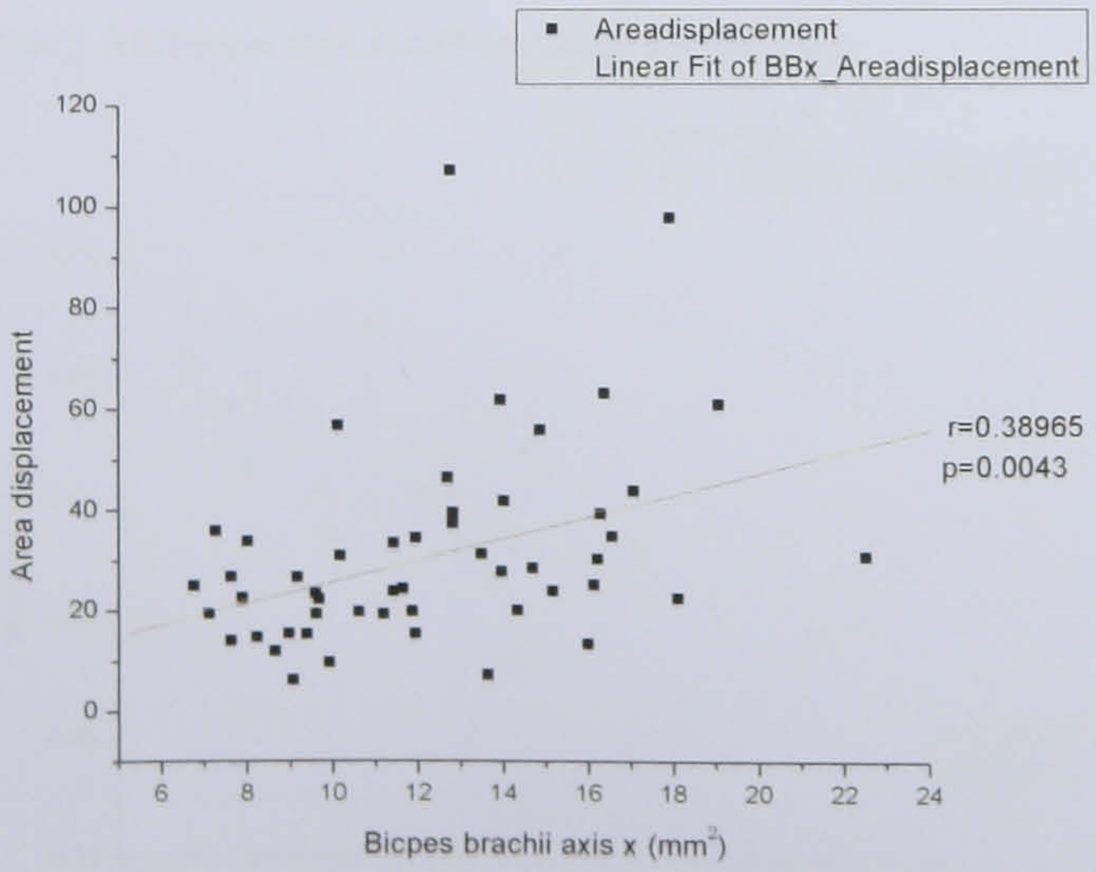


Figure 7.17 Linear fit for HSC over length of *Biceps brachii* axis x (mm^2).

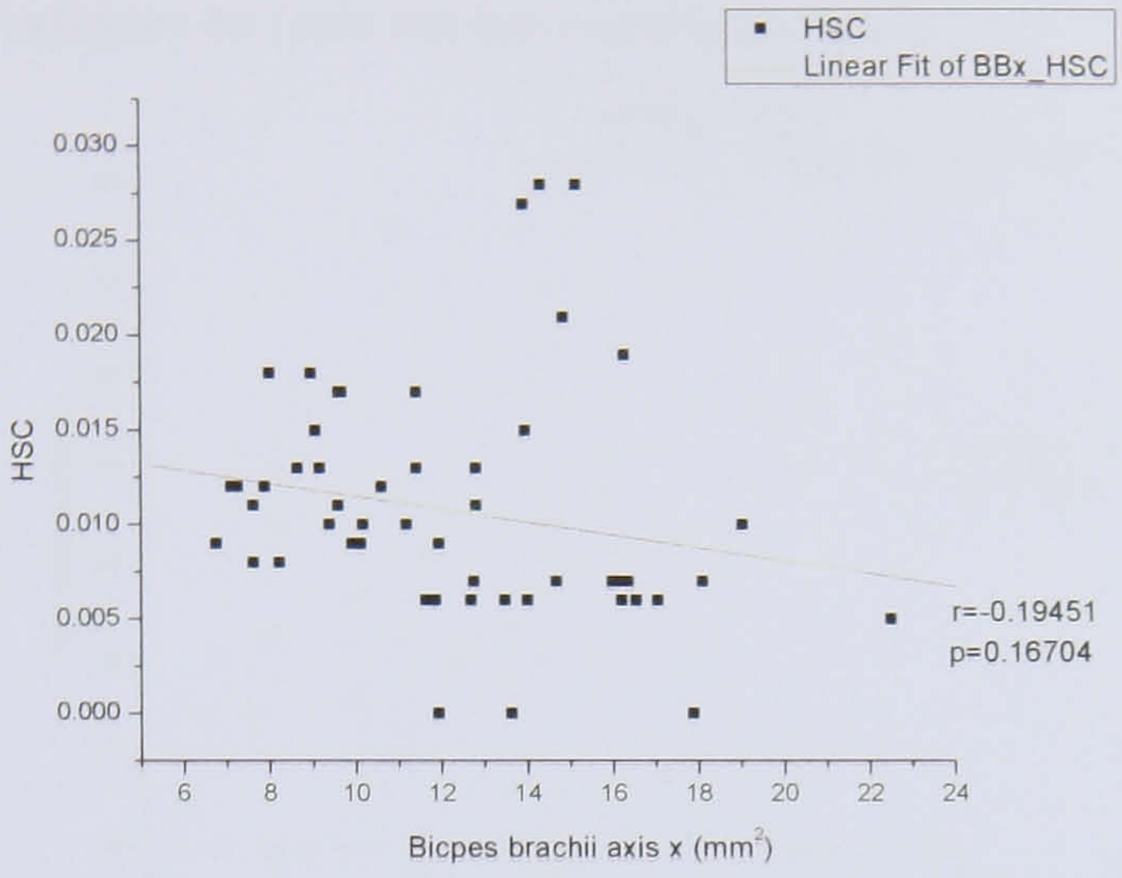


Figure 7.18 Linear fit for peak number over length of *Biceps brachii* axis x (mm^2).

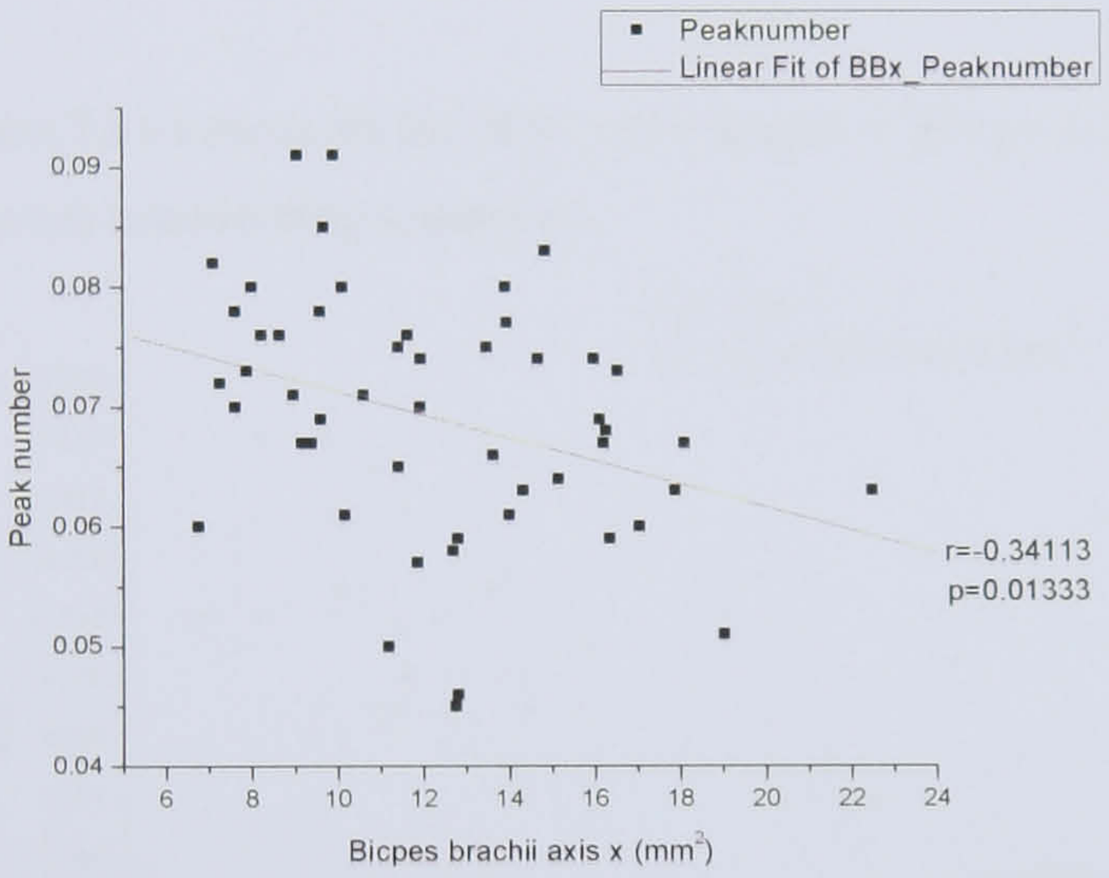


Figure 7.19 Linear fit for peak number over length of *Biceps brachii* axis x (mm^2) for category 1a (axis not intersecting anomaly).

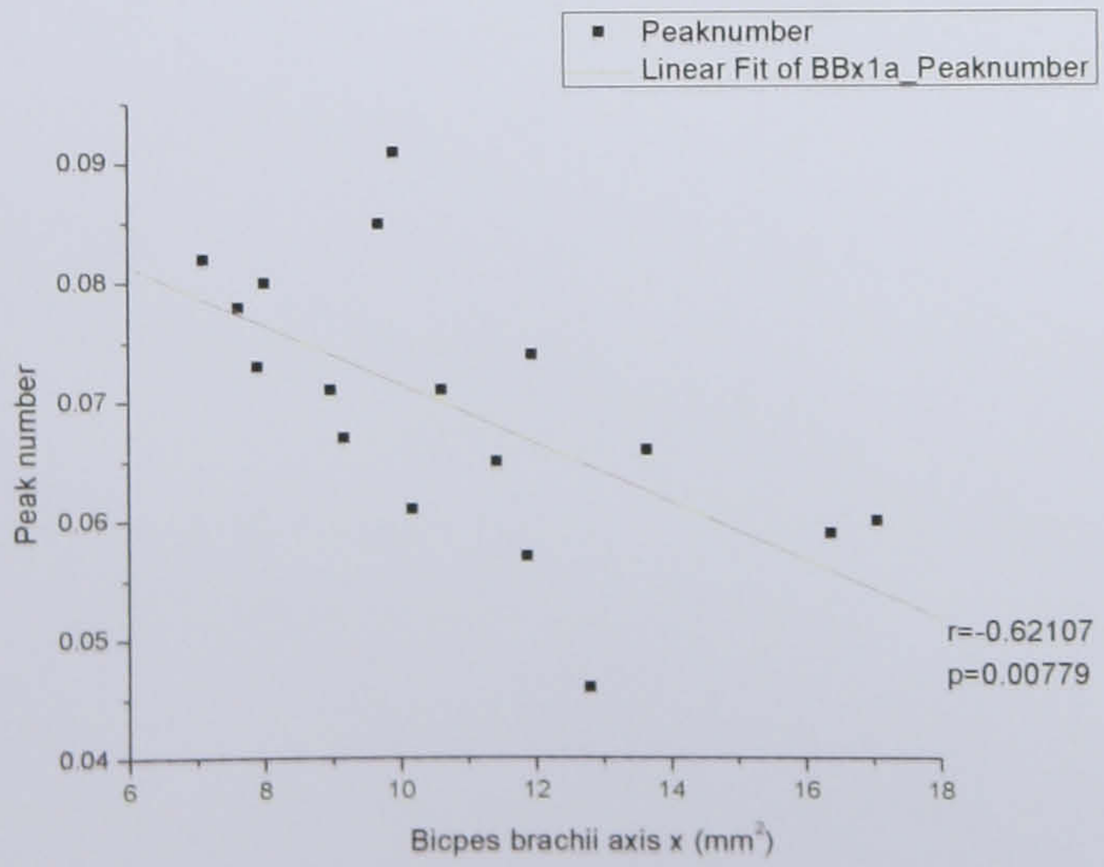


Figure 7.20 Linear fit for area displacement over length of *Biceps brachii* axis x (mm^2) for category 1a (axis not intersecting anomaly).

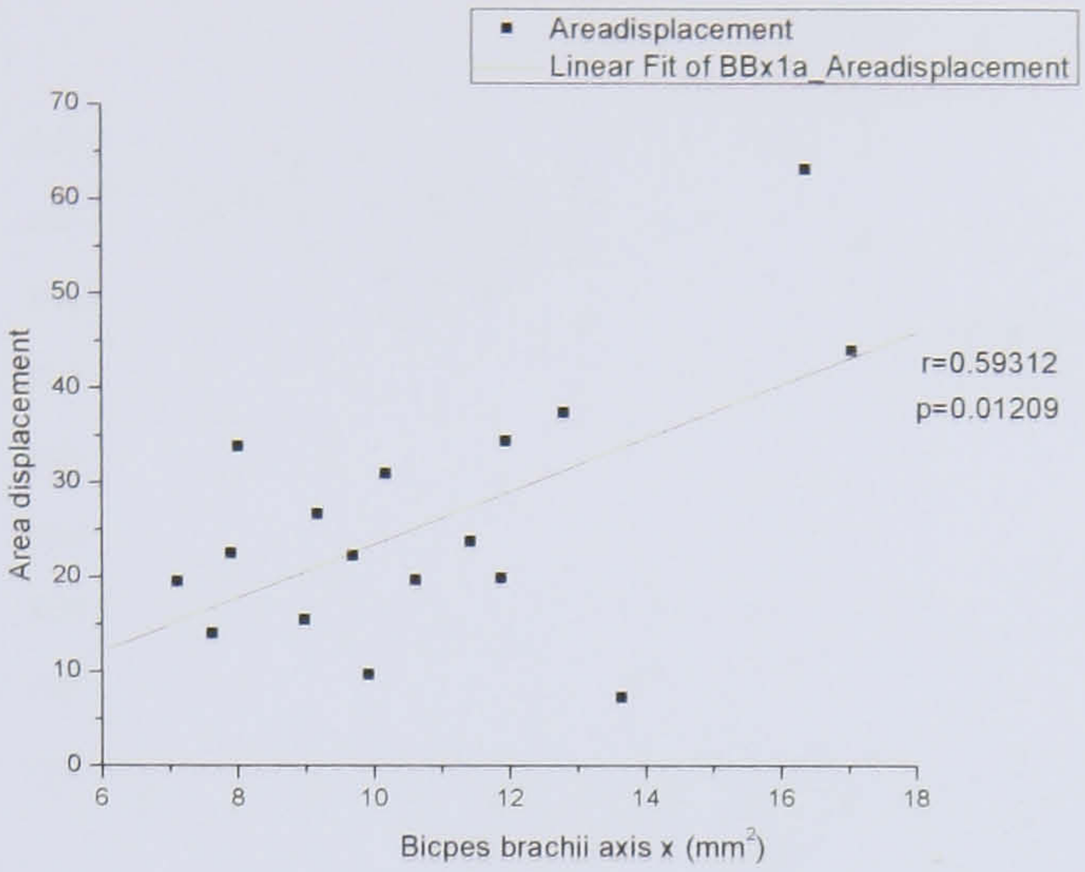


Figure 7.21 Linear fit for HSC over length of *Biceps brachii* axis x (mm^2) for category 1a (axis not intersecting anomaly).

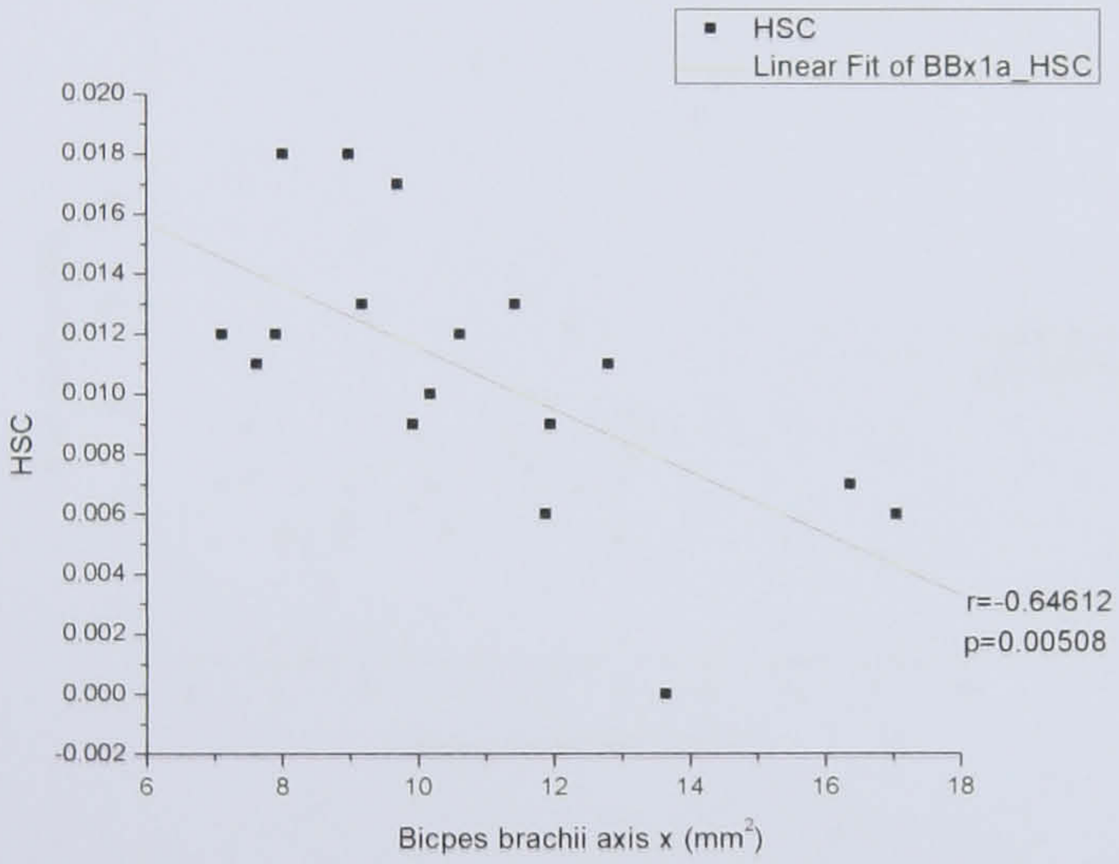


Figure 7.22 Linear fit for mean slope over length of *Biceps brachii* axis x (mm^2) for category 4 (axis intersecting anomaly).

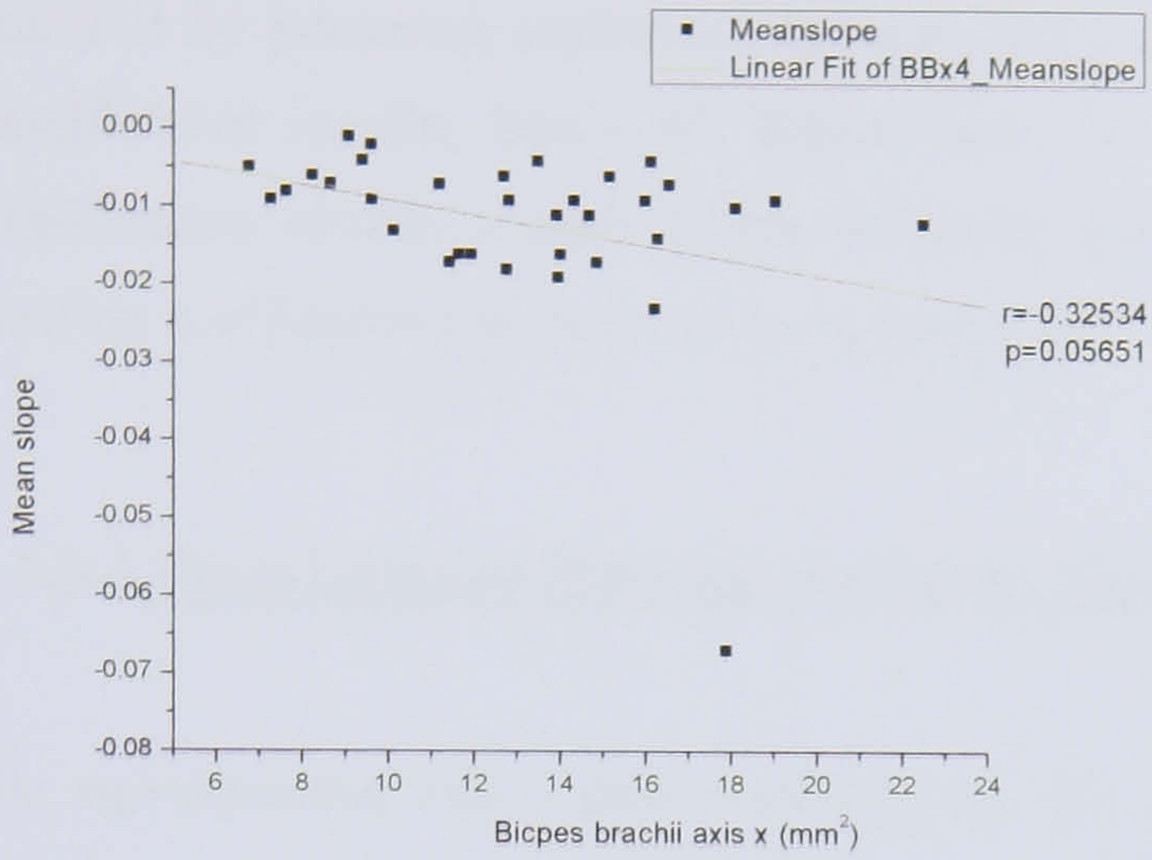
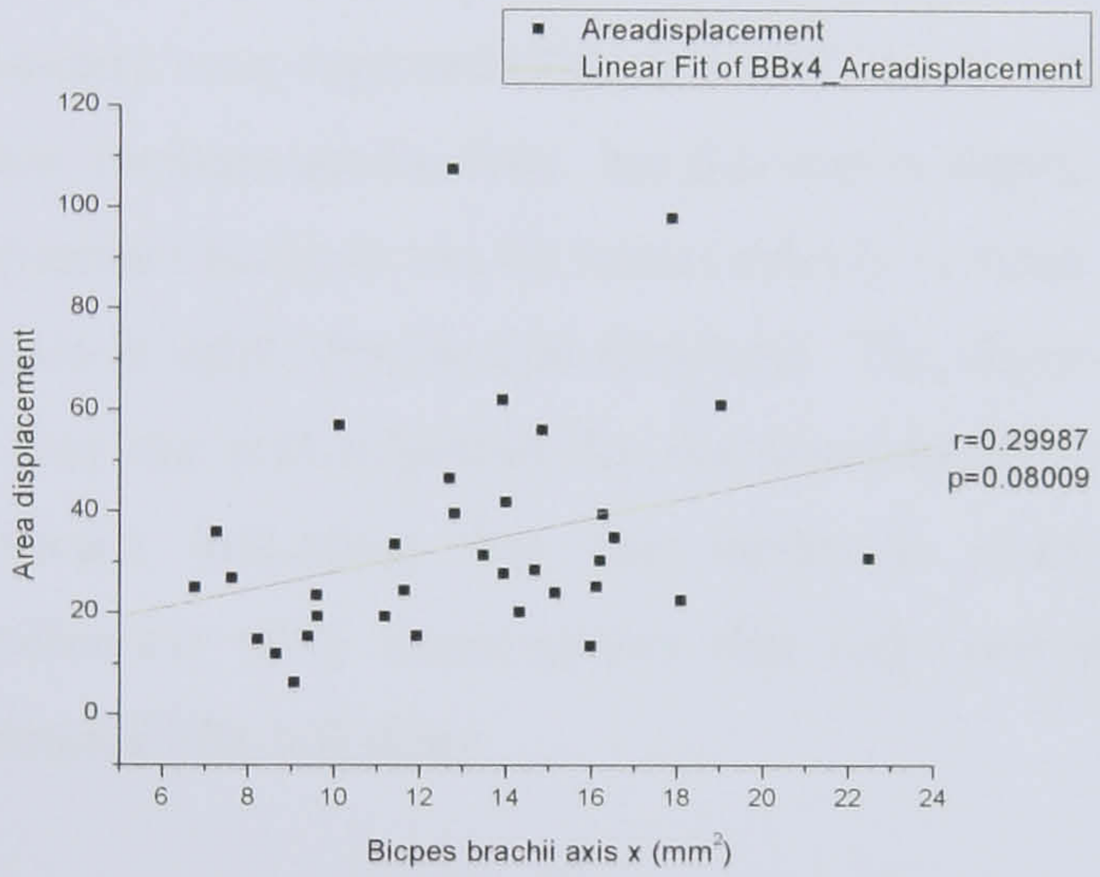


Figure 7.23 Linear fit for area displacement over length of *Biceps brachii* axis x (mm^2) for category 4 (axis intersecting anomaly).



7.4.3 Roughness parameters' use in distinguishing normal and abnormal entheses

This section and sub-sections present the discriminant function analysis data. This was performed to determine whether the roughness parameters were appropriate for the task of classifying entheses according to the presence of enthesopathies or bone-forming conditions. The tests performed and the reasoning behind the category designations were described in Chapter 6. If discriminant function analysis demonstrates that the roughness parameters can be used to differentiate between these categories, then it demonstrates that further research using these parameters can

be undertaken. For a discussion of these results and in particular which of the roughness parameters were best at describing entheses, see Chapter 8. Each enthesis axis will be presented separately. In each sub-section tables will present the best classification results, Box`s M, Eigenvalues, Wilks` lamda and a table of the classification results. Further tables, including standardised canonical discriminant function coefficients can be found in Appendix III.

7.4.3.1 Discriminant function analysis: *Supraspinatus* X

The *supraspinatus* axis x data were divided into three categories, as described in Chapter 6. Using just two roughness parameters 97.1 percent (33 of 34) were correctly classified. One hundred percent correct classification could be achieved, but required more than double the number of parameters, for this reason the data using just two parameters were explored (Tables 7.23-7.26). Box`s M was significant which violates the test for homoscedasticity, but this test is sensitive to a number of factors and the discriminant analysis can be robust even if violated. It is, therefore, assumed that the analysis is valid, despite this drawback. The eigenvalues for both functions indicate that they are both important for the discriminant function and the Wilks' lambda is significant indicating that the model is discriminating. Finally, the overall classification table demonstrates that only one enthesis is incorrectly classified (skeleton F120, left side).

Table 7.23 *Supraspinatus* dimension x. 3 categories (1 = normal, 2 = abnormal, 3 = "bone former").

Variables	Box's M p-value	Correctly assigned (%)	Comment
Relative length and area displacement	p = 0.000	97.10%	
Rq, Ra, relative length, area displacement, and Rq of FFT	p = 0.000	100%	

Table 7.24 *Supraspinatus* axis x discriminant function analysis results using roughness parameters: relative length and area displacement.

Eigenvalues

Function	Eigenvalue	% of Variance	Cumulative %	Canonical Correlation
1	5629.371[a]	100.0	100.0	1.000
2	1.652[a]	.0	100.0	.789

a. First 2 canonical discriminant functions were used in the analysis.

Table 7.25 *Supraspinatus* axis x discriminant function analysis results using roughness parameters: relative length and area displacement.

Wilks' Lambda

Test of Function(s)	Wilks' Lambda	Chi-square	df	Sig.
1 through 2	.000	293.137	4	.000
2	.377	29.741	1	.000

Table 7.26 *Supraspinatus* axis x discriminant function analysis results using roughness parameters: relative length and area displacement. Classification Results (a).

		Status 3tier	Predicted Group Membership			Total
			1	2	3	
Original	Count	1	21	0	1	22
		2	0	9	0	9
		3	0	0	3	3
	%	1	95.5	.0	4.5	100.0
		2	.0	100.0	.0	100.0
		3	.0	.0	100.0	100.0

(a) 97.1% of original grouped cases correctly classified.

To determine if the roughness parameters could distinguish between entheses in which the profile gauge intersected an anomaly (category 4) and in which it did not (category 1a), the data were divided into two categories. However, only six out of 28 entheses could be included in category 4 and only 66.7 percent (four out of six) of these were correctly classified. Nevertheless, this demonstrated that area displacement alone was a good parameter for discriminating between these categories. as can be

seen from the significance of Box` M and Wilks' lambda (Tables 7.27-7.30). The sample sizes were too small to subdivide the data into five categories (Chapter 6).

Table 7.27 *Supraspinatus* dimension x. 2-categories (1=anomaly not present or not intersected by profile gauge, 4=anomaly present and intersected by profile gauge).

Variables	Box's M p-value	Correctly assigned (%)	Comment
Area displacement	0.779	85.30%	Only 66.7% (4/6) of category 4 correctly classified
All	Sample size too small	88.20%	Only 66.7% (4/6) of category 4 correctly classified

Table 7.28 *Supraspinatus* axis x 2 category discriminant function analysis. Roughness parameter used: Area displacement.

Eigenvalues

Function	Eigenvalue	% of Variance	Cumulative %	Canonical Correlation
1	.608[a]	100.0	100.0	.615

a. First 1 canonical discriminant functions were used in the analysis.

Table 7.29 *Supraspinatus* axis x 2 category discriminant function analysis. Roughness parameter used: Area displacement.

Wilks' Lambda

Test of Function(s)	Wilks' Lambda	Chi-square	df	Sig.
1	.622	14.960	1	.000

Table 7.30 *Supraspinatus* axis x 2 category discriminant function analysis. Roughness parameter used: Area displacement.

Classification Results[a]

		Status 2tier (1=norm; 4=intersect)	Predicted Group Membership		Total
			1	4	
Original	Count	1	25	3	28
		4	2	4	6
	%	1	89.3	10.7	100.0
		4	33.3	66.7	100.0

a. 85.3% of original grouped cases correctly classified.

7.4.3.2 Discriminant function analysis: *Supraspinatus* Y

The *Supraspinatus* axis y data were divided into three categories, as described in Chapter 6. Using just two roughness parameters 75 percent were correctly classified, but category 2 were very poorly classified with only two out of eight correct. The addition of three further parameters (Rq, mean slope and area displacement) increased the correct classification by one enthesis, to three out of eight. However, Wilks' lambda indicated that the model was not discriminating. It was decided that the bone formers may have skewed the results and the process was repeated using categories 1 (normal) and 2 (abnormal). Using a combination of the roughness parameters (Tables 7.31-7.39) 93.5 percent of entheses included were correctly assigned and Wilks' lambda indicated that the model was discriminating.

Table 7.31 *Supraspinatus* dimension y 3 categories.

Variables	Box' M p-value	Correctly assigned (%)	Comment
HSC, Ra	0.188	75%	91.3% of category 1 correctly assigned, 25% of category 2 correctly assigned, and 80.0% of category 3 correctly assigned
HSC, Ra, Rq, Mean slope, and Area displacement	0	77.80%	91.3% of category 1 correctly assigned, 37.5% of category 2 correctly assigned, and 80% of category 3 correctly assigned

Table 7.32 *Supraspinatus* dimension y 3 category. Eigenvalues. HSC, Ra, Rq, mean slope and area displacement.

Eigenvalues

Function	Eigenvalue	% of Variance	Cumulative %	Canonical Correlation
1	.506[a]	80.2	80.2	.580
2	.125[a]	19.8	100.0	.333

a. First 2 canonical discriminant functions were used in the analysis.

Table 7.33 *Supraspinatus* dimension y 3 category. Wilks' Lambda. HSC, Ra, Rq, mean slope and area displacement.

Wilks' Lambda

Test of Function(s)	Wilks' Lambda	Chi-square	df	Sig.
1 through 2	.590	16.344	10	.090
2	.889	3.652	4	.455

Figure 7.34 *Supraspinatus* dimension y 3 category. Canonical discriminant functions. HSC, Ra, Rq, mean slope and area displacement.

Standardized Canonical Discriminant Function Coefficients

	Function	
	1	2
HSC	1.004	-.405
Ra	.579	-.116
Rq	.056	1.386
Mean slope	-.188	.740
Area displacement	-.015	-1.002

Figure 7.35 *Supraspinatus* dimension y 3 category. Classification result. HSC, Ra, Rq, Mean slope and Area displacement.

Classification Results[a]

			Predicted Group Membership			
		Status 3 tier	1	2	3	Total
Original	Count	1	21	1	1	23
		2	5	3	0	8
		3	1	0	4	5
	%	1	91.3	4.3	4.3	100.0
		2	62.5	37.5	.0	100.0
		3	20.0	.0	80.0	100.0

a. 77.8% of original grouped cases correctly classified.

Table 7.36 *Supraspinatus* axis y. Normal (category 1) and abnormal (category 2), bone formers excluded.

Variables	Box' M p-value	Correctly assigned (%)	Comment
Rq, skewness, Ra, kurtosis, peak frequency and mean displacement	0.565	93.5%	

Table 7.37 *Supraspinatus* axis y. Normal (category 1) and abnormal (category 2), bone formers excluded. Discriminant function analysis using: Rq, skewness, Ra, kurtosis, peak frequency and mean displacement.

Eigenvalues

Function	Eigenvalue	% of Variance	Cumulative %	Canonical Correlation
1	.868(a)	100.0	100.0	.682

(a) First 1 canonical discriminant functions were used in the analysis.

Table 7.38 *Supraspinatus* axis y. Normal (category 1) and abnormal (category 2), bone formers excluded. Discriminant function analysis using: Rq, skewness, Ra, kurtosis, peak frequency, and mean displacement.

Wilks' Lambda				
Test of Function(s)	**Wilks' Lambda**	**Chi-square**	**df**	**Sig.**
1	.535	16.246	6	.012

Table 7.39 *Supraspinatus* axis y. Normal (category 1) and abnormal (category 2), bone formers excluded. Discriminant function analysis using: Rq, skewness, Ra, kurtosis, peak frequency, and mean displacement.

Classification Results (a)					
		Status 3 tier	**Predicted Group Membership**		**Total**
			1	**2**	
Original	**Count**	**1**	22	1	23
		2	1	7	8
	%	**1**	95.7	4.3	100.0
		2	12.5	87.5	100.0

(a) 93.5% of original grouped cases correctly classified.

To determine if the roughness parameters could distinguish between entheses in categories 1a and 4, the same tests were conducted. Despite an overall high percentage of correctly assigned cases, only 33.3% (3 out of 9) were correctly classified (Tables 7.40 and 7.44). Neither this nor the eigenvalues (Table 7.41) nor Wilks' lambda (Table 7.42), indicated that this was a successful method for classification and this will be discussed in Chapter 8 (Table 7.43 presents the structure matrix). Subdivision into five categories could not be performed because of small sample sizes.

Table 7.40 *Supraspinatus* dimension y 2-categories.

Variables	Box' M p-value	Correctly assigned (%)	Comment
Rq of FFT	0.478	75.0%	96.3% of category 1 correctly assigned, but only 11.1% of category 4 correctly assigned.
Rq of FFT, Relative length, Peak frequency	0.179	80.6%	96.3% of category 1 correctly assigned, but only 33.3% of category 4 correctly assigned.

Table 7.41 *Supraspinatus* dimension y 2-categories. Eigenvalues. Rq of FFT, relative length, and peak frequency.

Eigenvalues

Function	Eigenvalue	% of Variance	Cumulative %	Canonical Correlation
1	.172(a)	100.0	100.0	.383

(a) First 1 canonical discriminant functions were used in the analysis.

Table 7.42 *Supraspinatus* dimension y 2 category. Wilks' lambda. Rq of FFT, relative length, and peak frequency.

Wilks' Lambda

Test of Function(s)	Wilks' Lambda	Chi-square	df	Sig.
1	.853	5.157	3	.161

Figure 7.43 *Supraspinatus* dimension y 2 category. Structure matrix. Rq of FFT, relative length, and peak frequency.

Structure Matrix

	Function
	1
Rq of FFT	.905
Relative length	.901
Peak frequency	.184

Pooled within-groups correlations between discriminating variables and standardized canonical discriminant functions
Variables ordered by absolute size of correlation within function.

Figure 7.44 *Supraspinatus* dimension y 2 category. Classification results using Rq of FFT, relative length, and peak frequency.

Classification Results[a]

			Predicted Group Membership		
		Status 2tier	1	4	Total
Original	Count	1	26	1	27
		4	6	3	9
	%	1	96.3	3.7	100.0
		4	66.7	33.3	100.0

a. 80.6% of original grouped cases correctly classified.

7.4.3.3 Discriminant function analysis: Common extensor origin x

The same approach was used for the common extensor origin axis x. However, there were a greater number of entheses present in all categories making it possible to use subdivisions not possible for the *supraspinatus* insertion. Initially, division into three categories was performed, as described in Chapter 6, and discriminant function analysis was performed using different combinations of variables. Overall classification was poor (Table 7.45), but eigenvalues (Table 7.46) and Wilks' lambda (Table 7.47) indicated that the first function of the model has statistically significant discriminating power. This can be seen in Figure 7.24 and in the classification results (Table 7.48) as good classification for categories 1 and 2, with only the third being poorly classified. Removal of the final category (the bone formers) led to an improved overall classification, with an increase to 82.9 percent, but the canonical correlation of the eigenvalue indicates that the relation between the categories and the function is not strong, whilst Wilks' lambda is significant (at $\alpha = 0.05$), indicating that the model is discriminating. The classification results indicate that both categories were well classified using these parameters (Tables 7.49-7.52).

Table 7.45 Common extensor origin 3 category (1 = normal, 2 = abnormal and 3 = bone former) classification results.

Variables	Box' M p-value	Correctly assigned (%)	Comment
Relative length	p=0.313	50.00%	
Relative length, area displacement and mean displacement	p=0.000	70.80%	53.8% of category 3 correctly assigned (7 cases), rest of these assigned as category 2 (6 cases).
Relative length, area displacement, mean displacement and Ra	p=0.002	72.90%	No improvement for category 3 from above
Relative length, area displacement, mean displacement, Ra and mean slope	p=0.022	75.00%	No improvement for category 3 from above

Table 7.46 Common extensor origin axis x. 3 categories. Eigenvalues for discriminant function analysis using Relative length, area displacement, mean displacement, Ra, and mean slope.

Eigenvalues

Function	Eigenvalue	% of Variance	Cumulative %	Canonical Correlation
1	.669(a)	92.9	92.9	.633
2	.051(a)	7.1	100.0	.220

(a) First 2 canonical discriminant functions were used in the analysis.

Table 7.47 Common extensor origin axis x. 3 categories. Wilks' lambda for discriminant function analysis using Relative length, area displacement, mean displacement, Ra, and mean slope.

Wilks' Lambda

Test of Function(s)	Wilks' Lambda	Chi-square	df	Sig.
1 through 2	.570	24.171	10	.007
2	.951	2.138	4	.710

Figure 7.24 Common extensor origin axis x. 3 categories. Canonical discriminant functions using Relative length, area displacement, mean displacement, Ra, and mean slope.

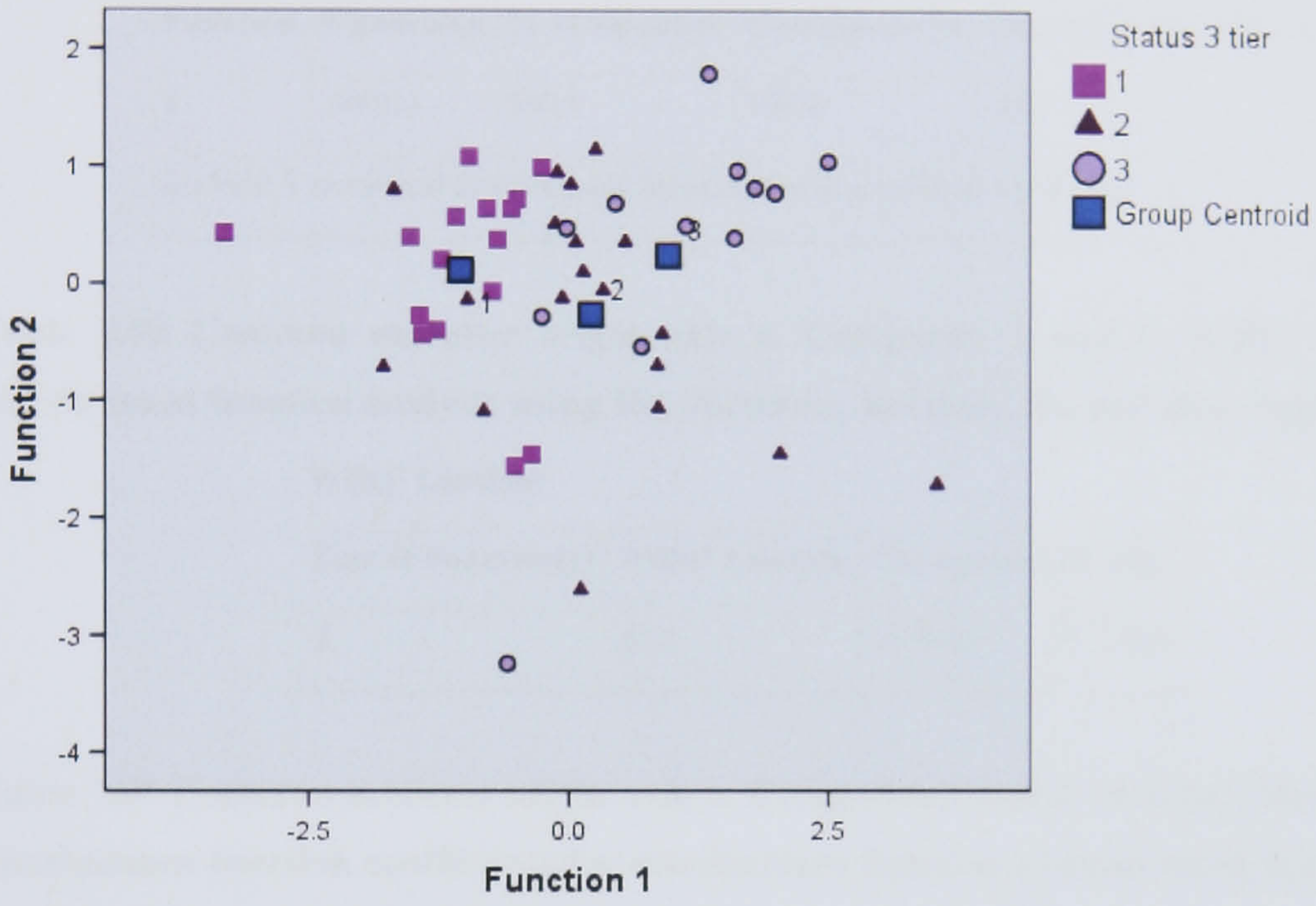


Table 7.48 Common extensor origin axis x. 3 categories. Canonical discriminant functions classification results using Relative length, area displacement, mean displacement, Ra, and mean slope.

Classification Results (a)						
		Status 3 category	Predicted Group Membership			Total
			1	2	3	
Original	Count	1	14	2	0	16
		2	3	15	1	19
		3	0	6	7	13
	%	1	87.5	12.5	.0	100.0
		2	15.8	78.9	5.3	100.0
		3	.0	46.2	53.8	100.0
(a) 75.0% of original grouped cases correctly classified.						

Table 7.49 Common extensor origin axis x. Categories 1 and 2 (category 3 is removed). Eigenvalues for discriminant function analysis using Rq, skewness, kurtosis, Ra, and area displacement.

Eigenvalues

Function	Eigenvalue	% of Variance	Cumulative %	Canonical Correlation
1	.480(a)	100.0	100.0	.570

(a) First 1 canonical discriminant functions were used in the analysis.

Table 7.50 Common extensor origin axis x. Categories 1 and 2. Wilks' lamda for discriminant function analysis using Rq, skewness, kurtosis, Ra, and area displacement.

Wilks' Lambda

Test of Function(s)	Wilks' Lambda	Chi-square	df	Sig.
1	.676	11.964	5	.035

Table 7.51 Common extensor origin axis x. Categories 1 and 2. Standardised canonical discriminant function coefficients for discriminant function analysis using Rq, skewness, kurtosis, Ra, and area displacement.

Standardized Canonical Discriminant Function Coefficients

	Function
	1
Rq	-.090
Skewness	1.646
Kurtosis	2.029
Ra	1.479
Area displacement	-1.151

Table 7.52 Common extensor origin axis x. Categories 1 and 2. Classification results for discriminant function analysis using Rq, skewness, kurtosis, Ra, and area displacement.

Classification Results (a)

		Status 3 category	Predicted Group Membership		Total
			1	2	
Original	Count	1	15	1	16
		2	5	14	19
	%	1	93.8	6.3	100.0
		2	26.3	73.7	100.0

(a) 82.9% of original grouped cases correctly classified.

Just two roughness parameters (relative length and mean displacement) were required to correctly assign categories 1a and 4 in 79.2 percent of cases. The canonical correlation of the eigenvalues and Wilks' lamda indicate the strength of the model. There is no link between misclassification and status as a bone former (as can be seen in Table 7.53-7.56, Appendix III).

Table 7.53 2 category classification results.

Variables	Box's p-value	Correctly assigned (%)
Relative length and mean displacement	p=0.025	79.20%

Table 7.54 Common extensor origin axis x. 2 categories. Eigenvalues for discriminant function analysis using Relative length and mean displacement.

Eigenvalues

Function	Eigenvalue	% of Variance	Cumulative %	Canonical Correlation
1	.566(a)	100.0	100.0	.601

(a) First 1 canonical discriminant functions were used in the analysis.

Table 7.55 Common extensor origin axis x. 2 categories. Wilks' lambda for discriminant function analysis using relative length and mean displacement.

Wilks' Lambda

Test of Function(s)	Wilks' Lambda	Chi-square	df	Sig.
1	.639	20.176	2	.000

Table 7.56 Classification Results (a). Common extensor origin axis x. 2 categories. Relative length and mean displacement.

		Status category 2	Predicted Group Membership		Total
			1	4	
Original	Count	1	16	4	20
		4	6	22	28
	%	1	80.0	20.0	100.0
		4	21.4	78.6	100.0

(a) 79.2% of original grouped cases correctly classified.

Finally, the entheses were subdivided into five categories (1 = normal; 21 = abnormal, but enthesopathy not intersected by the profile gauge; 22 = abnormal, with the enthesopathy intersected by the profile gauge; 31 = bone former with no enthesopathy or enthesopathy not intersected by the profile gauge; and 33 = bone former with enthesopathy intersected by the profile gauge). Although the overall classification may appear poor, the Wilks' lamda indicates that the model is discriminating. Further study of the classification results reveals that all entheses are correctly classified in over 60 percent of cases. However, it should be noted that the sample sizes of categories 21 and 31 are small and caution should be exercised in interpreting these results (Tables 7.57-5.60).

Table 7.57 Common extensor origin axis x 5 category classification results.

Variables	**Box' M p-value**	**Correctly assigned (%)**	**Comment**
Relative length and area displacement	p=0.28	62.50%	100% of category 21 classified as category 1
All	p=0.000	68.80%	

Table 7.58 Common extensor origin axis x. 5 categories. Eigenvalues for discriminant function analysis using all roughness parameters.

Eigenvalues				
Function	**Eigenvalue**	**% of Variance**	**Cumulative %**	**Canonical Correlation**
1	1.116(a)	49.9	49.9	.726
2	.817(a)	36.6	86.5	.670
3	.218(a)	9.8	96.3	.423
4	.083(a)	3.7	100.0	.278
(a) First 4 canonical discriminant functions were used in the analysis.				

Table 7.59 Common extensor origin axis x. 5 categories. Wilks' lambda for discriminant function analysis using all roughness parameters.

Wilks' Lambda				
Test of Function(s)	**Wilks' Lambda**	**Chi-square**	**df**	**Sig.**
1 through 4	.197	64.140	40	.009
2 through 4	.417	34.542	27	.151
3 through 4	.758	10.962	16	.812
4	.923	3.166	7	.869

Table 7.60 Common extensor origin axis x. 5 categories. Classification results for discriminant function analysis using all roughness parameters.

Classification Results (a)

		Status 5 category	Predicted Group Membership					Total
			1	21	22	31	33	
Original	Count	1	13	0	3	0	0	16
		21	0	1	0	0	0	1
		22	5	0	11	0	2	18
		31	0	0	1	2	0	3
		33	2	0	2	0	6	10
	%	1	81.3	.0	18.8	.0	.0	100.0
		21	.0	100.0	.0	.0	.0	100.0
		22	27.8	.0	61.1	.0	11.1	100.0
		31	.0	.0	33.3	66.7	.0	100.0
		33	20.0	.0	20.0	.0	60.0	100.0

(a) 68.8% of original grouped cases correctly classified.

7.4.3.4 Discriminant function analysis: Common extensor origin y

Discriminant function analysis was performed on common extensor origin axis y in the same manner as for the other entheses. Overall, three tier classification appeared to fit reasonably well (Tables 7.61-7.63) and Wilks' lambda indicated that the first function provides a discriminating model. However, there is considerable overlap in the cases, as visually demonstrated in Figure 7.25 and the classification results in Table 7.64 indicate that this model is poor at discriminating the normal entheses.

Table 7.61 Common extensor origin axis y. 3 category classification results.

Variables	Box' M p-value	Correctly assigned (%)	Comment
All	p=0.000	66.00%	66.7% of category 1, 75.0% of category 2, and 53.3% of category 3
Rq of FFT, mean slope, peak number, and area displacement	p=0.013	68.00%	Overall better classification, but category 1 is only 60.0% correctly classified

Table 7.62 Common extensor origin axis y. 3 categories. Eigenvalues for discriminant function analysis using: Rq of FFT, mean slope, peak number, and area displacement.

Eigenvalues

Function	Eigenvalue	% of Variance	Cumulative %	Canonical Correlation
1	.499(a)	80.4	80.4	.577
2	.121(a)	19.6	100.0	.329

(a) First 2 canonical discriminant functions were used in the analysis.

Table 7.63 Common extensor origin axis y. 3 categories. Wilks' lambda for discriminant function analysis using: Rq of FFT, mean slope, peak number, and area displacement.

Wilks' Lambda

Test of Function(s)	Wilks' Lambda	Chi-square	df	Sig.
1 through 2	.595	23.640	8	.003
2	.892	5.214	3	.157

Figure 7.25 Common extensor origin axis y. 3 categories. Canonical discriminant functions using: Rq of FFT, mean slope, peak number, and area displacement.

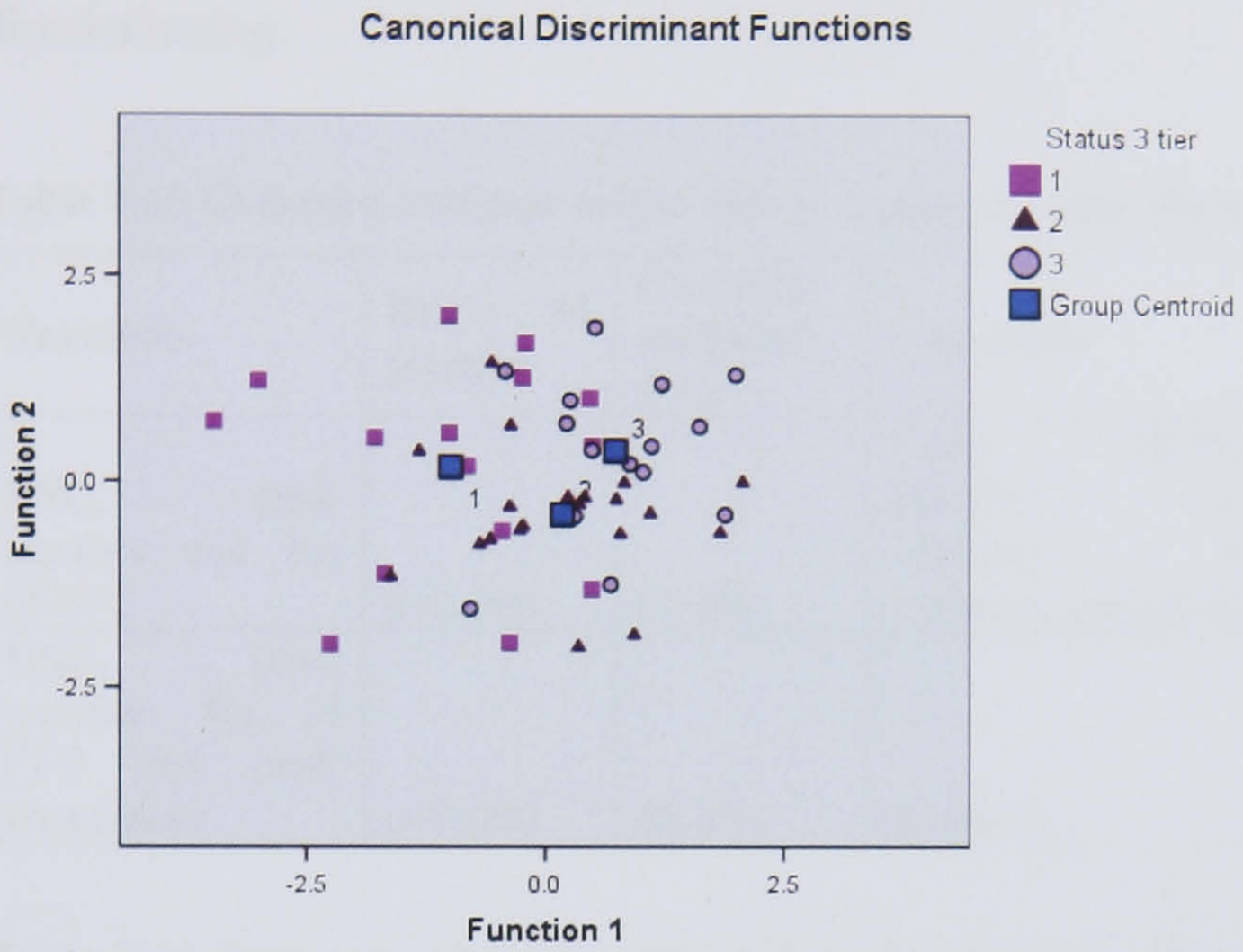


Table 7.64 Common extensor origin axis y 3 categories. Classification results for discriminant function analysis using: Rq of FFT, mean slope, peak number, and area displacement.

Classification Results (a)						
		Status 3 category	Predicted Group Membership			Total
			1	2	3	
Original	Count	1	9	3	3	15
		2	4	14	2	20
		3	1	3	11	15
	%	1	60.0	20.0	20.0	100.0
		2	20.0	70.0	10.0	100.0
		3	6.7	20.0	73.3	100.0
(a) 68.0% of original grouped cases correctly classified.						

When divided into two categories the overall classification results are good using only four roughness parameters, but category four is poorly classified (Tables 7.65-7.68). The Box's M indicates internal covariation, which is not surprising given that some of

the roughness parameters measure similar features of the enthesis. The canonical correlation of the eigenvalues does not indicate that there is a strong relation between the categories and the function, but Wilks' lamda indicates that the model is discriminating.

Table 7.65 Common extensor origin axis y. 2 category classification results.

Variables	Box's M p-value	Correctly assigned (%)	Comment
HSC, peak number and Rq of FFT	p=0.000	86.0%	Only 65.7% (11/17) of category 4 correctly classified
HSC, peak number, Rq of FFT and peak frequency	p=0.000	88.0%	as above

Table 7.66 Common extensor origin axis y. 2 categories. Eigenvalues for discriminant function analysis using: HSC, peak number, Rq of FFT, and peak frequency.

Eigenvalues

Function	Eigenvalue	% of Variance	Cumulative %	Canonical Correlation
1	.515(a)	100.0	100.0	.583

(a) First 1 canonical discriminant functions were used in the analysis.

Table 7.67 Common extensor origin axis y. 2 categories. Wilks' lambda for discriminant function analysis using: HSC, peak number, Rq of FFT, and peak frequency.

Wilks' Lambda

Test of Function(s)	Wilks' Lambda	Chi-square	df	Sig.
1	.660	19.116	4	.001

Table 7.68 Common extensor origin axis y. 2 categories. Classification results for discriminant function analysis using: HSC, peak number, Rq of FFT, and peak frequency.

Classification Results (a)					
		Status 2 category	Predicted Group Membership		Total
			1	4	
Original	Count	1	33	0	33
		4	6	11	17
	%	1	100.0	.0	100.0
		4	35.3	64.7	100.0
(a) 88.0% of original grouped cases correctly classified.					

Sample sizes for each category were fairly large even when divided into five categories (defined above). Overall classification results were poor and Box's M demonstrated that there was internal covariation (Tables 7.69-7.72). Wilks' lambda and the eigenvalues demonstrated that the model was of some success and the roughness parameters appear to be able to correctly classify entheses in the majority of these cases. This will be discussed further in Chapter 8.

Table 7.69 Common extensor origin axis y 5 categories: classifications.

Variables	Box' M p-value	Correctly assigned (%)	Comment
All	p=0.000	64.00%	50% (4/8) of category 33 and only 42.9% (3/7) of category 31 correctly classified
HSC, peak number, Rq of FFT, peak frequency, mean displacement and mean slope	p=0.008	62%	This improves classification of category 31 to 71.4% (5/7) correctly classified

Table 7.70 Common extensor origin axis y. 5 categories. Eigenvalues for discriminant function analysis using all roughness parameters.

Eigenvalues				
Function	**Eigenvalue**	**% of Variance**	**Cumulative %**	**Canonical Correlation**
1	1.127(a)	60.8	60.8	.728
2	.450(a)	24.3	85.1	.557
3	.192(a)	10.4	95.4	.402
4	.085(a)	4.6	100.0	.280
(a) First 4 canonical discriminant functions were used in the analysis.				

Table 7.71 Common extensor origin axis y. 5 categories. Wilks' lambda for discriminant function analysis using all roughness parameters.

Wilks' Lambda				
Test of Function(s)	**Wilks' Lambda**	**Chi-square**	**df**	**Sig.**
1 through 4	.251	57.418	40	.037
2 through 4	.533	26.105	27	.513
3 through 4	.773	10.679	16	.829
4	.922	3.380	7	.848

Table 7.72 Common extensor origin axis y. 5 categories. Classification results for discriminant function analysis using all roughness parameters.

Classification Results (a)

		Status 5 category	Predicted Group Membership					Total
			1	21	22	31	33	
Original	Count	1	12	2	0	1	0	15
		21	4	7	0	0	0	11
		22	1	1	6	0	1	9
		31	0	3	0	3	1	7
		33	2	1	1	0	4	8
	%	1	80.0	13.3	.0	6.7	.0	100.0
		21	36.4	63.6	.0	.0	.0	100.0
		22	11.1	11.1	66.7	.0	11.1	100.0
		31	.0	42.9	.0	42.9	14.3	100.0
		33	25.0	12.5	12.5	.0	50.0	100.0

(a) 64.0% of original grouped cases correctly classified.

7.4.3.5 Discriminant function analysis: *Biceps brachii* x

The *biceps brachii* insertion was studied, as described in Chapter 6. When divided into three categories, the roughness parameters were not ideal for discriminant function analysis. The percentage of correctly assigned in total (Table 7.73) and by category (Table 7.76) was poor. The canonical correlation of the eigenvalue indicated that neither function demonstrated a strong relation between category and function, whilst Wilks' lambda was statistically significant for the first function (Tables 7.74 and 7.75), indicating that the model was discriminating. However, it was decided that it was likely that a better performance could be achieved without the bone formers and so these were removed for the next analysis. This analysis proved more successful with higher overall classification results (Tables 7.77- 7.79) and an increased statistical significance of Wilks' lambda (Table 7.78).

Table 7.73 *Biceps brachii* axis x. 3 category discriminant function analysis results.

Variables	Box's M p-value	Correctly assigned (%)	Comment
Peak number, mean slope, peak frequency, relative length, and mean displacement.	0.092	66.00%	Only 58.3% (7/11) of category 1 and 33.3% (5/15) correctly classified, but 88.5% (23/26) of category 2 correctly classified
Peak number, mean slope, peak frequency, relative length, and HSC	0.092	66.00%	As above for category 1, but improved to 40.0% (6/15) for category 3

Table 7.74 *Biceps brachii* axis x discriminant function analysis using roughness parameters: Peak number, mean slope, peak frequency, relative length, and HSC.

Eigenvalues

Function	Eigenvalue	% of Variance	Cumulative %	Canonical Correlation
1	.365(a)	80.4	80.4	.517
2	.089(a)	19.6	100.0	.286

(a) First 2 canonical discriminant functions were used in the analysis.

Table 7.75 *Biceps brachii* axis x discriminant function analysis using roughness parameters: Peak number, mean slope, peak frequency, relative length, and HSC.

Wilks' Lambda

Test of Function(s)	Wilks' Lambda	Chi-square	df	Sig.
1 through 2	.673	19.016	10	.040
2	.918	4.087	4	.394

Table 7.76 *Biceps brachii* axis x discriminant function analysis using roughness parameters: Peak number, mean slope, peak frequency, relative length, and HSC.

Classification Results (a)

		Status 3-categories	Predicted Group Membership			Total
			1	2	3	
Original	Count	1	7	4	1	12
		2	1	22	3	26
		3	1	8	6	15
	%	1	58.3	33.3	8.3	100.0
		2	3.8	84.6	11.5	100.0
		3	6.7	53.3	40.0	100.0
(a) 66.0% of original grouped cases correctly classified.						

Table 7.77 *Biceps brachii* axis x. Categories 1 (normal only) and 2 (all abnormal). Results of discriminant function analysis using Rq, Ra, meanslope, HSC, mean displacement, area displacement, and Rq of FFT.

Eigenvalues

Function	Eigenvalue	% of Variance	Cumulative %	Canonical Correlation
1	.674(a)	100.0	100.0	.635
(a) First 1 canonical discriminant functions were used in the analysis.				

Table 7.78 *Biceps brachii* axis x. Categories 1 (normal only) and 2 (all abnormal). Results of discriminant function analysis using Rq, Ra, meanslope, HSC, mean displacement, area displacement and, Rq of FFT.

Wilks' Lambda

Test of Function(s)	Wilks' Lambda	Chi-square	df	Sig.
1	.597	16.237	7	.023

Table 7.79 *Biceps brachii* axis x. Categories 1 (normal only) and 2 (all abnormal). Results of discriminant function analysis using Rq, Ra, meanslope, HSC, mean displacement, area displacement, and Rq of FFT.

Classification Results (a)

		Status 3-categories	Predicted Group Membership		Total
			1	2	
Original	Count	1	7	4	11
		2	1	25	26
	%	1	63.6	36.4	100.0
		2	3.8	96.2	100.0

(a) 86.5% of original grouped cases correctly classified.

It was hypothesised that the best discrimination should be made between the categories 1a and 4, as discussed in Chapter 6. Overall classification results seemed positive (Table 7.80), but the canonical correlation of the eigenvalues indicated that the relation between the categories and the function was not strong, but Wilks' lambda indicated that the model was significant (Tables 7.81 and 7.82). Category 4 membership was almost universally correctly classified, but just under half of the entheses in category 1a were incorrectly classified (Table 7.83).

Table 7.80 *Biceps brachii* axis x. 2 category (1a and 4) discriminant function analysis results.

Variables	Box's M p-value	Correctly assigned (%)	Comment
All	0.004	78.0%	Only 43.8% (7/16) of category 1a correctly classified
Rq of FFT, mean slope, relative length and peak frequency	0.000	78.0%	Only 37.5% (6/16) of category 1a correctly classified
Rq of FFT, mean slope, relative length and mean displacement	0.000	78.0%	Only 43.8% (7/16) of category 1a correctly classified
Rq of FFT, mean slope, relative length, mean displacement and area displacement	0.001	80.00%	50% of category 1a correctly classified
Rq of FFT, mean slope, relative length, mean displacement, Rq and peak frequency	0.004	82.00%	56.3% of category 1a correctly classified

Table 7.81 *Biceps brachii* axis x. 2 category (1a and 4) discriminant function analysis using roughness parameters: Rq of FFT, mean slope, relative length, mean displacement, Rq, and peak frequency.

Eigenvalues				
Function	**Eigenvalue**	**% of Variance**	**Cumulative %**	**Canonical Correlation**
1	.331(a)	100.0	100.0	.499
(a) First 1 canonical discriminant functions were used in the analysis.				

Table 7.82 *Biceps brachii* axis x. 2 category (1a and 4) discriminant function analysis using roughness parameters: Rq of FFT, mean slope, relative length, mean displacement, Rq, and peak frequency.

Wilks' Lambda				
Test of Function(s)	**Wilks' Lambda**	**Chi-square**	**df**	**Sig.**
1	.751	12.883	6	.045

Table 7.83 *Biceps brachii* axis x. 2 category (1a and 4) discriminant function analysis using roughness parameters: Rq of FFT, mean slope, relative length, mean displacement, Rq, and peak frequency.

Classification Results (a)					
		Status 2 category	Predicted Group Membership		Total
			1	4	
Original	Count	1	9	7	16
		4	2	32	34
	%	1	56.3	43.8	100.0
		4	5.9	94.1	100.0
(a) 82.0% of original grouped cases correctly classified.					

Further subdivisions of the data into five categories were tested, to determine whether the effect of pooling data from entheses with anomalies intersected by the profile gauge and those not. However, the sample size of categories 21 and 31 were very small compared to that of category 22. This must be borne in mind when the results of this study are interpreted. The overall highest classification achieved with the roughness parameters was 60 percent (Table 7.84), but Wilks' lambda was not significant indicating that this model was not discriminating (Table 7.85). The canonical correlation of the eigenvalues on the other hand indicated that some functions were related to categories, but the individual category classification indicates that the model is not ideal (Table 7.86).

Table 7.84 *Biceps brachii* axis x 5 category discriminant function analysis using all roughness parameters.

Eigenvalues				
Function	Eigenvalue	% of Variance	Cumulative %	Canonical Correlation
1	.845(a)	54.1	54.1	.677
2	.463(a)	29.7	83.8	.563
3	.218(a)	13.9	97.7	.423
4	.036(a)	2.3	100.0	.186
(a) First 4 canonical discriminant functions were used in the analysis.				

Table 7.85 *Biceps brachii* axis x 5 category discriminant function analysis using all roughness parameters.

Wilks' Lambda			
Test of Function(s)	**Wilks' Lambda**	**Chi-square**	**df**	**Sig.**
1 through 4	.294	50.836	40	.117
2 through 4	.542	25.425	27	.551
3 through 4	.793	9.636	16	.885
4	.965	1.462	7	.984

Table 7.86 *Biceps brachii* axis x 5 category discriminant function analysis using all roughness parameters.

Classification Results (a)								
		Status 5 category	**Predicted Group Membership**					**Total**
			1	**21**	**22**	**31**	**33**	
Original	**Count**	**1**	6	0	4	1	0	11
		21	0	2	1	0	0	3
		22	2	2	17	0	2	23
		31	0	0	1	1	0	2
		33	0	0	7	0	4	11
	%	**1**	54.5	.0	36.4	9.1	.0	100.0
		21	.0	66.7	33.3	.0	.0	100.0
		22	8.7	8.7	73.9	.0	8.7	100.0
		31	.0	.0	50.0	50.0	.0	100.0
		33	.0	.0	63.6	.0	36.4	100.0
(a) 60.0% of original grouped cases correctly classified.								

7.4.3.6 Discriminant function analysis: *Biceps brachii* y

The approach described in Chapter 6, was applied to *biceps brachii* axis y (Tables 7.87-7.93). Despite fairly high overall classification results, Wilks' lambda indicated that the best classifying model was not discriminating. Box's M also indicates that the categories were not homoscedastic and that covariance matrices were significantly

different. This may explain these results. However, as can be seen in Table 7.94, 92 percent of category 2 is correctly classified. For this reason it was decided to re-attempt discriminant function analysis using the categories 1 and 2 (excluding all bone formers), but although category 2 membership classification improved there was no improvement in category 1. Nevertheless, Wilks' lambda was significant indicating that the model was discriminating.

Table 7.87 *Biceps brachii* axis y 3 category classification using discriminant function analysis.

Variables	Box's M p-value	Correctly assigned (%)	Comment
All	p=0.000	72.0%	Only 41.7% (5/12) of category 3 correctly classified.
Rq, Ra, HSC, relative length, peak number, mean displacement, area displacement and Rq of FFT	p=0.000	66.0%	Only 46.2% (6/13) of category 1 and 33.3% (4/12) of category 3 correctly classified.
Rq, Ra, HSC, mean slope, relative length, peak number, mean displacement, area displacement and Rq of FFT	p=0.000	72.0%	Only 33.3% (4/12) of category 3 correctly classified.

Table 7.88 *Biceps brachii* axis y. 3 category discriminant function analysis results using Rq, Ra, HSC, mean slope, relative length, peak number, mean displacement, and area displacement.

Eigenvalues

Function	Eigenvalue	% of Variance	Cumulative %	Canonical Correlation
1	.607(a)	76.6	76.6	.615
2	.185(a)	23.4	100.0	.395

(a) First 2 canonical discriminant functions were used in the analysis.

Table 7.89 *Biceps brachii* axis y 3 category discriminant function analysis results using Rq, Ra, HSC, mean slope, relative length, peak number, mean displacement and area displacement.

Wilks' Lambda

Test of Function(s)	Wilks' Lambda	Chi-square	df	Sig.
1 through 2	.525	27.717	18	.067
2	.844	7.311	8	.503

Table 7.90 *Biceps brachii* axis y. 3 category discriminant function analysis results using Rq, Ra, HSC, mean slope, relative length, peak number, mean displacement, and area displacement.

Classification Results (a)

		Status 3-categories (1=normal, 2=abnormal, 3=BF)	Predicted Group Membership			Total
			1	2	3	
Original	Count	1	9	2	2	13
		2	2	23	0	25
		3	1	7	4	12
	%	1	69.2	15.4	15.4	100.0
		2	8.0	92.0	.0	100.0
		3	8.3	58.3	33.3	100.0

(a) 72.0% of original grouped cases correctly classified.

Table 7.91 Discriminant function analysis results for *Biceps brachii* axis y categories 1 (normal) and 2 (abnormal).

Variables	Box's M p-value	Correctly assigned (%)	Comment
All		86.50%	Only 54.5% (6/11) of category 1 correctly classified, with 100% of category 2 correctly classified
Rq, area displacement, mean slope and Rq of FFT	0.028	83.80%	Only 45% (5/6) of category 1 correctly classified
Ra, Rq, area displacement, mean slope, mean displacement, Rq of FFT, and HSC	0.027	86.50%	

Table 7.92 *Biceps brachii* axis y. Categories 1 (normal) and 2 (abnormal). Discriminant function analysis results using Ra, Rq, area displacement, mean slope, mean displacement, Rq of FFT, and HSC.

Eigenvalues

Function	Eigenvalue	% of Variance	Cumulative %	Canonical Correlation
1	.674(a)	100.0	100.0	.635

(a) First 1 canonical discriminant functions were used in the analysis.

Table 7.93 *Biceps brachii* axis y. Categories 1 (normal) and 2 (abnormal). Discriminant function analysis results using Ra, Rq, area displacement, mean slope, mean displacement, Rq of FFT, and HSC.

Wilks' Lambda

Test of Function(s)	Wilks' Lambda	Chi-square	df	Sig.
1	.597	16.237	7	.023

Table 7.94 *Biceps brachii* axis y. Categories 1 (normal) and 2 (abnormal). Discriminant function analysis results using Ra, Rq, area displacement, mean slope, mean displacement, Rq of FFT, and HSC.

Classification Results (a)					
		Status 3-categories	Predicted Group Membership		Total
			1	2	
Original	Count	1	7	4	11
		2	1	25	26
	%	1	63.6	36.4	100.0
		2	3.8	96.2	100.0
(a) 86.5% of original grouped cases correctly classified.					

Discriminant function analysis of two categories was expected to perform best for all enthesis axes, as discussed in Chapter 6. However, Box's M was significant (Table 7.95), indicating lack of covariation between matrices and the canonical correlation of the eigenvalue was low, indicating a lack of relationship between the function and the categories. Nevertheless, each enthesis was correctly classified in over 60 percent of cases and Wilks' lambda indicated that the model was discriminating (Tables 7.96-7.98).

Table 7.95 *Biceps brachii* axis y 2 category classification using discriminant function analysis.

Variables	Box's M p-value	Correctly assigned (%)	Comment
All	p=0.000	72.0%	category 3 has 69.6% (16/23) correctly assigned as opposed to only 60.9% (14.23) using HSC, peak frequency and Ra
HSC, peak frequency, Ra	p=0.003	76.0%	

Table 7.96 *Biceps brachii* axis y. 2 categories. Discriminant function analysis results using HSC, peak frequency, and Ra.

Eigenvalues				
Function	**Eigenvalue**	**% of Variance**	**Cumulative %**	**Canonical Correlation**
1	.298(a)	100.0	100.0	.479
(a) First 1 canonical discriminant functions were used in the analysis.				

Table 7.97 *Biceps brachii* axis y. 2 categories. Discriminant function analysis results using HSC, peak frequency, and Ra.

Wilks' Lambda				
Test of Function(s)	**Wilks' Lambda**	**Chi-square**	**df**	**Sig.**
1	.770	12.134	3	.007

Table 7.98 *Biceps brachii* axis y. 2 categories. Discriminant function analysis results using HSC, peak frequency, and Ra.

Classification Results (a)					
		Status 2 category (1a=not intersected; 4=intersected)	**Predicted Group Membership**		**Total**
			1	**4**	
Original	**Count**	**1**	24	3	27
		4	9	14	23
	%	**1**	88.9	11.1	100.0
		4	39.1	60.9	100.0
(a) 76.0% of original grouped cases correctly classified.					

There was a fairly even distribution of entheses in each of the five categories (defined in Chapter 6), except for category 31, which consisted of only three entheses. Overall classification was poor, perhaps because of the violation of homoscedasticity, as can be seen from Box's M (Table 7.99). The canonical correlation of the eigenvalue of the first function was strong, but none of the functions had a statistically significant Wilks' lambda indicating that model was not discriminating (Tables 7.100-7.102).

Table 7.99 *Biceps brachii* axis y 5 category classification using discriminant function analysis.

Variables	Box's M p-value	Correctly assigned (%)	Comment
all	p=0.000	58.0%	categories 31 and 33 correctly assigned in only 33.3% of cases (1/3 and 3/9 respectively)
HSC, area displacement and Rq of FFT	p=0.000	54.0%	category 31 correctly classified in 0% of cases
HSC, area displacement, Rq of FFT, Rq, peak number, mean displacement and peak frequency	p=0.000	58.0%	category 31 correctly classified in 0% of cases

Table 7.100 *Biceps brachii* axis y. 5 categories. Discriminant function analysis results using all roughness parameters.

Eigenvalues

Function	Eigenvalue	% of Variance	Cumulative %	Canonical Correlation
1	.841(a)	58.1	58.1	.676
2	.349(a)	24.1	82.2	.509
3	.195(a)	13.5	95.7	.404
4	.063(a)	4.3	100.0	.243

(a) First 4 canonical discriminant functions were used in the analysis.

Table 7.101 *Biceps brachii* axis y. 5 categories. Discriminant function analysis results using all roughness parameters.

Wilks' Lambda

Test of Function(s)	Wilks' Lambda	Chi-square	df	Sig.
1 through 4	.317	47.686	40	.189
2 through 4	.584	22.348	27	.719
3 through 4	.787	9.927	16	.870
4	.941	2.533	7	.925

Table 7.102 *Biceps brachii* axis y. 5 categories. Discriminant function analysis results using all roughness parameters.

Classification Results (a)

		Status 5-categories (1=normal, 21=abnormal not intersected, 22=abnormal intersected, 31=BF not intersected, 32 BF intersected)	Predicted Group Membership					Total
			1	21	22	31	33	
Original	Count	1	8	2	1	0	2	13
		21	1	8	2	0	0	11
		22	2	2	9	0	1	14
		31	0	1	1	1	0	3
		33	1	1	4	0	3	9
	%	1	61.5	15.4	7.7	.0	15.4	100.0
		21	9.1	72.7	18.2	.0	.0	100.0
		22	14.3	14.3	64.3	.0	7.1	100.0
		31	.0	33.3	33.3	33.3	.0	100.0
		33	11.1	11.1	44.4	.0	33.3	100.0

(a) 58.0% of original grouped cases correctly classified.

7.4.3.7 Discriminant function analysis: Summary

Discriminant function analysis of the entheses by axis demonstrated that the roughness parameters can be used to distinguish between categories of enthesis. Some models were better than others, but sample size and covariance will have affected the results. The roughness parameters were not discussed at length in this chapter, but will be in Chapter 8.

7.5 Summary

This chapter has demonstrated that the new recording method can be applied to three entheses and that the roughness parameters can be used to describe the surfaces. It also demonstrates the importance of taking into account factors other than activity-related stress when analysing enthesopathy presence. Enthesopathies have higher

frequencies in individuals with fractures and in individuals with possible disease presence (categorised as bone formers). In this sample there was very little difference in size, DJD presence or roughness parameters between left and right sides of the skeleton. This enabled data to be pooled without the concern that side differences may be affecting the results. Difference in size of bone and enthesis were found between the normal skeletons and those with abnormalities. This was expected, as discussed in Chapter 6. However, differences in size were not expected between normal skeletons and bone formers, or between abnormal skeletons and bone formers. This demonstrated that, in general, skeletons with enthesopathies were larger than those without and that their entheses were also larger. Bone formers were largest of all. This will be discussed in Chapter 8. The measurements of the entheses studied compared to that of bones were correlated in unexpected ways, as described above. Development of entheses requires further study to elucidate the causes of these findings. Correlations were tested between the size of entheses and the values of the roughness parameters. Statistically significant correlations were found and will be discussed in context in Chapter 8. Finally, the discriminant function analysis demonstrated that roughness parameters have a value as descriptors of enthesis shape. Interestingly, these also distinguish between normal skeletons and bone formers. This was another unexpected finding, but again demonstrates the importance of distinguishing between different causes of enthesopathy formation. Chapter 8 will discuss all these findings in relation to the chapters on activity-related stress in bioarchaeology, anatomy of entheses and aetiology of enthesopathies.

Chapter 8. Discussion

The initial concept of this dissertation involved the use of anonymous medical records with radiographs to determine the relationship between life histories and enthesopathy formation. However, the National Health Service (NHS) in Britain does not collect and retain information on occupation or activity patterns. This was, consequently, not possible.

8.1 Introduction

This research had two aims: firstly, to determine whether MSM can be used as indicators of physical activity by bioarchaeologists and, secondly, to develop a new recording method for MSM. The first aim was studied using literature reviews covering bioarchaeological understandings of MSM (and other indicators of activity) and clinical data on entheses and enthesopathy formation. This aim was achieved. It was found that enthesopathies cannot be used alone as indicators of physical activity. Their aetiology is complex and not fully understood clinically. However, it is known that many diseases can contribute to their formation making this one of the most important factors to be considered by bioarchaeologists. This was a primary factor to be taken into account in the new recording method. Simplicity is often the key to the adoption of new recording methods; for this reason the new method developed had to be simple, cheap, repeatable and ideally quantitative. To achieve the second aim, several pilot studies were performed to test different recording methods. It was decided early on that a visual method was vital to record the different types of enthesopathy that occur. Visual study of the entheses also determined that the shape of the enthesis should be recorded. For this reason methods were developed which recorded the size of the enthesis and its curvature. Following this, roughness parameters used by material scientists were applied to the enthesis curvature to determine which were most applicable for the description of enthesis shape and for the differentiation between normal entheses and those with enthesopathies. Chapter 7 presented the results of this analysis and this secondary aim was fulfilled. It will be discussed in detail in the present chapter.

8.2 First Aim: Necessity of the Research for Bioarchaeology

If archaeology is the study of culture in the past, then bioarchaeology is the use of bioarchaeological artefacts in this search. Human skeletal remains, without doubt, are the best means to understanding human behaviour at the individual and population level. Skeletons, unlike any other artefact are remnants of individuals who lived in the past, so should be the starting point for any archaeological research where skeletal remains are found. Those studying markers of occupational stress (MOS) have, in some cases used these as markers of specific activities (*e.g.* rowing; Hawkey and Merbs 1995); whereas others have used them as indicators of changes in the larger population (*e.g.* subsistence pattern changes; Bridges 1989). This (and the discussion in Chapter 2) is a clear demonstration of their practical use at the individual level and the potential scaling of their use to population studies. These studies lead to the creation of models of human activity. Chapter 2 was also used to critique the literature published and to determine whether bioarchaeologists have discovered a direct link between physical activity and enthesopathy formation. As discussed in Chapter 2, no such a link exists. What is highlighted, and is crucial to this study, are the many bioarchaeological questions which could be answered using MSM, if scientific evidence of their value could be obtained. This demonstrates the necessity of the research for bioarchaeology.

8.2.1 Stage 1: Anatomy of Entheses

The first step on the road to determining whether enthesopathies could be used as indicators of physical activity was to determine the anatomy of entheses. Chapter 2 demonstrated that bioarchaeologists have conflicting views about the anatomy of these sites. Some mention Sharpey's fibres, but the majority of papers seem to ignore the anatomy completely. However, the interface between two materials with different mechanical properties is complex and the most likely to fail under stress (Currey 2002). Consequently, the anatomy and biochemistry of these sites is vitally important to understanding the cause of enthesopathies.

Chapter 3 addressed the anatomy of entheses. The goal of understanding enthesopathy formation was also addressed through the discussion of their development during

growth and in particular the adolescent growth spurt. It was clear from the review that the anatomy and biochemistry of these sites has had a recent resurgence in research following a dearth of interest since German papers from the 1930s. New terminology was developed following a paradigm shift in the understanding of the enthesis (Benjamin, *et al.* 2002). This has been discussed in Chapter 3. The new terminology is based on the cell biology and extra-cellular matrix of these sites. Broadly, entheses are divided into two groups: fibrocartilaginous and fibrous. The term "Sharpey's fibres" is restricted to the collagen fibres which anchor the soft tissue to the bone. Similar to an anchor which fixes a ship (through water) onto the seabed; these fibres are surrounded by bone extra-cellular matrix anchoring them to bone. The term "Sharpey's fibres" is restricted to the description of fibrous entheses.

Fibrous entheses are primarily those which attach soft tissues to the diaphysis of long bones (not phalanges). In many cases they anchor the strongest muscles in the body to bone, *e.g.* the deltoid to the humerus. Stress at the interface is dissipated by increasing the surface area of the enthesis. During development the interface is mediated by periosteum (Benjamin and Ralphs 1995). This is lost during later life. As a consequence, these sites present a diversity of macroscopic appearances on human skeletal remains. In juveniles, their macroscopic appearance on dry bone is smooth, but ill-defined. With age the intermediate periosteum can be lost and the surface appearance becomes roughened. Consequently, age, at fibrous entheses, is probably the primary factor to consider when studying enthesopathies.

Fibrocartilaginous entheses, by comparison, attach soft tissues (including the joint capsule) to the epiphysis of long bones and to areas in the short bones of hands and feet. Joint movement at these sites is great, which affects the angle at which the tendon (or other soft tissue) attaches. Consequently, stress dissipation is important as is control over the direction of the force to be distributed. Some researchers have compared fibrocartilage to the less flexible (the grommet) part of an electric cable just before the cable joins the plug (Benjamin and Ralphs 1999). To achieve this, the enthesis consists of the following four layers: tendon, unmineralised fibrocartilage, mineralised fibrocartilage and bone. The divide between mineralised (bone and mineralised fibrocartilage) and non-mineralised layers is known as the "tidemark", which also exists in hyaline joints. In general terms, these entheses are very similar to

hyaline cartilaginous joints, unsurprisingly given the similarity in characteristics between the hyaline cartilage and fibrocartilage (Benjamin and Ralphs 2004). Their macroscopic appearance is a smooth, well-defined area very much like that of a synovial joint. The bone and mineralised fibrocartilage zones of these entheses interdigitate like a jigsaw, thereby increasing the surface area of the enthesis.

Enthesopathies should be divided into those involving new bone formation (spurs): bone destruction (lytic lesions); or a combination of both at a single site (see Chapter 7). Enthesopathies have many causes, as discussed in Chapters 4 and 5; this section will focus on how they form. In bone spurs regions of mineralised fibrocartilage were found in the bone portion of the spur and are thought to be created by endochondral ossification (it should be remembered that the bone below a fibrocartilaginous enthesis is subchondral bone) brought on by repeated micro-tears or from compressive loading. Bone spurs obviously increase the surface area of the enthesis, which should help in load distribution. Whether bone spurs act as stabilisers or increase surface area to reduce stress is still unknown. Subchondral bone does not underlie fibrous entheses, but it should be remembered that the difference between the two types of enthesis is not absolute. It has been demonstrated that fibrocartilage can form where required (Benjamin, *et al.* 2002). Longitudinal fissuring has been reported in the clinical literature at entheses, but little is known about the mechanics and cell biology of these types of injury.

Chapter 3 illustrated that, despite the attempt by bioarchaeologists to use enthesopathies as indicators of physical stress, the biological understanding of entheses is still incomplete. Two types of enthesis have been described, but only fibrocartilaginous ones have been studied in great detail. This is primarily because these are more commonly injured or affected by diseases (as was discussed in Chapters 4 and 5). Further research is necessary before the formation of enthesopathies can be fully understood. However, from this anatomical approach it is clear that the normal appearance of fibrocartilaginous attachments is smooth with a well-defined margin. For this reason it seemed obvious to focus the rest of this research on this type of enthesis. Further reasons for focussing on fibrocartilaginous entheses were discussed in Chapters 4 and 5.

8.2.2 Stage 2: Enthesopathies of Traumatic Aetiology

The primary purpose of Chapter 4, and this research in general, was to determine whether there is a link between repetitive activity and enthesopathy formation. A direct link between the two seems to be an underlying assumption in much of the bioarchaeological literature. However, if the situation is not as simple as this, then the foundation stone of this aspect of the discipline is not sound. Consequently, the discipline needs to be up-to-date with the current clinical paradigm. The World Health Organisation perceives that occupational health (including musculoskeletal health) is multifactorial in origin and therefore clear data are difficult to obtain. To expand the raft of knowledge, the literature review focused on both upper and lower limb enthesopathy formation. Literature on hyaline joint injuries (particularly osteochondritis dissecans and osteophyte formation) was also studied to see if parallels could be drawn from these studies to enthesopathy formation.

The enthesis is a zone which few clinicians appear to research and the majority of the literature focuses on either the bone or the soft tissues and not the whole enthesis. It is of interest to bioarchaeologists to understand the bone changes, but the musculoskeletal system needs to be considered as a unit (especially at the enthesis, which often transmits immense force between the skeleton and muscle) and not as compartmentalized as the clinical research seems to be because bioarchaeologists are using the bone to understand the activity occurring in the soft tissues.

Experiments in animals have proved that a ruptured tendon can heal to join the bone with the fibrocartilage layers in between. However, it was also determined that the insertion site (rat *supraspinatus* insertion on the humerus) heals poorly when compared to the healing of other musculoskeletal structures (Thomopoulos *et al.* 2002). This is unsurprising given that the mechanical requirements of entheses rely on the attachment of materials with different mechanical properties. If difficulties with healing occur, then the injuries should be recognisable in human skeletal remains. The question is: are spurs and lytic lesions caused by injury or the healing of injury and are they a sign of acute (*i.e.* one-off) or chronic (*i.e.* repetitive and possibly activity-related) processes?

There seems to be a dearth of clinical literature on the formation of spurs in relation to activity or occupational stress, despite the existence of literature on treatment either of the soft tissue or bone. The primary locations discussed relate to the rotator cuff, the Achilles tendon and plantar fascia. Injuries to all of these sites are relatively common in sport and occupational activities (Benjamin, *et al.* 2006; Sadat-Ali 1998). Factors affecting their aetiology in the lower limb include footwear and body mass, but the amount of walking was not a factor. This is an important point that should be noted by bioarchaeologists who have discussed amount of walking and terrain walked over in their studies of enthesopathies [*e.g.* (Al-Oumaoui, *et al.* 2004)]. Similarly, lytic lesions cannot be directly linked to physical activity. Numerous causes have been linked, including avulsion injuries, but even these have a multifactorial origin. When compared to causes of injury at hyaline joints, one further cause is possible: that of osteochondritis dissecans. The clear thesis from this review of the literature is that enthesopathies are not caused by physical activity alone.

8.2.3 Stage 3: Disease and Enthesopathy Formation

The multifactorial aetiology of enthesopathies was demonstrated in Chapters 3 and 4. Chapter 5 covered their pathological aetiology. The aim of Chapter 5, apart from providing a list of pathological causes, was to present diagnostic criteria to use in the later stages of this research. Modern clinical diagnostic criteria were used for this and it was hoped that some of these new criteria would be useful to the field of palaeopathology. The limitations of this are that many of the pathognomonic signs and symptoms do not affect the musculoskeletal system; and if they do, this is rarely the mineralised parts. One of the other problems faced were the many rare diseases with only a minimal record of clinical study (*e.g.* SAPHO syndrome) or those more common diseases with rare occurrence of enthesopathy (*e.g.* Lyme disease). In the latter cases it is not evident whether the enthesopathies are a sign of the disease or caused by a different factor, such as age. It must be remembered that individuals can suffer from more than one condition at once; sometimes with similar skeletal changes (*e.g.* DISH and AS; Moreno *et al.* 1996). Additional research is required (at a clinical level) to answer these questions.

One disease cluster which appears to be dominant, both in quantity of clinical literature published and in prevalence, is that of the seronegative spondyloarthropathies. These diseases are thought to have a prevalence of 0.3 percent in the modern world. Considering that recent research has indicated that sacroiliitis and enthesopathy formation are hallmarks of this cluster of diseases, it is surprising that so few cases exist in the palaeopathological literature. Such a high clinical presence of these, and other diseases covered in this chapter, indicated that stringent diagnostic criteria were needed to avoid under-diagnosis of these diseases. These criteria, described in Chapter 6, led to the classification of many skeletons as "bone formers". This term is merely used to indicate that these individuals had a greater propensity to form bone at any enthesis. This does not mean that these skeletons had definitely suffered from any of the diseases discussed in Chapter 5, but this was a possibility.

These literature reviews demonstrated that the aetiology of enthesopathy formation is multifactorial and many of these factors are only seen in soft tissue. It is obvious from these reviews that previous bioarchaeological research has been built on shaky foundations, as demonstrated by the clinical research. However, there is very little clinical data on the enthesis itself (it is possible that this is caused by specialisation of clinical research into either bone or soft tissue, but not of the interface). It is also apparent that pathological changes may play a greater role in enthesopathy formation than seems to be assumed in bioarchaeological literature.

8.3 Aim 2: Pilot Methods

It was stated in the introduction that the second aim of this research was to create a new recording method based on the outcome of the first aim. The starting point was that the method could be able to answer questions posed by bioarchaeologists. For this to be effective it must have widespread usage so that populations can be compared. To achieve this it had to be: simple, affordable, repeatable, and quantitative.

Chapter 3 made it quite clear that there are so many factors involved that only a small number of entheses (*supraspinatus* insertion, common extensor origin, *biceps brachii*

insertion) could be covered fully. They were all chosen because they are fibrocartilaginous and should have a smooth, well-defined area when normal. They are also some of the best described entheses in clinical literature in the upper extremity. This, it was hoped, would keep the methodology for visual recording as simple as possible and avoid problems dealt with in Chapter 2. Visual recording is, obviously, the simplest and cheapest method. Drawbacks are repeatability and although some researchers claim them to be quantitative methods, the quantification is bound up in the visual recording method. As discussed in detail in Chapter 6, the visual recording method used in this research defines entheses as: normal (no enthesopathy), abnormal (a bone spur, a lytic lesion, or woven bone on surface), damaged, or missing. Where an enthesopathy exists a note was made of whether it was proliferative, lytic or a combination of the two. The visual system was also extended to include all of the following enthesis: *subscapularis*, *supraspinatus*, *infraspinatus*, *teres minor*, common extensor origin, *anconeus*, common flexor origin, *triceps brachii*, *brachialis*, *biceps brachii* (all insertion, unless otherwise stated).

Entheses are essentially surfaces comparable to landscapes with hills and valleys, or road surfaces, or grades of sandpaper. These surfaces are studied mathematically (in the case of small surfaces this is called metrology) and there are standardized methods of studying them. However, it is the collection of the data which has to take in many considerations, foremost of them all is the preservation and conservation of bone. Many of the data collection methods used in metrology are only appropriate for items which can be crossed by a metal stylus, or are only appropriate for items smaller than bones. Further considerations were cost and portability. Chapter 6 described the many pilot methods tested to achieve this.

8.3.1 Aim 2: Main Study

The final method involved the use of a profile gauge to map the curvature of the enthesis along two predefined bisecting axes. Further quantitative data were collected from measurements of the entheses (along the same predefined axes as used for the profile gauge) and the size and robusticity of the humerus, radius and ulna. Stringent criteria, based on the data from Chapter 5 and presented in Chapter 6, were applied to

separate those individuals with possible bone-forming diseases, from those with no signs.

Adult skeletons from late medieval Fishergate House, York (UK) were used for this analysis, as described in Chapter 6 and 7. Only male skeletons were used to avoid hormonal effects on enthesopathy morphology. However, all age groups were pooled because the ageing methods employed in this study found only two young males. Other ageing techniques were not used because they rely on degenerative changes which are a factor in enthesopathy formation. Using these would create inconsistencies in the results. Left and right upper limbs were also pooled because of the negligible left to right asymmetry (see Chapter 7). Three categories were selected: "normal", "abnormal" and "bone forming". The stringent new criteria for separating "normal" skeletons from "bone forming" were applied. The term "abnormal" was applied to entheses with enthesopathies of any kind (but not defined as bone formers). The hypothesis that bone formers had a higher number of appendicular enthesopathies than the other skeletons was upheld (as demonstrated in the previous chapter). This is important as it demonstrated the necessity of analysing the data from these skeletons separately.

8.3.2 Aim 2: Performance of New Recording Method

This section discusses the results of the final recording method as tested on the male skeletons from Fishergate House, York. The results of the discriminant function analysis will be discussed in relation to the question of which roughness parameters were found to be the most useful to the study of enthesopathies. The results will be discussed in relation to the individual entheses and will be tied together at the end of this chapter, but prior to this the general findings of the skeletal analysis will be discussed. Further research required will be presented in Chapter 9.

The skeletal analysis demonstrated that many different types of enthesopathy existed. The high frequency of enthesopathies at some entheses was also demonstrated. The entheses with the three highest frequencies were those for the *subscapularis*, the common extensor origin, and the *biceps brachii*. It was expected that the

supraspinatus entheses would have the highest frequency because this has the highest reported frequency in the clinical literature. The reasons for this difference are unclear. In general, proliferative enthesopathies are the most common at all entheses, but the *biceps brachii* has the highest level of variation in types of enthesis found. This is unsurprising, given that this tendon has a wide variety of insertion angles and insertion sites (Forthman *et al.* 2008). Individual variation in this enthesis is, therefore, to be expected. Left and right sides were pooled for all the final analyses. Measurements of the entheses indicated that there were no significant differences in size of entheses between the left and right sides. DJD frequencies were also highly similar, which may indicate similar levels of arm use, if DJD is degenerative in origin. Skeletons with fractures were found to have high levels of enthesopathy frequency, which may indicate an acute trauma-related aetiology for some of these enthesopathies. It is also possible that this is merely coincidental.

One of the hypotheses of this study was that bone formers would have a higher frequency of appendicular enthesopathies than other skeletons. This was indicated as a possibility in Chapter 5 and had to be tested to determine whether it was necessary to separate these skeletons from the rest of the sample. The findings of this analysis indicated that the hypothesis was correct. Bone formers had a higher frequency of enthesopathies at all sites (except the *subscapularis* insertion). In the majority of cases, this was found to be a statistically significant ($\alpha = 0.05$) finding. Consequently, this must be taken into account in all future bioarchaeological analyses of MSM. It must also be borne in mind when interpreting past studies, as this factor has rarely been taken into account.

8.3.2.1 Supraspinatus

The *supraspinatus* enthesis is located at the lateral edge of the greater tuberosity of the humerus. Clinically, this muscle is found to be more commonly injured than any of the other rotator cuff muscles. However, in this study the *subscapularis* insertion was found to be abnormal in more skeletons than any of the other rotator cuff insertions. Nevertheless, the *supraspinatus* insertion is useful for this analysis because

of the mass of clinical literature with which to interpret the data.

8.3.2.1.1 Supraspinatus: enthesopathies and skeleton size

There were indications from the preliminary data used to create the methodology that size differences would exist between the categories: "normal", "abnormal", and "bone former". The hypotheses were that the measurements of the enthesis (and the bone) would fulfil the following:

- *Normal < With enthesopathies (abnormal)*
- *Normal < Bone formers*
- *With enthesopathies (abnormal) < Bone formers*

The measurements of the bone did not follow all of these hypotheses (Chapter 7). None of the bone measurements (except the size of the *supraspinatus* axis x) for the bone formers were statistically significantly larger (Student's T-test at $\alpha = 0.05$). However, the length of the humerus for the abnormal entheses and bone formers was statistically significantly larger than those with normal entheses. The vertical and transverse measurements of the humeral head also followed this pattern. The humeral head index (vertical head diameter ÷ transverse head diameter) was statistically significantly smaller in the normal cases compared to the abnormal ones. The condylar and epicondylar widths also followed this pattern. Therefore, it seems that bone formers and individuals with abnormal *supraspinatus* entheses are larger than those with normal entheses.

It was found that the size of the *supraspinatus* axis x followed these hypotheses. However, the *supraspinatus* axis y did not. It could be presumed that this relates to the ability of the enthesis to grow in different directions. The axis y is bounded by the humeral head and the joint capsule. The axis x is bounded by the *infraspinatus* enthesis and the bicipital groove. However, the entheses of this region are not so neatly divided. The tendons of both the *supraspinatus* and *infraspinatus* muscles blend together near the insertion, thus the middle portion of the facets represent the entheses of both tendons (Minagawa, *et al.* 1998). Note, however, that there is normally a slight ridge running in the direction of the y axis part-way along the

enthesis (Figure 8.1). This ridge was defined, for the purposes of this study, as the edge of the *supraspinatus* enthesis. The fibres of these tendons also merge with the joint capsule (Benjamin, *et al.* 2004). Furthermore, it has been demonstrated that the *supraspinatus* enthesis also extends over the edge of the greater tuberosity (Curtis, *et al.* 2006), but this extension is not visible on the bone as a smooth, well-defined "footprint" (Figure 8.1). For this reason it was not measured or included as part of the surface roughness test. Table 8.1 demonstrates the difference in measurement between entheses measured with soft tissue and the ones in this study.

Figure 8.1 Ridge running across *supraspinatus* enthesis. Arrow points to ridge. Arrow head demonstrates rough area.



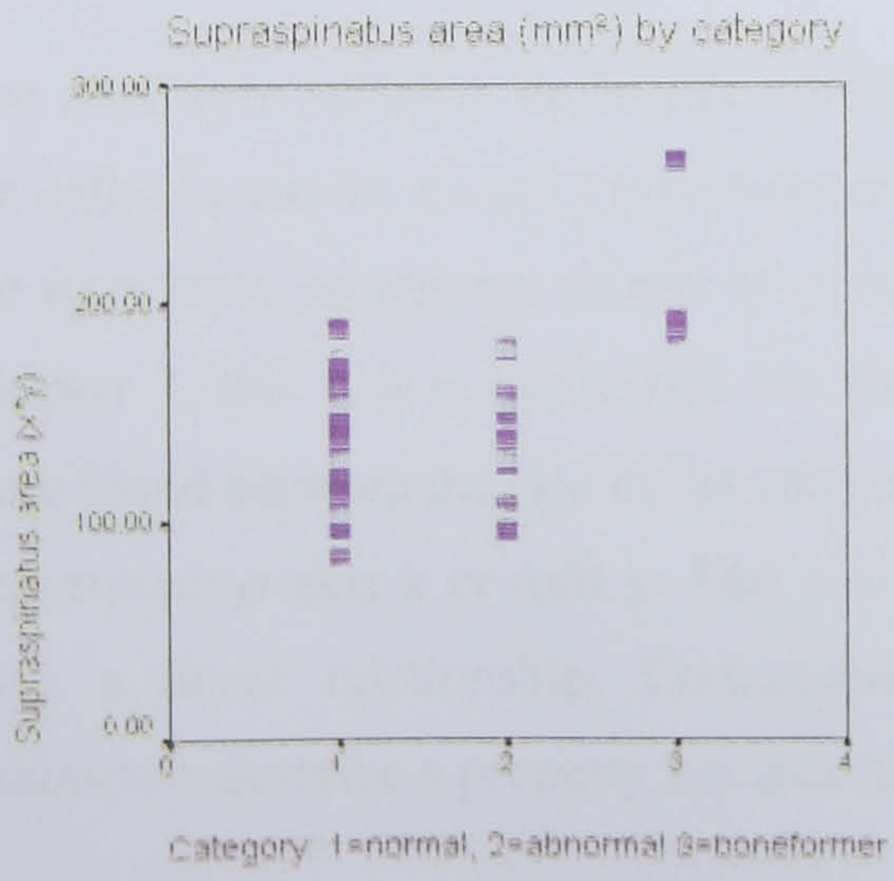
Table 8.1 Published measurements of the *supraspinatus* insertion discussed here, with this study's results for comparison.

Enthesis	Publication	Mean	Range	Comment
Supraspinatus x axis	This study	16 mm (n = 39)	11.2 to 22.5 mm	
Supraspinatus x axis	Curtis *et al.* (2006) p.606	23 mm	18 to 33 mm	Age and sex unknown
Supraspinatus x axis	Minagawa *et al.* (1998) p305 (distance a-b*)	12.6 mm	11.3 to 14.5 mm; standard deviation 1.1 mm	Males and females all over 50 years
Supraspinatus x	Minagawa *et al.* (1998) p.305 (distance a-c**)	22.5 mm	18.2 to 27.3 mm; standard deviation 3.1 mm	Males and females all over 50 years
Supraspinatus y axis	This study	8.9 mm (n = 40)	6.1 to 17.4 mm	
Supraspinatus y axis	Curtis *et al.* (2006) p.606	16 mm	12 to 21 mm	Age and sex unknown

*a-b: measured from the anterior margin of the greater tuberosity to the anterior margin of the *infraspinatus* tendon

**a-c: measured from the anterior margin of the greater tuberosity to the posterior margin of the *supraspinatus* tendon

Figure 8.3 *Supraspinatus* area (mm^2) by category of enthesis. Note that there is little difference in size between the abnormal (2), normal (1) entheses, and the bone formers (3).



Student's T-test indicated that there were no statistically significant ($\alpha = 0.05$)

differences for the approximation of the area (calculated as axis x multiplied by axis y) between the abnormal and normal entheses (Figure 8.3). The bone formers could not be included because of the small sample size. The surface area of an attachment site is important, as this allows force to be dissipated over a greater area, thus reducing localised stress. However, the shape of the enthesis is also of importance because it has been demonstrated that different regions of the tendon are active with different movements at the shoulder (Fallon, *et al.* 2002). For this reason, measuring the x- and y-axis of the fibrocartilaginous portion of the enthesis should provide valuable information for understanding muscle usage.

8.3.2.1.2 *Supraspinatus*: Measurement Correlations

No statistically significant ($\alpha = 0.05$) correlation was found using Pearson correlation coefficients for the size of the *supraspinatus* enthesis and any of the measurements of the humerus, or the indices calculated. Therefore, the size of the enthesis has no linear correlation with the size of the humerus. This is surprising as the head of the humerus and the greater tubercle fuse between the ages of two and six years (Scheuer and Black 2000a) and so their growth should be linked. More surprisingly, the x- and y-axes do not correlate in size. This may reflect the problems with measuring this enthesis, as discussed above.

The data were tested to determine whether a correlation existed between the size of the enthesis and the roughness parameters. This was undertaken to determine whether the roughness parameters should be normalised by enthesis size: as demonstrated in Chapter 7, this was not required. No statistically significant ($\alpha = 0.05$) correlations were found between the size of the enthesis and the roughness parameters of either the *supraspinatus* axis x or axis y. This indicates that the size and the roughness do not have a linear relationship. Consequently, this demonstrates that the roughness parameters describe a property separate to that of size for these entheses.

8.3.2.1.3 *Supraspinatus*: Discriminant Function Analysis

Discriminant function analysis was used to determine whether the roughness parameters could be used to quantitatively define the entheses into categories, *e.g.* bone formers (Table 8.2). With the *supraspinatus* axis x divided into the three categories (1 = normal, 2 = abnormal, and 3 = bone former), the best discriminating of the parameters were the relative length, area displacement, and the peak number. These parameters provided 73.5 percent accuracy. Interestingly the bone formers are 100 percent correctly classified. However, the small size of the sample, in particular the number of bone formers (a total of three skeletons), calls into question the applicability of using these parameters on larger sample sizes without further testing. When the data were divided into two categories (1 = profile gauge does not intersect anomaly; 4 = profile gauge intersects anomaly) the best classification was achieved using relative length, area displacement, peak number and Rq; a higher accuracy was achieved (85.3 percent). However, the classification results indicate that only one case of category 4 is accurately classified. This should, theoretically, be the most accurate method to split the data, but for some reason this is not the case. It is most likely to be caused by small sample size and because many of the normal entheses are very convex giving them comparatively high values of relative length. A further test should have been performed to determine whether the shape of bone formers affected the category 2 results, by subdividing into five categories (1 = normal; 21 = abnormal, but axis not intersecting the anomaly; 22 = abnormal, axis intersects the anomaly; 31 = bone former, but axis not intersecting any anomaly; and 33 = bone former, axis intersects the anomaly). Unfortunately, the sample sizes were too small for this to be appropriate.

The *supraspinatus* enthesis size of axis y did not vary between the different categories of enthesis as classified in this research, as discussed above. It is possible that the lack of ability to change size in this axis may lead to greater variation in roughness than in axis x, or that the small size of this enthesis would make the roughness less variable because the number of peaks and troughs would always be fewer than possible in a larger enthesis. Discriminant function analysis of the three category data (1 = normal, 2 = abnormal, and 3 = bone former) provides 77.8 percent overall accuracy using

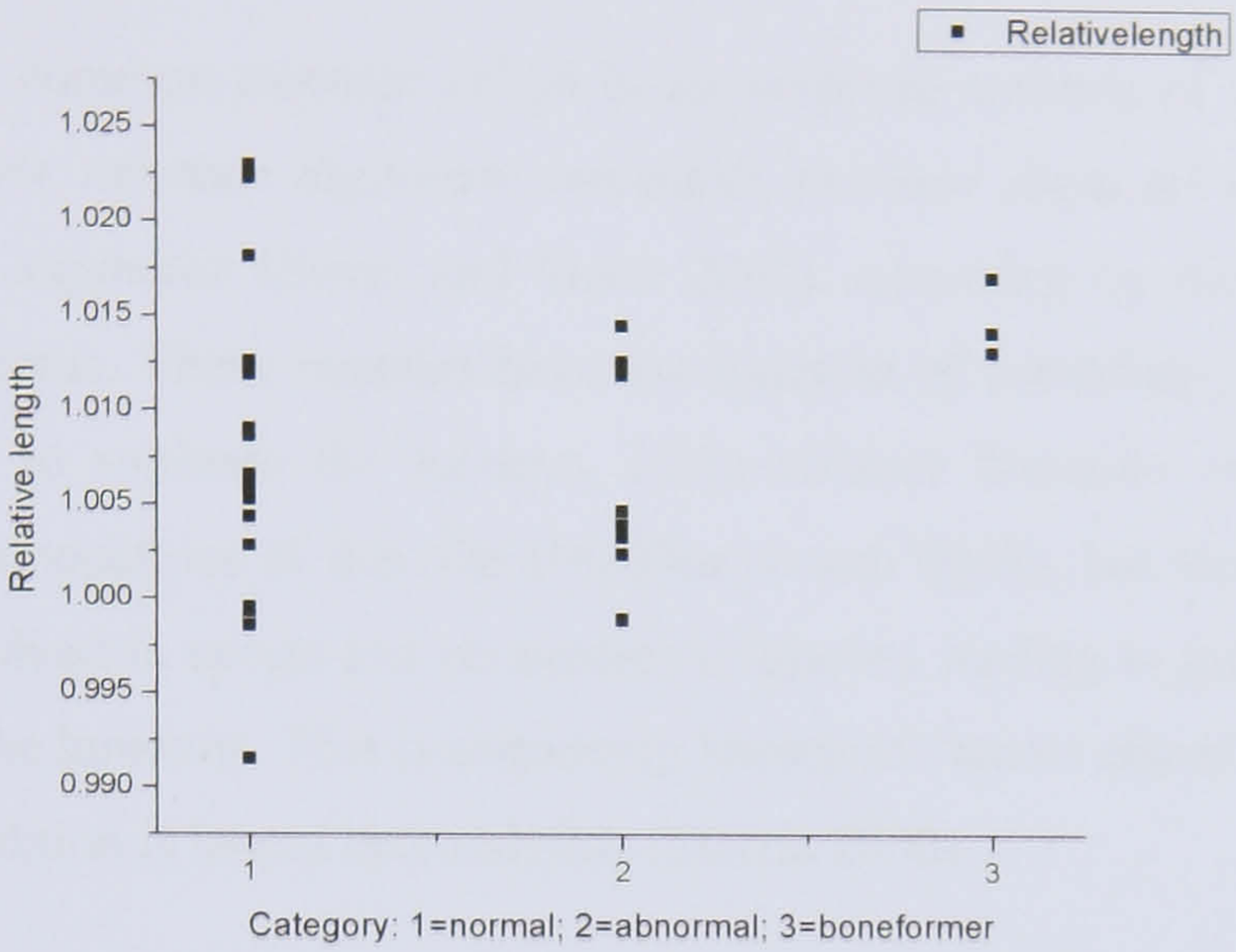
roughness parameters: HSC, Ra, Rq, mean slope, and area displacement. The eigenvalues and Wilks' lambda of both functions do not have statistical significance ($\alpha = 0.05$ level). The classification table indicates that these roughness parameters correctly classify category 1 and category 3 entheses, but are less effective for category 2 entheses at only 37.5 percent accuracy (three cases correctly assigned) with the remaining five cases assigned into category 1 (normal). The cases misclassified included categories 21 and 22 (21 = abnormal, but axis not intersecting the anomaly; 22 = abnormal, axis intersects the anomaly). It is unclear why these should be misclassified when the bone formers are correctly classified in all but one case (skeleton F164 R). To determine if this relates to whether abnormalities are intersected by the profile gauge, the data were divided into two categories (1 = profile gauge does not intersect anomaly; 4 = profile gauge intersects anomaly). When this was performed the best classification of the entheses using discriminant function analysis was achieved using Rq of FFT, relative length, and peak frequency. This achieved 80.6 percent accuracy, but only 33.3 percent of category 4 was correctly classified. All abnormal entheses with exostoses intersected by the profile gauge were incorrectly classified as normal. This indicates that in general these classification methods for this enthesis have a tendency to classify all entheses as normal. Unfortunately, the data set were too small to subdivide the data into five categories (1 = normal; 21 = abnormal, but axis not intersecting the anomaly; 22 = abnormal, axis intersects the anomaly; 31 = bone former, but axis not intersecting any anomaly; and 33 = bone former, axis intersects the anomaly). It would be interesting to determine if the problems with accuracy of the abnormal data were caused by the combination of groups 21 and 22 along with 31 and 33.

Table 8.2 Roughness parameters for *supraspinatus* x and y.

Enthesis, axis, category division	Roughness parameters	Comment
Supraspinatus x 3 categories	Relative length, area displacement, and peak number	100% classification accuracy for category 3 (only 66.7% accuracy for category 2)
Supraspinatus x 2 categories	Relative length, area displacement, peak number and Rq	
Supraspinatus x 5 categories	not applicable, sample sizes too small	
Supraspinatus y 3 categories	HSC, Ra, Rq, mean slope, and area displacement	Poor classification accuracy for category 2
Supraspinatus y 2 categories	Rq of FFT, relative length, peak frequency	Poor classification accuracy for category 4
Supraspinatus y 5 categories	not applicable, sample sizes too small	

It can be seen from the curves of axis x that, although there is some variation, the general trend of this surface is to be a slightly convex shape with a sharp incline from the medial aspect (the bicipital groove) and flattening off towards the infraspinatus insertion (Appendix VI). However, the convexity of the normal surfaces varies leading to a wide variation in roughness parameter value, as demonstrated in (Figure 8.4). Despite this, good levels of accuracy were achieved in the discriminant function analysis. Further tests, with larger sample sizes are needed so that the ability of the roughness parameters to accurately classify the entheses can be tested.

Figure 8.4 *Supraspinatus* axis x. Variation of relative length within and between the 3 categories.



The smooth part of *supraspinatus* axis y ranges from concave to convex. It must be remembered here that the *supraspinatus* enthesis continues into the rough region and that the tendon merges with the joint capsule. This makes the y-axis of the enthesis much harder to model. There is wide variation in shape and, more importantly, slope. Slope has considerable effect on many of the roughness parameters. It is likely that this has considerable effect on the results. However, the more important question is why the bone formers have entheses which are so readily classifiable into their own category. In general, these curves appear (visually) to be more concave than many of the other entheses. This may be by chance, but if not, it raises questions about the pathogenesis of bone-forming diseases and when they start to act on the skeleton. To understand this it would be necessary to undertake research into the development of entheses and the onset of bone-forming diseases.

8.3.3.2 Common Extensor Origin

The common extensor origin is the common enthesis of the *extensor carpi radialis brevis*, *extensor digitorum communis*, *extensor digiti minimi*, *extensor carpi ulnaris* and *supinator* (Stone and Stone 2000), occurring on the lateral epicondyle of the humerus. These muscles have the function of extending the hand, fingers and wrist and to supinate the forearm. Little clinical literature could be found concerning enthesopathies at this site (Medline search 2008), but these muscles are commonly involved in sports and occupational injuries, leading to pain at the lateral epicondyle of the humerus. This is commonly known as "tennis elbow". The clinical term for this condition is lateral epicondylitis (Martin 2000).

8.3.3.2.1 Common extensor origin: enthesopathies and skeleton size

The common extensor origin on the lateral epicondyle of the humerus was measured and the surface curvature calculated using the methodology described in Chapter 6. The results of these measurements were very interesting. It was found that the size of the humerus in general was not statistically significantly different between normal entheses and those with enthesopathies (not bone formers). In contrast, the overall length, size of the humeral head, and epicondylar width were all larger in bone formers than normal skeletons. The transverse head of the humerus was also statistically significantly larger in the bone formers than in those skeletons with enthesopathies at the common extensor origin (not diagnosed with bone-forming disease). It is surprising that measurements remote from the lateral epicondyle demonstrate these changes. At the lateral epicondyle statistically significant differences were found. Measurements of both the x- and y-axis were significantly smaller in the normal skeletons compared with either those skeletons with enthesopathies or bone formers. This contradicts the hypothesis that individuals with entheses too small to effectively dissipate stress are more likely to have enthesopathies. No statistically significant difference was found between the skeletons with enthesopathies and the bone formers. It is also surprising that bone formers differ significantly from the other skeletons, despite the fact that the diseases thought to

cause these changes occur primarily in adulthood and not during the growth of the skeleton. Perhaps this hypothesis is incorrect and that these diseases cause skeletal change prior to growth completion. Future research to test this hypothesis would be required. However, it is possible that it is a result of small sample size or sample bias.

8.3.3.2.2 Common extensor origin: Measurement Correlations

It was hypothesised in Chapter 6 that the size of the bone should correlate with enthesis size, *i.e.* larger individuals should have larger entheses. To test this, Pearson correlation coefficients (and where appropriate Spearman`s rho) were calculated between measurements of the bone and the x- and y-axis of the entheses. The primary test was to determine whether the x- and y-axes of the entheses correlated; which they did, unlike those of the *supraspinatus* insertion. It is probable that this is because there is more space around the common extensor origin enthesis because it is located outside the joint capsule (Gray 1974). Further correlations were expected between the common extensor origin size and the anatomical landmarks close by: the condylar and epicondylar width. These were expected because development of these structures occurs together (Scheuer and Black 2000b). The proposed correlations were found. Correlations were not expected between the common extensor origin size and measurements of the humeral head because the muscles originating at this enthesis do not act upon the shoulder, but only upon the hand, wrist and elbow. However, correlations were found. They were also found between the enthesis and minimum circumference and maximum length, but not for either the robusticity or the humeral head index. Correlations probably occur for developmental reasons.

Correlations between enthesis size and roughness parameters were analysed to determine whether the size alone affected the roughness parameter values. If this were found to be the case, then these roughness parameters may not be useful for the analysis of roughness itself. However, the parameters chosen should not be affected by size of the enthesis, so if size and roughness do correlate then this may demonstrate shape variation with size. Pearson correlation coefficients (and where appropriate Spearman's rho) were calculated for all the roughness parameters and both common extensor axes x and y. Statistically significant (at $\alpha = 0.05$ level)

correlations were found between the common extensor origin axis x dimensions and peak number ($p = 0.001$). It was possible that pooling the normal data with that for entheses with enthesopathies may have had an effect on this data; consequently, the data were subdivided into two categories: axis not intersecting anomaly = 1 and axis intersecting anomaly = 4. Peak number was found to correlate with both categories ($p = 0.025$ and $p = 0.020$, respectively). The plots of these data indicate that as the x-axis of the enthesis increased the peak number (defined as the number of peak turning points per unit length) decreased. This means that the surfaces became "less rough" relative to their length. This roughness parameter should, perhaps, be altered to be the number of peaks without dividing by unit length. Then this relationship would not occur.

The same procedure was adopted for the common extensor origin axis y. Common extensor origin axis y size correlated with the Rq of FFT ($p = 0.002$). When subdivided into two categories (axis not intersecting anomaly = 1a and axis intersecting anomaly = 4), no statistically significant (at $\alpha = 0.05$) correlations were found for category 4. Peak frequency ($p = 0.031$), peak number ($p = 0.002$) and Rq of FFT ($p = 0.026$) all demonstrated statistically significant (at $\alpha = 0.05$) Pearson correlation coefficients with common extensor origin axis y size. Spearman's rho demonstrated a statistically significant difference between common extensor origin axis y size and HSC ($p = 0.01$), but this is likely the cause of outliers (Chapter 7). Therefore, common extensor origin axis y size and shape correlate for entheses in which the axis does not intersect the anomaly.

8.3.3.2.3 Common extensor origin: Discriminant Function Analysis

Discriminant function analysis of this data indicates that relative length is the best overall method of classifying the common extensor origin x by enthesopathy presence (Table 8.3). With the common extensor origin axis x divided into the three categories (1 = normal, 2 = abnormal, and 3 = bone former), the best discriminating of the parameters was relative length. This parameter alone correctly accounted for 50.0 percent of the entheses. The best classification result achieved was 75 percent using

relative length, area displacement, mean displacement, Ra, and mean slope. The eigenvalues and Wilks' lambda of the first function demonstrate that this is statistically significant, but the second function was not. Box's M was significant, indicating internal covariation. However, unlike the *supraspinatus* entheses the bone formers are not readily classified. Only 53.8 percent (7 out of 13) were correctly classified, the rest were classified as category 2. The bone formers were removed to determine whether roughness parameters could be used to distinguish between normal and abnormal entheses. It was found that 82.9 percent of the remaining entheses could be correctly classified using Rq, skewness, kurtosis, Ra, and area displacement. All the data, including the bone formers, were then divided into two categories (axis not intersecting anomaly = 1 and axis intersecting anomaly = 4) to determine if better results could be achieved by studying the presence of anomalies visible on the curves. The best results were achieved using relative length and mean displacement, producing 79.2 percent classification accuracy with both categories having almost equal accuracy. This data set was larger than that present for the *supraspinatus* enthesis, so the data were subdivided into five categories: (1 = normal, 21 = abnormal but axis not intersecting anomaly, 22 = abnormal with axis intersecting anomaly, 31 = bone former but axis not intersecting anomaly and 33 = bone former with axis intersecting anomaly). Only 68.8 percent accuracy could be achieved when the data were divided into five categories. This is almost certainly caused by the small sample sizes involved; for example there is only one enthesis classified in category 21. However, this analysis does indicate that future studies with larger and more equal sample sizes are necessary.

Discriminant function analysis for common extensor origin axis y was more problematic than for the x-axis. For the three category analysis (1 = normal, 2 = abnormal, and 3 = bone former), no combination of roughness parameters correctly assigned more than 68.0 percent of cases correctly. The roughness parameters used to achieve this were: Rq of FFT, mean slope, peak number, and area displacement. It was decided not to reanalyse this data with the bone formers removed because it is unlikely that this would affect the classification of category 1. However, when divided into two categories (1a = axis not intersecting anomaly 4 = axis intersecting anomaly), to determine if better results could be achieved by studying the presence of anomalies visible on the curves, the maximum percentage of entheses correctly assigned was

88.0 percent, using Rq of FFT, peak number, HSC, and Rq of FFT. This improvement in classification was as expected because part of the aim of this research was to develop a method that could be used to distinguish between those entheses with and those without anomalies. It is possible that the small sample sizes led to the poor classification when entheses were divided into five categories (1 = normal, 21 = abnormal but axis not intersecting anomaly, 22 = abnormal with axis intersecting anomaly, 31 = bone former but axis not intersecting anomaly and 33 = bone former with axis intersecting anomaly). The best classification achieved was 64.0 percent, but this did represent 80.0 percent correct classification for category 1, again demonstrating that the method does have potential.

Table 8.3 Common extensor origin: Parameters best suited to describe this enthesis.

	Roughness parameters	**Comment**
Common extensor origin x 3 categories	Relative length, area displacement, mean displacement, Ra and mean slope	Only 75% overall accuracy, but 87.5% accuracy for category 1 and 78.9% for category 2. Category 3 has only 53.8% accuracy
Common extensor origin x 2 categories (1a = axis not intersecting anomaly 4 = axis intersecting anomaly)	Relative length and mean displacement	Overall 79.2% accuracy. Box's M p-value 0.025
Common extensor origin x 5 categories	All	100% (1/1) of category 21 assigned as category 1
Common extensor origin y 3 categories	Rq of FFT, mean slope, peak number, and area displacement	
Common extensor origin y 2 categories (1a = axis not intersecting anomaly 4 = axis intersecting anomaly)	HSC, peak number, Rq of FFT and peak frequency	All of these roughness parameters correlated with the size of this enthesis axis
Common extensor origin y 5 categories	All (for 64.0%)	HSC, peak number, Rq of FFT, peak frequency, mean displacement and mean slope for 62.0%

The trend in shape is for a slope from the most lateral point, where an exostosis is often present in the abnormal entheses, down towards the condyle of the humerus. The roughness parameters which seem to best classify axis x of this enthesis are the hybrid parameter relative length which measures both horizontal and vertical elements and displacement of the curve from the mean line. This is unsurprising given the general sloping tendency which these curves have, which would have had considerable effect on such roughness parameters as Rq and Ra. The curves indicate

that the bone formers have variable shape, which probably accounts for the difficulty of their classification. In contrast, the common extensor origin axis y is generally convex in shape with occasional additional peaks. It is these additional peaks which seem to be most important in terms of classification because the best classifying roughness parameters are those that measure variation in height. Note also that these correlated with the size of the enthesis, as hypothesised. This relationship between enthesis size and shape, which clearly exists for this enthesis, might indicate that size itself could be used to distinguish between the different types of entheses.

8.3.3.3 *Biceps Brachii*

The *biceps brachii* insertion occurs on the bicipital (or radial) tuberosity of the radius. It also inserts into an aponeurosis which ends in the deep fascia of the forearm (Chew and Giuffré 2005). The muscle supinates and flexes the forearm from its origin on the scapula (Stone and Stone 2000).

8.3.3.3.1 *Biceps brachii*: enthesopathies and skeleton size

Size differences in the whole bone measurements between different classes of entheses (1 = normal, 2 = abnormal and 3 = bone former) were only found for the maximum length of the radius between the normal and the abnormal entheses. However, normal enthesis size (both in the x- and y-axes) was smaller than either the abnormal or bone former class, with the bone formers also larger than the abnormal entheses. This reflects the findings found for the other entheses. It indicates that enthesopathies do not form in entheses which are least capable of dissipating force because they have a small surface area. Clinical literature indicates that the *biceps brachii* tendon insertion does not cover the entire bicipital tuberosity (Table 8.4), but occurs on a small section within this area (Forthman, *et al.* 2008; Mazzocca, *et al.* 2007). It also indicates that there is a small, smooth attachment area surrounded by a rough area and that the attachment does not include the ridge (Mazzocca, *et al.* 2007). This is in contrast to this study which only recorded the smooth area of the bicipital tuberosity quantitatively, but nevertheless found that in the majority of cases the entire

tuberosity was smooth. It is possible that the pressure on an overlying bursa, which exists on the radial side, may cause fibrocartilage to form on the tuberosity, but this is mere supposition. However, clinical findings must be taken into account for all results arising from the measurement of this enthesis.

Table 8.4 Size of the *biceps brachii* enthesis.

Enthesis	Publication	Mean	Range	Comment
Biceps brachii axis x	This study	12.3 mm, standard deviation 3.5	6.76-22.49 mm	
Biceps brachii axis x	Mazzocca *et al.* 2007	15 mm, standard deviation 2 mm	10-19mm	The soft tissue footprint has a mean width of 2 mm, standard deviation 0.3 mm
Biceps brachii axis x	Forthman *et al.* 2008	7.1 mm, standard deviation 2.8 mm	3.6-12.7 mm	
Biceps brachii axis y	This study	23.7 mm, standard deviation 3.2 mm	15.82-32.21 mm	
Biceps brachii axis y	Mazzocca *et al.* 2007	22 mm, standard deviation 3 mm	16-30 mm	The soft tissue footprint has a mean length of 14 mm, standard deviation 2 mm
Biceps brachii axis y	Forthman *et al.* 2008	21.5 mm, standard deviation 2.3 mm	13.8-27.3mm	

8.3.3.3.2 *Biceps brachii*: Measurement Correlations

Biceps brachii x and y axis dimensions demonstrated a statistically significant ($p = 0.000$) linear correlation using Spearman's rho. One further statistically significant linear correlation in size was found between the x-axis and the medio-lateral diameter of the radius ($p = 0.016$), using Pearson's correlation coefficient. No further correlations were found. Features of the development of the radial tuberosity during growth are not fully understood. One hypothesis for the development is that the radial tuberosity is a flake epiphysis with a very short ossification and fusion time making it difficult to study (Scheuer and Black 2000b). Consequently, these findings are difficult to interpret.

Pearson correlation coefficients were not statistically significant between *biceps brachii* axis y and any of the roughness parameters. However, statistical significance was found between *biceps brachii* axis x and peak number ($p = 0.043$) and area displacement ($p = 0.000$). Where the x-axis did not intersect an anomaly (category 1a), this statistical significance occurred for HSC ($p = 0.005$) and peak number ($p = 0.008$). These correlations indicate that the larger the enthesis was, the lower the roughness parameter value. This was expected because the number of peaks is measured per unit length. The visual appearance of this enthesis indicated that many of the peaks occurred at either end of the enthesis whilst little activity occurred in the centre. Consequently, the number of peaks is similar, but because length varies this negative correlation occurs. Statistically significant Pearson correlation coefficients and Spearman's rho ($\alpha = 0.05$) were found for other roughness parameters, but linear fit and outlier removal indicated that these were not relevant correlations (Chapter 7).

8.3.3.3.3.3 ***Biceps brachii*: Discriminant Function Analysis**

Discriminant function analysis of the three categories (1 = normal, 2 = abnormal, and 3 = bone former) was poor at correctly classifying the entheses, even when multiple roughness parameters were combined. The best classification was achieved using: peak number, meal slope, peak frequency, relative length and HSC (Table 8.5). However, this achieved only 66.0 percent accuracy and only 40.0 percent for category 3. It was decided that the bone formers were probably causing these poor results because the majority of bone formers had enthesopathies intersected by the profile gauge. Therefore, bone formers should be expected to cluster with the abnormal entheses for which the majority also had enthesopathies intersected by the profile gauge. Removal of the bone formers leaving only categories normal (1) and abnormal (2) led to an improvement in classification: 86.5 percent could be correctly classified using the roughness parameters Rq, Ra, mean slope, HSC, mean displacement, area displacement, and Rq of FFT. However, category 1 entheses were still poorly classified with only 63.6 percent correct. Those four incorrectly classified entheses all appear to be less curved than the others (see Figure 8.5 and Appendix VI.).

Figure 8.5 *Biceps brachii* x: skeleton F219 right side versus skeleton F98 right side.



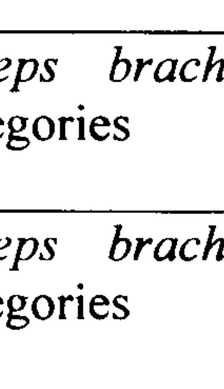
F219 F98

To determine if this was caused by the combination in category 2 of curves which did intersect the line with those which did not, these categories were separated. The following categories were formed: 1a = axis not intersecting anomaly (includes normal, abnormal and bone formers) and 4 = axis intersecting anomaly (includes abnormal and bone formers). The percentage correctly assigned was higher than the 3 category model at 82.0 percent, but again category 1a was only correctly classified in 56.3 percent of cases (9 out of 16). This may well be caused by the sample size difference, or the normal variation in shape of this enthesis. The roughness parameters used to achieve this were: Rq, mean slope, peak frequency, relative length, mean displacement, and Rq of FFT. These parameters have internal covariance (Box's M p = 0.004), however, this is to be expected given the overlap in their mathematical definitions. The data were then subdivided into five categories (1 = normal, 21 = abnormal but axis not intersecting anomaly, 22 = abnormal with axis intersecting anomaly, 31 = bone former but axis not intersecting anomaly, and 33 = bone former with axis intersecting anomaly) to determine if the poor classification results for category 1a were caused by the pooling of normal, abnormal and bone former data. However, sample sizes for categories 21 and 31 were extremely small (3 and 2, respectively). It is likely that this affected the overall classification results, as the overall classification was 60.0 percent correct using all roughness parameters.

Discriminant function analysis of the *biceps brachii* axis y data demonstrates that for 3 categories (1 = normal, 2 = abnormal, and 3 = bone former) the classification using the majority of the roughness parameters was poor at only 72.0 percent accurate. For the bone formers this was reduced to 33.3 percent. For this reason discriminant function analysis was performed on the normal and abnormal data with the bone formers removed. This improved accuracy to 86.5 percent, but only 63.6 percent (7 out of 11) of the normal entheses were correctly classified. Those incorrectly

classified typically had a "peak" near the midpoint of the axis (Figure 8.6). When subdivided into two categories (axis not intersecting anomaly = 1a and axis intersecting anomaly = 4), the maximum percentage correctly classified was 76.0 percent. Using this classificatory system only 60.9 percent of the category 4 entheses were correctly classified, but the Wilks' lambda is statistically significant, indicating that the model is discriminating. When subdivided into five categories (1 = normal, 21 = abnormal but axis not intersecting anomaly, 22 = abnormal with axis intersecting anomaly, 31 = bone former but axis not intersecting anomaly, and 33 = bone former with axis intersecting anomaly) only 58.0 percent were correctly classified. However, it was only the bone formers (categories 31 and 33) which were poorly classified. This is unsurprising given that no differences were expected to be found between these and other entheses, excepting in the frequency of appendicular enthesopathies found.

Figure 8.6 *Biceps brachii* y: skeleton F35 left side in comparison with skeleton F98 left side.



F98 F35

Table 8.5 *Biceps brachii*: Parameters best suited to describe this enthesis.

	Roughness parameters	**Comments**
Biceps brachii x 3 categories	Peak number, mean slope, peak frequency, relative length, and mean displacement	Only 40% of category 3 correctly classified. Peak number correlated with the size of this enthesis axis
Biceps brachii x 2 categories (1a and 4)	Rq, mean slope, peak frequency, relative length, mean displacement, and Rq of FFT	only 56.3% of category 1a correctly classified
Biceps brachii x 5 categories	All	Box's M p = 0.005 and category 33 only 36.4% (4/11) correctly classified
Biceps brachii y 3 categories	Rq, Ra, HSC, mean slope, relative length, peak number, mean displacement, area displacement, and Rq of FFT	only 33.3% of category 3 correctly classified
Biceps brachii y 2 categories	HSC, peak frequency, and Ra	
Biceps brachii y 5 categories	HSC, area displacement, and Rq of FFT	only 33.3% of both category 31 and 33 correctly classified

Clinically, the *biceps brachii* enthesis is described as having a high degree of

individual variation (Forthman *et al.* 2008). The enthesis shape has, recently, been subdivided into five different shapes (Mazzocca *et al.* 2007). The high degree of individual variation can be attested to by the differences in shape seen in the profile gauge curves, particularly, of the x-axis. This may explain some of the poor findings of the discriminant function analysis. The findings may also not reflect the true anatomy of the site, if the enthesis does only occupy a small internal subsection of the bicipital tuberosity. Future research would require the entheses to be visually categorised following the clinical data, prior to analysis, to avoid this problem. Nevertheless, the roughness parameters still describe the shape of the enthesis and could, therefore, be applied to such future studies.

8.4 Summary of Discussion

The main aims of this research were to determine the aetiology of enthesopathy formation and to create new recording criteria based on these findings. It was also decided that the new recording criteria must be simple, cheap, quantitative and repeatable (low intra- and inter-observer error). Three-dimensional methods were eschewed because of the difficulties of comparing structures without landmarks (O'Higgins pers. comm.; Bookstein 1991). For this reason, two-dimensional methods were explored, enabling both size and surface shape to be recorded. The use of the profile gauge enabled the surface of the enthesis to be recorded with little intra- or inter-observer error. Visual recording was used to supplement the data on enthesopathy type, *e.g.* spur or lytic lesion presence. Clinical data could not be used to determine the cause of the different lesions, nor could it supply information on whether acute or chronic trauma could be differentiated on the basis of lesions. This clearly contradicts Hawkey and Merbs (1995) who stated that lytic lesions were supposedly caused by micro-trauma and bone spurs by macro-trauma. Consequently, interpretations of activity based on the Hawkey and Merbs method is highly questionable. Enthesopathy formation is also related to the ageing process, but it is not possible to distinguish between normal ageing and activity-related enthesopathy formation. Enthesopathies caused by diseases cannot be distinguished either. There is also no basis for the concept that activity affects enthesopathy location in the seronegative spondyloarthropathies, as posited by Hawkey (1998).

It has been demonstrated that enthesopathies occur more frequently in larger entheses. This appears to contradict the hypothesis that enthesopathies should be most common in smaller entheses because there is a smaller surface area to dissipate force. However, in the case of the common extensor origin there was a correlation between larger entheses and larger bone size (as measured using normal anatomical landmarks). This may indicate that larger individuals had larger entheses and that this increased size predisposed these individuals to injury at entheses. Not all entheses demonstrated correlations between their size and local bone structures. This is probably caused by developmental factors and local constraints on enthesis size, particularly in those entheses within joint capsules. Further research is required to determine the relationship between size of entheses and size of the individual and development of entheses. This would enable conclusions to be drawn on size-related enthesopathy formation and on enthesopathy size in bone formers.

It has been demonstrated that bone formers have more appendicular enthesopathies than normal individuals. In this study bone formers were distinguished by the presence of sacroiliac joint enthesopathy in combination with spinal enthesopathy. It is not clear whether all of these individuals have a bone-forming disease, have an ossifying diathesis, or have sacroiliac and spinal enthesopathy caused by activity-related stress. Further research is required to determine the cause of these changes. Clinically, there are no simple tests to determine the presence of these diseases, but many individuals with seronegative spondyloarthropathies have HLA-B27. It may be possible to test for this in skeletal remains, but it is not a *sine qua non* of these diseases. Clinical studies of these diseases need monitoring by palaeopathologists to remain up to date with new diagnostic criteria. The aetiology of these diseases is currently uncertain, and it may be possible that palaeopathology can add to the understanding of these diseases.

Most importantly this research has demonstrated that there is shape variation within normal entheses. This is of immense importance for the understanding of how force is dissipated at the enthesis. Consequently, it is also of importance for understanding the pathogenesis of abnormality development. This is supported by clinical data of size and shape of the *biceps brachii* insertion, which is proving to be important for

reconstruction of ruptured entheses (Forthman, *et al.* 2008).

Chapter 9. Conclusions

9.1 Review of Clinical and Bioarchaeological Literature

The purpose of the literature reviews was to place enthesopathy formation in context and to determine the causes of enthesopathy formation. In the bioarchaeological literature, there have been many studies of activity-related stress in archaeologically derived human skeletal remains. Methods used range from the study of DJD, the measurement of the shape of the bone structure (*e.g.* cross-sectional geometry), the presence of trauma as well as the study of MSM (see Chapter 2). MSM are enthesopathies in the skeleton, thought to be caused by activity-related repetitive movement. This means that their aetiology is fixed in the mind of these researchers. The aim of this research was to determine if this is a tenable hypothesis. If it were confirmed, then no other causes of enthesopathies should exist and the link between repetitive movement and enthesopathies would have to be direct. The review of the anatomical literature indicates that this is not the case. There are different types of enthesis, with different developmental features in differing mechanical environments. Consequently, enthesopathies cannot all be recorded using the same methodology and interpretation of the results must occur with these factors in mind.

Two further literature reviews were undertaken. The first studied the role of physical stress, occupation and one-off trauma on entheses (see Chapter 4). The second reviewed the literature on disease-related enthesopathy formation (see Chapter 5). Whilst bioarchaeologists have often assumed a direct link between MSM and activity-related stress, clinical literature paints a different picture. Injury to entheses has many causes. The ageing process, biological sex, obesity and smoking are all important factors in enthesopathy formation. Many differing types of injury can occur, from one-off trauma to chronic (repetitive) trauma. However, the healing process of entheses after injury is not fully understood, so the differing appearance of entheses (discussed in Chapter 2) cannot be attributed to a single cause. Causes of bone spur formation have been recorded with differing aetiologies, as have lytic lesions. For these reasons each type of lesion cannot be attributed to a particular cause. Some diseases also cause enthesopathy formation, and this must be taken into account when studying MSM. It is clear from the literature that the appearance of these

enthesopathies does not differ from those caused by repetitive stress, this is because there are a limited number of responses of these tissues to injury or disease processes. For this reason it is necessary to have a rigorous method for the diagnosis of these diseases in archaeologically derived human skeletal remains. Without this enthesopathies caused by disease will be recorded incorrectly as being caused by activity-related stress.

9.2 Pilot study

The pilot study was used to develop a new digital recording method that did not require large data sets or encounter conservation problems. It was also important that the final method should be cheap, simple and repeatable, so that it can be widely used. It was decided that only fibrocartilaginous entheses should be recorded because of the lack of literature on the normal and abnormal appearance of fibrous entheses (as discussed in Chapter 3). The upper limb was chosen because this thought to be the best part of the body to study occupational stress; the lower limb is affected by normal locomotion and body weight (see Chapter 2).

A visual system was also created to increase the information on types of enthesopathy found at entheses. The Hawkey and Merbs (1995) recording method was considered for use, but it does not take into account the normal appearance of entheses, nor do any of the methods published prior to 2006 (Villotte 2006). For this reason a new method had to be developed. The normal appearance of fibrocartilaginous entheses is smooth and well-delimited (Benjamin, *et al.* 2002). Any deviation from this was considered to be an enthesopathy. Spurs and lytic lesions are the most commonly discussed, but porosity and woven bone can occur on the surface of fibrocartilaginous entheses. They also have "speed bump-like" structures along the surface, giving an uneven appearance to an otherwise normal enthesis. In some cases, and this was especially common at the *subscapularis* insertion, the surface had completely lost smoothness and had the appearance of cortical bone. This may indicate total rupture of the tendon leading to the loss of the enthesis (which is no longer required if the muscle is not attached to the bone). This is conjecture because clinical literature tends to focus either on the soft tissue changes or damage to the bone, but not to the injury

or healing of the enthesis itself. This variation was recorded descriptively. Visual appearance was also used to find the edges of the enthesis for measurement. Measurement was undertaken to quantify their size and to compare with the size of the dry bones. Measurement of the bones had low inter- and intra-observer error rates.

Cheap digitisation of the entheses was more problematic (see Chapter 6). Three-dimensional laser scanning was considered, but this equipment is not available to all bioarchaeologists. Artificial drawing of a line across an enthesis was attempted using a laser beam and a camera on a long exposure setting. However, determining the start and end points of the enthesis was hard on the final image. This method also required motorisation of the laser to keep it tracking along a straight line. This method was difficult to use and required specialist equipment. The second method used FIMO, a moulding agent used by conservation units. However, bone can be very friable and this method required contact between the bone and the FIMO. It was decided that for conservation reasons, this was an inappropriate method for storing the enthesis data. The final method tested involved the use of a profile gauge and a scanner to record the two dimensional curvature of the enthesis. This formed the basis of the new recording method.

9.3 New Method

The aim of the experimental study was to create a new recording method which was simple and cheap to use, repeatable and quantitative. Most importantly, it had to be based on the information derived from the literature reviews. Two key features stood out from these: firstly, that two types of enthesis exist (fibrous and fibrocartilaginous) and, secondly, that many diseases can cause enthesopathy formation. Therefore, differential diagnoses for enthesopathies were considered vital and criteria developed from the literature review of disease-related enthesopathy formation were created to group the skeletons into "normal" individuals (*i.e.* those with no sign of these diseases) and "bone formers" (*i.e.* individuals with possible disease-related enthesopathy formation). It should be noted here that the definition for "bone formers" (defined in Chapter 1 as: individuals with a propensity to have enthesopathies. By definition in this thesis, this requires enthesopathies at the

sacroiliac joint and in the spine) is not the same as the definition proposed by Rogers and colleagues (1997) because the presence of osteophytes is not required.

A further goal of the experimental research was the creation of a quantitative recording method. Reburial of archaeologically derived human skeletal remains is becoming more common. With a digital method, it is possible to store data and reinterpret it at a later date without recourse to study the skeleton. Therefore, a digital method was created with a quantitative method of analysis. For simplicity and cost-effectiveness a two dimensional recording method was created using a profile gauge (commonly used in archaeology for the analysis of pottery). The line drawn was then scanned onto a computer. This enabled the surface curvature to be recorded in a repeatable manner (see Chapter 7). Measurements of the entheses were also made to record size. In this manner size and curvature were recorded and the data stored indefinitely. Curvature of the entheses was then assessed using roughness parameters commonly used in materials science. This was performed to determine which of the roughness parameters were best at differentiating between normal and abnormal entheses. Bone formers were also tested.

Summary of the experimental study:

- A new recording method for fibrocartilaginous entheses was created based on the anatomical literature and taking into account the clinical literature on physical stress and disease-related enthesopathy formation.
    - One recording method was visual and was defined by the smoothness of the enthesis. If the enthesis was not smooth, then it was considered abnormal and the type of abnormality was described.
    - A quantitative method for analysis of the data was created based on the size and curvature of the enthesis.
        - The data on curvature and size is stored digitally. This means that the data can be analysed using different quantitative methods, based on the research questions posed or new breakthroughs in the understanding of enthesopathy formation.

Results of the experimental study:

- Many different types of abnormality occur at entheses. Some of these have not

been described in the bioarchaeological literature previously, such as the presence of woven bone on the surface of an enthesis.

- Bone formers have more appendicular enthesopathies than other skeletons.
- Individuals with fractures have more enthesopathies, which may be related to the trauma that caused the fracture.
- The size of entheses varies between normal entheses, entheses with abnormalities and bone formers. Unexpectedly, statistically significant differences exist in the size of entheses in bone formers. The cause of this is unknown, but may indicate systemic changes occurring during development and growth.
- The size of entheses does not always correlate (in a linear manner) with the size of the bone or the size of the joint upon which they act. In the case of the *supraspinatus* and *biceps brachii* insertions, this is probably caused by localised anatomical constraints, such as the presence of joint capsules or bursae.
- The curvature of the entheses can be described using roughness parameters. These roughness parameters were able to distinguish between normal and abnormal entheses and differentiate bone formers (using discriminant function analysis). The success rate was not 100 percent, but this is not surprising given that there is considerable normal variation in curvature of entheses.

9.4 Limitations

The following limitations were found:

- This study was not performed on skeletons of known occupation. This is the greatest limitation of this study because it is unclear which features of enthesis structures are best for recording occupation.
- Sample sizes were small.
- More entheses of the upper limb need to be studied.
- There is a lack of clinical information on the effects of activity-related stress on fibrous entheses.
- A method for recording fibrous entheses is required.
- Modern clinical evidence of the effect of activity-related stress on entheses is

required.

9.5 Future research

New recording methods for enthesopathies were required because bioarchaeological literature on MSM did not take into account new clinical and anatomical findings. Further research is necessary to fully understand enthesopathy aetiology, but this cannot be achieved through literature review. Instead, clinical studies are required on the mechanisms of enthesopathy formation (in particularly the different types of enthesopathy recorded experimentally) and their causes. Further bioarchaeological studies are required on skeletons of known age and occupation (such as the crypt sample from Christ Church, Spitalfields, London) to determine if this new method can be used to differentiate between manual labourers and non-manual workers. Changes in the method of quantification of the surface curvature may be required to best achieve this goal.

9.6 Summary

In summary, the new recording methods developed (and interpreted) on the basis of clinical literature reviews have proved valuable in distinguishing between normal and abnormal entheses. These new recording methods have demonstrated that there is normal variation in surface curvature of entheses and that the entheses of bone formers differ in size and shape from other entheses. Further research is required to elucidate this latter finding. Digital recording of entheses is also important in the current climate of reburial of archaeologically derived human remains. This allows re-study and re-interpretation of the size and shape of entheses without recourse to the remains themselves. This avoids the problem of gathering large samples of data from different researchers who use different recording methods.

10 Bibliography

Abrahams, PH, Hutchings, R and Marks, SC. 1998. *McMinn's Colour Atlas of Human Anatomy.* Mosby: London.

Abreu, MR, Chung, CB, Mendes, L, Mohana-Borges, A, Trudell, D and Resnick, D. 2003. Plantar calcaneal enthesophytes: new observations regarding sites of origin based on radiographic, MR imaging, anatomic and palaeopathologic analysis. *Skeletal Radiology.* 32: 13-21

Akfirat, M, Sen, C and Günes, T. 2003. Ultrasonographic appearance of the plantar fasciitis. *Journal of Clinical Imaging.* 27: 353-357

Aldridge, K, Ruff, CB and Beck, TJ. 1998. The effects of physical fitness in the structure of long bone diaphyses: A study of U.S. female Marine recruits [abstract]. *American Journal of Physical Anthropology, Supplement.* 26: 63

Allard, SA, Bayliss, MT and Maini, RN. 1990. The synovium-cartilage junction of the normal human knee. Implications for joint destruction and repair. *Arthritis and Rheumatism.* 33 (8): 1170-1190

Al-Oumaoui, I, Jiménez-Brobeil, S and du Souich, P. 2004. Markers of Activity Patterns in some Populations of the Iberian Peninsula. *International Journal of Osteoarchaeology.* 14: 343-359

Amiel, D, Chu, CR and Lee, J. 1995. Effect of Loading on Metabolism and Repair of Tendons and Ligaments. SL Gordon, SJ Blair and LJ Fine (ed.) *Repetitive Motion Disorders of the Upper Extremity.* American Academy of Orthopaedic Surgeons: Rosemont, Illinois. 217-230

Amor, B, Dougades, M and Mijiyawa, M. 1990. Critères de Classification des Spondyloarthropathies. *Revue du Rhumatisme.* 57 (2): 85-89

Andersson, GBJ. 1995. Epidemiology of Occupational Neck and Shoulder Disorders. SL Gordon, SJ Blair and LJ Fine (ed.) *Repetitive Motions Disorders of the Upper Extremity.* American Academy of Orthopaedic Surgeons: Rosemont, Illinois. 31-42

Ando, W, Sakai, T, Kuduwara, I, Ieguchi, M, Miyamoto, T and Ohzono, K. 2004. Bilateral achilles tendon ruptures in a patient with ochronosis: a case report. *Clinical Orthopaedics and Related Research.* 424: 180-182

Andriacchi, T, Sabiston, P, DeHaven, K, Dahners, L, Woo, SLY, Frank, CB, Oakes, B, Brand, R and Lewis, J. 1988. Ligament: Injury and Repair. SLY Woo and JA Buckwalter (ed.) *Injury and Repair of the Musculoskeletal Soft Tissues.* American Academy of Orthopaedic Surgeons: Park Ridige, Illinois. 103-128

Anonymous. 1997-2003. *Online Medical Dictionary.* Department of Oncology, University of Newcastle Upon Tyne: http://www.medical_dictionary.com/results.php

Anonymous. 2000. *Pseudogout and Calcium Crystal Diseases.* Arthritis Research Campaign: Chesterfield, Derbyshire.

Apley, AG and Solomon, L. 1982. *Apley's System of Orthopaedics and Fractures.* Butterworths: London.

Arayssi, T and Hamden, A. 2004. New insights into the pathogenesis and therapy of Behçet's disease. *Current Opinion in Pharmacology.* 4: 1-6

Arnett, FC. 2001. Ankylosing Spondylitis. WJ Koopman (ed.) *Arthritis and Allied Conditions.* Lippincott Williams and Wilkins: Philadelphia. 1311-1323

Arriaza, B. 1997. Spondylolysis in Prehistoric Human Remains From Guam and its Possible Etiology. *American Journal of Physical Anthropology.* 104: 393-397

Arriaza, B and Standen, V. 2006. 75th Annual Meeting of the American Association of Physical Anthropologists: Skeletal Robusticity and Economies of the Ancient African Populations in northern Chile [abstract]. *American Journal of Physical Anthropology.* 129 (S42): 58

Astruc, L, Vargiolu, R and Zahouani, H. 2003. Wear assessments of prehistoric instruments. *Wear.* 255: 341–347

Auerbach, BM and Ruff, CB. 2006. Limb bone bilateral asymmetry: variability and commonality among modern humans. *Journal of Human Evolution.* 50: 203-218

Aufderheide, AC and Rodríguez-Martín, C. 1998. *The Cambridge Encyclopedia of Paleopathology.* Cambridge University Press: Cambridge.

Awada, H, Abi-Karam, G and Fayad, F. 2003. Musculoskeletal and other extrapulmonary disorders in sarcoidosis. *Best Practice and Research Clinical Rheumatology.* 17 (6): 971-987

Ayers, RS and Westcot, DW. 1984. *Water quality for agriculture.* Food and Agriculture Organization, United Nations: Rome.

Balaban, B, Taskaynatan, M, Yasar, E, Tan, K and Kalyon, T. 2005. Ochronotic spondyloarthropathy: spinal involvement resembling ankylosing spondylitis. *Clinical Rheumatology.*

Bamford, M. 1995. Introduction to occupational health. M Bamford (ed.) *Work and Health: An introduction to occupational health care.* Chapman and Hall: London. 1-21

Banes, AJ, Hu, P, Xiao, H, Sanderson, MJ, Boitano, S, Brigman, B, Fisher, T, Tsuzaki, M, Brown, TD, Almekinders, LC and Lawrence, WT. 1995. Tendon Cells of the Epitenon and Internal Tendon Compartment Communicate Mechanical Signals Through Gap Junctions and Respond Differentially to Mechanical Load and Growth Factors. SL Gordon, SJ Blair and LJ Fine (ed.) *Repetitive Motion Disorders of the Upper Extremity.* American Academy of Orthopaedic Surgeons: Rosemont. 231-245

Barozzi, L, Olivieri, I, De Matteis, M, Padula, A and Pavlica, P. 1998. Seronegative spondyloarthropathies: imaging of spondylitis, enthesitis and dactylitis. *European Journal of Radiology.* 27: S12-S17

Bass, WM. 1995. *Human Osteology: A Laboratory and Field Manual.* Missouri Archaeological Society: Missouri.

Beauchesne, P, Agarwal, SC, Selbie, M, Gordon, C, Saunders, S and Webber, C. 2004. 74th Annual Meeting of the American Association of Physical Anthropologists: The examination of age and sex-related changes in cortical bone mineral density and geometric properties of the radius in a 19th century archaeological population [abstract]. *American Journal of Physical Anthropology.* 126 (S40): 61

Benchakroun, M, El Bardouni, A, Zaddoug, O, Kharmaz, M, Lamrani, MO, El Yaacoubi, M, Hermas, M, Wahbi, S, Ouazzani, N and El Manouar, M. 2004. Tuberculous sacroiliitis. Four cases. *Joint Bone Spine.* 71: 150-153

Benfer, RA and McKern, TW. 1966. The Correlation of Bone Robusticity with the Perforation of the Coronoid-olecranon Septum in the Humerus of Man. *American Journal of Physical Anthropology.* 24: 247-252

Benjamin, M, Evans, EJ, Rao, RD, Findley, JA and Pemberton, DJ. 1991. Quantitative differences in the histology of the attachment zones of the meniscal horns in the knee joint of man. *Journal of Anatomy.* 177: 127-134

Benjamin, M, Kumai, T, Milz, S, Boszczyk, BM, Boszczyk, AA and Ralphs, JR. 2002. The skeletal attachment of tendons - tendon 'entheses'. *Comparative Biochemistry and Physiology Part A.* 133 (4): 931-945

Benjamin, M and McGonagle, D. 2001. The anatomical basis for disease localisation in seronegative spondyloarthropathy at entheses and related sites. *Journal of Anatomy.* 199: 503-526

Benjamin, M, Moriggl, B, Brenner, E, Emery, P, McGonagle, D and Redman, S. 2004. The "Enthesis Organ" Concept: Why Enthesopathies May Not Present as Focal Insertional Disorders. *Arthritis and Rheumatism.* 50 (10): 3306-3313

Benjamin, M, Newell, RLM, Evans, EJ, Ralphs, JR and Pemberton, DJ. 1992. The structure of the insertions of the tendons of biceps brachii, triceps and brachialis in elderly dissecting room cadavers. *Journal of Anatomy.* 180: 327-332

Benjamin, M and Ralphs, JR. 1995. Functional and Developmental Anatomy of Tendons and Ligaments. SL Gordon, SJ Blair and LJ Fine (ed.) *Repetitive Motion Disorders of the Upper Extremity.* American Academy of Orthopaedic Surgeons: Rosemont. 185-203

Benjamin, M and Ralphs, JR. 1996. Tendons in Health and Disease. *Manual Therapy.* 1 (4): 186-191

Benjamin, M and Ralphs, JR. 1997. Tendons and ligaments - an overview. *Histology and Histopathology.* 12: 1135-1144

Benjamin, M and Ralphs, JR. 1998. Fibrocartilage in tendons and ligaments - an adaptation to compressive load. *Journal of Anatomy.* 193: 481-494

Benjamin, M and Ralphs, JR. 1999. The Attachment of Tendons and Ligaments to Bone. CW Archer, B Caterson, M Benjamin and JR Ralphs (ed.) *Biology of the Synovial Joint.* Harwood Academic Publishers: Amsterdam. 361-371

Benjamin, M and Ralphs, JR. 2004. Biology of Fibrocartilage Cells. *International Review of Cytology.* 233: 1-45

Benjamin, M, Rufai, A and Ralphs, JR. 2000. The Mechanism of Formation of Bony Spurs (Enthesophytes) in the Achilles Tendon. *Arthritis and Rheumatism.* 43 (3): 576-583

Benjamin, M, Toumi, H, Ralphs, JR, Bydder, G, Best, TM and Milz, S. 2006. Where tendons and ligaments meet bone: attachment sites ('entheses') in relation to exercise and/or mechanical load. *Journal of Anatomy.* 208: 471-490

Benus, R and Masnicova, S. 2002. *Markers of occupational stress in great Moravian and early middle ages populations from Devin (Southwestern Slovakia) [abstract].* 14th European Meeting of the Paleopathology Association. Coimbra, Portugal.

Beresford, WA. 1981. *Chondroid Bone, Secondary Cartilage and Metaplasia.* Urban & Schwarzenberg: Baltimore.

Berget, KA and Churchill, SE. 1994. 63rd Annual Meeting of the American Association of Physical Anthropologists: Subsistence activity and humeral hypertrophy among western Aleutian Islanders [abstract]. *American Journal of Physical Anthropology, Supplement.* 55

Berkow, R. 1982. *The Merck Manual of Diagnosis and Therapy.* Merk and Company, Incorporated: Rathway, New York.

Bice, G. 2003. *Reconstructing behavior from archaeological skeletal remains: A critical analysis of the biomechanical model.* PhD. Michigan State University.

Biewener, AA, Fazzalari, NL, Konieczynski, DD and Baudinette, RV. 1996. Adaptive Changes in Trabecular Architecture in Relation to Functional Strain Patterns and Disuse. *Bone.* 19 (1): 1-8

Birkett, DA. 1986. The Human Burials in Daniels, R. The Excavation of the Church of the Franciscans, Hartlepool, Cleveland. *Archaeological Journal.* 143: 291-298

Blau, S. 2001. Limited Yet Informative: Pathological Alterations Observed on Human Skeletal Remains from Third and Second Millennia BC Collective Burials in the United Arab Emirates. *International Journal of Osteoarchaeology.* 11: 173-205

Bookstein, FL. 1991. *Morphometric tool for landmark data: geometry and biology.* Cambridge University Press: Cambridge.

Borman, P, Bodur, H and Cihz, D. 2002. Ochronotic arthropathy. *Rheumatology International.* 21: 205-209

Bosilkovski, M, Krteva, L, Caparoska, S and Dimzova, M. 2004. Osteoarticular involvement in brucellosis: study of 196 cases in the Republic of Macedonia. *Croatian Medical Journal.* 45 (6): 727-733

Boulle, E-L. 2000. Nouvelle interprétation d'une variation osseuse du talus. *Comptes Rendus de l'Académie des Sciences - Series IIA - Sciences de la Terre et des planètes.* 331: 615-620

Boulle, E-L. 2001a. Evolution of Two Human Skeletal Markers of the Squatting Position: A Diachronic Study From Antiquity to the Modern Age. *American Journal of Physical Anthropology.* 115: 50-56

Boulle, E-L. 2001b. Osteological Features Associated with Ankle Hyperdorsiflexion. *International Journal of Osteoarchaeology.* 11: 345-349

Bourbou, C. 2003. Health Patterns of Proto-Byzantine Populations (6th-7th centuries AD) in South Greece: The Cases of Eleutherna (Crete) and Messene (Peloponnese). *International Journal of Osteoarchaeology.* 13: 303-313

Boyde, A. 2003. The real response of bone to exercise. *Journal of Anatomy.* 203: 173-189

Boyer, GS, Templin, DW, Bowler, A, Lawrence, RC, Everett, DF, Heyse, SP, Cornoni-Huntley, J and Goring, WP. 1997. A comparison of patients with spondyloarthropathy seen in

specialty clinics with those identified in a communitywide epidemiologic study: has the classic case misled us? *Archives of Internal Medicine.* 157 (18): 2111-2117

Brandi, ML, Gennari, L, Cerinic, MM, Becherini, L, Falchetti, A, Masi, L, Gennari, C and Reginster, J-Y. 2001. Genetic markers of osteoarticular disorders: facts and hopes. *Arthritic Research.* 3: 270-280

Braun, J, Khan, MA and Sieper, J. 2000. Enthesitis and ankylosis in spondyloarthropathy: What is the target of the immune response? (A report from a symposium held at Klinikum Benjamin Franklin, Free University, Berlin, Germany, 25-26 February 2000). *Annals of the Rheumatic Diseases.* 59: 985-994

Braun, J and Sieper, J. 1999. Spondyloarthopathy (letter). *Lancet.* 353 (9163): 1526-1527

Brickley, M, Berry, H, Western, G, Hanccks, A and Richards, M. 2006. The People: Physical Anthropology. M Brickley, S Buteux, J Adams and R Cherrington (ed.) *St Martin's Uncovered: Investigations in the Churchyard of St. Martin's-in-the-Bull-Ring, Birmingham, 2001.* Oxbow Books: Oxford. 90-151

Brickley, M and McKinley, JI. 2004. *Guidelines to the Standards for Recording Human Remains.* British Association For Biological Anthropology and Osteoarchaeology. Institute of Field Archaeologists: Southampton.

Bridges, P. 1997. The relationship between muscle markings and diaphyseal strength in prehistoric remains from West-Central Illinois [abstract]. *American Journal of Physical Anthropology, Supplement.* 24: 82

Bridges, PS. 1989. Changes in Activities with the Shift to Agriculture in the Southeastern United States. *Current Anthropology.* 30 (3): 385-394

Bridges, PS. 1992. Prehistoric Arthritis in the Americas. *Annual Review of Anthropology.* 21: 67-91

Bridges, PS, Blitz, JH and Solano, MC. 2000. Changes in Long Bone Diaphyseal Strength With Horticultural Intensification in West-Central Illinois. *American Journal of Physical Anthropology.* 112: 217-238

Brock, SL. 1985. 54th Annual Meeting of the American Association of Physical Anthropologists: Biomechanical Adaptation of Human Lower Limb Bones in the Prehistoric American Southwest [abstract]. *American Journal of Physical Anthropology, Supplement.* 150

Brock, SL and Ruff, CB. 1987. Diachronic patterns of change in structural properties of the femur in the prehistoric American Southwest. *American Journal of Physical Anthropology.* 75 (1): 113-127

Brothwell, DR. 1981. *Digging up Bones: The excavation, treatment and study of human skeletal remains.* Cornell University Press: Ithaca, New York.

Buckwalter, JA, Rosenberg, L, Coutts, R, Hunziker, E, Reddi, AH and Mow, VC. 1988. Articular Cartilage: Injury and Repair. SLY Woo and JA Buckwalter (ed.) *Injury and Repair of the Musculoskeletal Soft Tissues.* American Academy of Orthopaedic Surgeons: Park Ridge, Illinois. 465-482

Buikstra, JE and Ubelaker, DH. 1994. *Standards for Data Collection from Human Skeletal Remains.* Arkansas Archeological Survey Research Series: Fayetteville, Arkansas.

Bui-Mansfield, LT. 2002. *Osteochondritis Dissecans*. EMedicine: www.emedicine.com/radio/topic495.htm

Burr, DB, Ruff, CB and Thompson, DD. 1990. Patterns of SKeletal Histologic Change Through Time: Comparison of an Archaic Native American Population with Modern Populations. *The Anatomical Record.* 226 (3): 307-313

Cammisa, M, Serio, A and Guglielmo, G. 1998. Diffuse idiopathic skeletal hyperstosis. *European Journal of Radiology.* 27: S7-S11

Cao, J, Zhao, Y, Liu, J, Xirao, R, Danzeng, S, Daji, D and Yan, Y. 2003. Brick tea flouride as a main source of adult fluorosis. *Food and Chemical Toxicology.* 41: 535-542

Capasso, L, Kennedy, KAR and Wilczak, CA. 1999. *Atlas of Occupational Markers on Human Remains.* Edigrafital S.p.A.: Teramo, Italy.

Cardoso, FA. 2008. *A Portrait of Gender in Two 19th and 20th Century Portuguese Populations: A Palaeopathological Perspective.* PhD. Durham. Durham University.

Carlson, KJ, Grine, FE and Pearson, OM. 2007. Robusticity and Sexual Dimorphism in the Postcranium of Modern Hunter-Gatherers From Australia. *American Journal of Physical Anthropology.* 134 (1): 9-23

Carpintero-Benítez, P, Logroño, C and Collantes-Estevez, E. 1996. Enthesopathy in Leprosy. *Journal of Rheumatology.* 23: 1020-1021

Cattaneo, C. 1991. Direct genetic and immunological information in the reconstruction of health and biocultural conditions of past populations: a new prospect for archaeology. H Bush and M Zvelebil (ed.) *Health in Past Societies.* British Archaeological Reports International Series: Oxford. 39-52

Chang, HK, Lee, DH, Jung, SM, Choi, SJ, Kim, JU, Choi, YJ, Baek, SK, Cheon, KS, Cho, EH and Won, KS. 2002. The Comparison Between Behcet's Disease and Spondyloarthritides: Does Behcet's Disease Belong to the Spondyloarthropathy Complex? *Journal of Korean Medical Science.* 17 (4): 524-9

Chapman, NEM. 1997. Evidence for Spanish Influence on Activity Induced Musculoskeletal Stress Markers at Pecos Pueblo. *International Journal of Osteoarchaeology.* 7: 497-506

Chary-Valckenaere, I, Jaulhac, B, Monteil, H and Pourel, J. 1995. Diagnosis of Lyme Disease: Current difficulties and prospects. *Revue du rhumatisme (English ed.).* 62 (4): 271-280

Chew, ML and Giuffré, BM. 2005. Disorders of the Distal Biceps Brachii Tendon. *RadioGraphics.* 25: 1227–1237

Chitnavis, J, Sinsheimer, JS, Suchard, MA, Clipsham, K and Carr, AJ. 2000. End-stage coxarthrosis and gonarthrosis. Aetiology, clinical patterns and radiological features of idiopathic osteoarthritis. *Rheumatology.* 39: 612-619

Choukri, F, Chakib, A, Himmich, H, Huë, S and Caillat-Zucman, S. 2001. HLA-B*51 and B*15 Alleles Confer Predisposition to Behçet's Disease in Moroccan Patients. *Human Immunology.* 62: 180-185

Churchill, SE and Formicola, V. 1997. A Case of Marked Bilateral Asymmetry in the Upper Limbs of an Upper Palaeolithic Male from Barma Grande (Liguria), Italy. *International*

Journal of Osteoarchaeology. 7: 18-38

Churchill, SE and Morris, AG. 1998. Muscle marking morphology and labour intensity in prehistoric Khoisan foragers. *International Journal of Osteoarchaeology*. 8: 390-411

Ciranni, R and Fornaciari, G. 2003. Luigi Boccherini and the Barocco Cello: an 18th Century Striking Case of Occupational Disease. *International Journal of Osteoarchaeology*. 13: 294-302

Clark, CS. 1999. 68th Annual Meeting of the American Association of Physical Anthropologists: Occupational Stress and Trends Toward Asymmetry in Two African Skeletal Populations [abstract]. *American Journal of Physical Anthropology, Supplement*. 108

Clark, J and Stechschulte, DJ. 1998. The interface between bone and tendon at an insertion site: a study of the quadriceps tendon insertion. *Journal of Anatomy*. 193: 605-616

Colao, A, Ferone, D, Marzullo, P and Lombardi, G. 2004. Systemic Complications of Acromegaly: Epidemiology, Pathogenesis, and Management. *Endocrine Reviews*. 25 (1): 102-152

Cole, TM. 1994. Size and shape of the femur and tibia in northern Plains Indians. DW Owsley and RL Jantz (ed.) *Skeletal Biology of the Great Plains: Migration, Warfare, Health, and Subsistence*. Smithsonian Institution Press: Washington. 219–234

Cooper, RR and Misol, S. 1970. Tendon and ligament insertion: a light and electron microscope study. *The Journal of Bone and Joint Surgery A*. 52A (1): 1-20, 170

Cope, JM, Adler, LM, Martin, DL and Potts, DD. 2004. 73rd Annual Meeting of the American Association of Physical Anthropologists: Synergistic musculosketal attachment sites in the upper extremity and activity patterns at Tell Abraq, United Arab Emirates, 2300 BC [abstract]. *American Journal of Physical Anthropology*. 123 (S38): 79

Cope, JM, Berryman, AC, Martin, DL and Potts, DD. 2005. Robusticity and Osteoarthritis at the Trapeziometacarpal Joint in a Bronze Age Population From Tell Abraq, United Arab Emirates. *American Journal of Physical Anthropology*. 126: 391–400

Cornwall, MW and McPoil, TG. 1999. Plantar Fasciitis: Etiology and Treatment. *Journal of Orthopaedic and Sports Physical Therapy*. 29 (12): 756-760

Cramp, R. 2005. *Wearmouth and Jarrow monastic sites*. English Heritage: Swindon.

Crubezy, E, Goulet, J, Bruzek, J, Jelinek, J, Rouge, D and Ludes, B. 2002. Epidemiology of osteoarthritis and enthesopathies in a European population dating back 7700 years. *Joint Bone Spine*. 69: 580-588

Currey, JD. 2002. *Bones: Structure and Mechanics*. Princeton University Press: Princeton.

Curtis, AS, Burbank, KM, Tierney, JJ, Scheller, AD and Curran, AR. 2006. The Insertional Footprint of the Rotator Cuff: An Anatomic Study. *Arthroscopy*. 22 (6): 603-609

Cush, J and Lipsky, PE. 2001. Reiter's Syndrome and Reactive Arthritis. WJ Koopman (ed.) *Arthritis and Allied Conditions*. Lippincott Williams and Wilkins: Philadelphia. 1324-1344

Dandy, DJ and Edwards, DJ. 1999. *Essential Orthopaedics and Trauma*. Harcourt Publishers Ltd.: Edinburgh.

Daneshvari, S and Pearson, OM. 2004. 74th Annual Meeting of the American Association of Physical Anthropologists: Estimation of living body mass from multiple skeletal elements [abstract]. *American Journal of Physical Anthropology.* 126 (S40): 82

Davidson, JM, Rose, JC, Gutmann, MP, Haines, MR, Condon, K and Condon, C. 2002. The Quality of African-American Life in the Old Southwest near the Turn of the Twentieth Century. RH Steckel and JC Rose (ed.) *The Backbone of History: Health and Nutrition in the Western Hemisphere.* Cambridge University Press: Cambridge. 226-277

de Gouw, HW, Westendorp, RG, Kunst, AE, Mackenbach, JP and Vandenbroucke, JP. 1995. Decreased mortality among contemplative monks in The Netherlands. *American Journal of Epidemiology.* 141 (8): 771-775

De Maeseneer, M, Lenchik, L, Everaert, H, Marcelis, S, Bossuyt, A, Osteaux, M and Beeckman, P. 1999. Evaluation of lower back pain with bone scintigraphy and SPECT. *Radiographics.* 19 (4): 901-912

De Paulis, F, Cacchio, A, Michelini, O, Damiani, A and Saggini, R. 1998. Sports injuries in the pelvis and hip: diagnostic imaging. *European Journal of Radiology.* 27: S49-S59

DeGroot, H. 1998. *Myositis Ossificans*. Bonetumor.org: http://www.bonetumor.org/tumors/pages/page177.htm

Denton, N. 2002. 71st Annual Meeting of the American Association of Physical Anthropologists: Osteological markers and habitual behaviors, assessing the connection at Hierakonpolis, Egypt [abstract]. *American Journal of Physical Anthropology, Supplement.* 62

Derevenski, JRS. 2000. Sex Differences in Activity-Related Osseous Change in the Spine and the Gendered Division of Labor at Ensay and Wharram Percy, UK. *American Journal of Physical Anthropology.* 111: 333–354

Devas, M. 1975. *Stress Fractures.* Churchill Livingstone: Edinburgh.

Devlin, MJ. 2004. 74th Annual Meeting of the American Association of Physical Anthropologists: Variation in estradiol level affects diaphyseal bone growth in response to mechanical loading [abstract]. *American Journal of Physical Anthropology.* 126 (S40): 86-87

Di Franco, M, Mauceri, MT, Sili-Scavalli, A, Iagnocco, A and Ciocco, A. 2000. Study of Peripheral Bone Mineral Density in Patients with Diffuse Idiopathic Skeletal Hyperostosis. *Clinical Rheumatology.* 19: 188-192

Dispenzieri, A, Kyle, RA, Lacy, MQ, Rajkumar, SV, Therneau, TM, Larson, DR, Greipp, PR, Witzig, TE, Basu, R, Suarez, GA, Fonseca, R, Lust, JA and Gertz, MA. 2003. POEMS syndrome: definitions and long-term outcome. *Blood.* 101: 2496-2506

Dobson, L. 2005. Time, Travel and Political Communities: Transportation and Travel Routes in Sixth- and Seventh-century Northumbria. *A Journal of Early Medieval Northwestern Europe.* 8: http://www.mun.ca/mst/heroicage/issues/8/dobson.html

Donnelly, LF, Bisset, GS, Helms, CA and Squire, DL. 1999. Chronic avulsive injuries of childhood. *Skeletal Radiology.* 28: 138-144

Dörfl, J. 1969a. Vessels in the Region of Tendinous Insertions. I. Chondroapophyseal Insertion. *Folia Morphologica.* 17 (1): 74-78

Dörfl, J. 1969b. Vessels in the Region of Tendinous Insertions. II. Diaphysoperiosteal

Insertion. *Folia Morphologica.* 17 (1): 79-82

Dörfl, J. 1980a. Migration of tendinous insertions. I. Cause and mechanism. *Journal of Anatomy.* 131 (1): 179-195

Dörfl, J. 1980b. Migration of tendinous insertions. II. Experimental modifications. *Journal of Anatomy.* 131 (2): 229-237

Dougades, M, van der Linden, S, Juhlin, R, Huitfeldt, B, Amor, B, Calin, A, Cats, A, Dijkmans, B, Olivieri, I, Pasero, G, Veys, E and Zeidler, H. 1991. The European Spondyloarthropathy Study Group Preliminary Criteria for the Classification of Spondyloarthropathy. *Arthritis and Rheumatism.* 34 (10): 1218-1227

Douglas, MT, Petrusewsky, M and Quebral, RMI. 1997. Skeletal Biology of Apurguan: A Precontact Chamorro Site on Guam. *American Journal of Physical Anthropology.* 104: 291-313

Drapeau, MSM. 2006. 75th Annual Meeting of the American Association of Physical Anthropologists:Upper-and lower-limb skeletal muscle site variability in modern humans [abstract]. *American Journal of Physical Anthropology.* 129 (S42): 84

Dürr, HR, Lienemann, A, Sübernagl, H, Nerlich, A and Refior, HJ. 1997. Acute calcific tendinitis of the pectoralis major insertion associated with cortical bone erosion. *European Radiology.* 7: 1215-1217

Dutour, O. 1986. Enthesopathies (lesions of muscular insertions) as indicators of the activities of neolithic Saharan populations. *American Journal of Physical Anthropology.* 71: 221-224

Econs, J. 1999. New Insights Into the Pathogenesis of Inherited Phosphate Wasting Disorders. *Bone.* 25 (1): 131–135

Elliott, D. 1967. The Biomechanical Properties of Tendon in Relation to Muscular Strength. *Annals of Physical Medicine.* 9 (1): 1-7

Enna, CD. 1982. Leprosy (Hansen's Disease). R Berkow (ed.) *The Merck Manual of Diagnosis and Therapy.* Merck and Company, Incorporated: Rahway, New York. 140-143

Erdem, CZ, Sarikaya, S, Erdem, LO, Ozdolap, S and Gundogdu, S. 2005. MR imaging features of foot involvement in ankylosing spondylitis. *European Journal of Radiology.* 53: 110-119

Etaouil, N, Benyahya, E, Bennis, R and Mkinsi, O. 2002. Ankylosing spondylitis and Behçet's disease in combination. Two case reports. *Joint Bone Spine.* 69: 95-96

Etxeberria, F and Herrasti, L. 1991. War Injuries in a Field Hospital Dating to the Beginning of the Nineteenth Century in th Basque Country (Spain). *International Journal of Osteoarchaeology.* 1: 279-282

Evereklioglu, C. 2005. Current concepts in the etiology and treatment of Behçet disease. *Survey of Ophthalmology.* 50 (4): 297-350

Evison, MP, Fieller, NRJ and Smillie, DM. 1999. Ancient HLA: A Preliminary Survey. *Ancient Biomolecules.* 3 (1): 1-28

Faccia, KJ and WIlliams, RC. 2008. Schmorl's Nodes: Clinical Significance and Implications for the Bioarchaeological Record. *International Journal of Osteoarchaeology.* 18 (1): 28-44

Fallon, J, Blevins, FT, Vogel, K and Trotter, J. 2002. Functional morphology of the supraspinatus tendon. *Journal of Orthopaedic Research.* 20: 920–926

Fiorato, V, Boylston, A and Knusel, CJ. 2001. *Blood Red Roses: The archaeology of a mass grave from the Battle of Towton AD 1461.* Oxbow: Oxford.

Flemming, DJ, Murphey, MD, Shekitka, KM, Temple, HT, Jelinek, JJ and Kransdorf, MJ. 2003. Osseous Involvement in Calcific Tendinitis: A Retrospective Review of 50 Cases. *American Journal of Roentgenology.* 181: 965-972

Formicola, V, Frayer, DW and Heller, JA. 1990. Bilateral Absence of the Lesser Trochanter in a Late Epigravettian Skeleton From Arene Candide (Italy). *American Journal of Physical Anthropology.* 83: 425-437

Forthman, CL, Zimmerman, RM, Sullivan, MJ and Gabel, GT. 2008. Cross-sectional anatomy of the bicipital tuberosity and biceps brachii tendon insertion: Relevance to anatomic tendon repair. *Journal of Shoulder and Elbow Surgery.* in press:

Foster, A. 1995. The effects of work on health. M Bamford (ed.) *Work and Health: An introduction to occupational health care.* Chapman and Hall: London. 22-38

Fournié, B. 1993. Le territoire enthésique, une approche élargie du concept d'enthèse. *Le Presse Médicale.* 22 (35): 1767-1769

Fournié, B. 2004. Pathology and clinico-pathologic correlations in spondyloarthropathies. *Joint Bone Spine.* 71 (6): 525-529

France, DL. 1988. Osteometry at Muscle Origin and Insertion in Sex Determination. *American Journal of Physical Anthropology.* 76: 515-526

Franck, C, Woo.S., Andriacchi, T, Brand, R, Oakes, B, Dahners, L, DeHaven, K, Lewis, J and Sabiston, P. 1988. Normal Ligament: Structure, Function, and Composition. SLY Woo and JA Buckwalter (ed.) *Injury and Repair of the Musculoskeletal Soft Tissues.* American Academy of Orthopaedic Surgeons: Park Ridge, Illinois. 45-101

Franco, G. 1999. Ramazzini and workers' health. *Lancet.* 354: 858-861

François, RJ, Braun, J and Khan, MA. 2001. Entheses and enthesitis: a histopathologic review and relevance to spondyloarthritides. *Current Opinion in Rheumatology.* 13: 255-264

François, RJ, Gardner, DL, Degrave, EJ and Bywaters, EGL. 2000. Histopathologic evidence that sacroiliitis in ankylosing spondylitis is not merely enthesitis. *Arthritis and Rheumatism.* 43 (9): 2011-2024

Fung, DT and Ng, GY. 2005. Herbal remedies improve the strength of repairing ligament in a rat model. *Phytomedicine.* 12 (1-2): 93-99

Gadelmawla, ES, Koura, MM, Maksoud, TMA, Elewa, IM and Soliman, HH. 2002. Roughness parameters. *Journal of Materials Processing Technology.* 123: 133-145

Ganong, WF. 2001. *Review of Medical Physiology.* Lange Medical Books: New York.

Garber, EK and Silver, S. 1982. Pedal manifestations of DISH. *Foot and Ankle.* 3 (1): 12-16

Gelberman, R, Goldberg, V, An, KN and Banes, A. 1988. Tendon. SLY Woo and JA

Buckwalter (ed.) *Injury and Repair of the Musculoskeletal Soft Tissues.* American Academy of Orthopaedic Surgeons: Park Ridge, Illinois. 3-40

Gibb, JA, White, AJ and Ward, CP. 1985. Population ecology of rabbits in the Wairarapa, New Zealand. *New Zealand Journal of Ecology.* 8: 55-82

Gibbon, WW and Long, G. 1999. Ultrasound of the plantar aponeurosis (fascia). *Skeletal Radiology.* 28: 21-26

Gjerdrum, T, Walker, PL and Andrushko, V. 2003. 72nd Annual Meeting of the American Association of Physical Anthropologists:Humeral retroversion: An activity pattern index in prehistoric southern California [abstract]. *American Journal of Physical Anthropology.* 120 (S36): 100-101

Gosling, JA, Harris, PF, Whitmore, I and Willan, PLT. 2002. *Human Anatomy: Color Atlas and Test.* Mosby: Edinburgh.

Goyal, S. 2006. *Pachydermoperiostosis*. eMedicine: http://www.emedicine.com/DERM/topic815.htm

Gray, H. 1974. Gray's Anatomy. TP Pick and R Howden (ed.) Running Press: Philadelphia.

Greenfield, EM and Goldberg, VM. 1997. Genetic determination of bone density (letter). *Lancet.* 350: 1263

Grimaldo, M, Borja-Aburto, VH, Ramirez, AL, Ponce, M, Rosas, M and Diaz-Barriga, F. 1995. Endemic Fluorosis in San Luis Potosi, Mexico. *Environmental Research.* 68: 25-30

Habicht, GS, Beck, G and Benach, JL. 1990. Lyme Disease. TD Brock (ed.) *Microorganisms: from Smallpox to Lyme Disease. Reading from Scientific American Magazine.* W.H. Freeman and Company: New York. 29-37

Haines, RW and Mohuiddin, A. 1968. Metaplastic bone. *Journal of Anatomy.* 103 (3): 527-538

Ham, AW. 1957. *Histology.* Pitman Medical Publishing Co., Ltd.: London.

Hamdi, N, Cooke, TDV and Hassan, B. 1999. Ochronotic arthropathy: case report and review of the literature. *International Orthopaedics.* 23: 122-125

Hardy, DC, Murphy, WA, Siegel, BA, Reid, IR and Whyte, MP. 1989. X-linked hypophosphatemia in adults: prevalence of skeletal radiographic and scintigraphic features. *Radiology.* 171 (2): 403-414

Hart, DA, Frank, CB and Bray, RC. 1995. Inflammatory Processes in Repetitive Motion and Overuse Syndromes: Potential Role of Neurogenic Mechanisms in Tendons and Ligaments. SL Gordon, SJ Blair and LJ Fine (ed.) *Repetitive Motion Disorders of the Upper Extremity.* American Academy of Orthopaedic Surgeons: Rosemont, Illinois. 247-262

Hartnett, K. 2002. 71st Annual Meeting of the American Association of Physical Anthropologists: An investigation of habitual activity patterns at the historic period Maya site of Tipu, Belize, using musculoskeletal stress markers (MSM) [abstract]. *American Journal of Physical Anthropology, Supplement.* 83

Harvey, B. 1993. *Living and Dying in England 1100-1540: The Monastic Experience.* Clarendon Press: Oxford.

Harvey, T and Salvato, P. 2003. 'Lyme disease': ancient engine of an unrecognized borreliosis pandemic? *Medical Hypotheses.* 60 (5): 742-759

Hashimoto, S, Creighton-Achermann, L, Takahashi, K, Amiel, D, Coutts, RD and Lotz, M. 2002. Development and regulation of osteophyte formation during experimental osteoarthritis. *Osteoarthritis and Cartilage.* 10: 180–187

Hauser, G and de Stefano, GF. 1989. *Epigenetic Variants of the Human Skull.* E. Schweizerbart'sche Verlagsbuchhandlung: Stuttgart.

Hawkey, DE. 1988. *Use of Upper Extremity Enthesopathies to Indicate Habitual Activity Patterns.* M.A. Arizona State University.

Hawkey, DE. 1998. Disability, Compassion and the Skeletal Record: Using Musculoskeletal Stress Markers (MSM) to Construct an Osteobiography from Early New Mexico. *International Journal of Osteoarchaeology.* 8: 326-340

Hawkey, DE and Merbs, CF. 1995. Activity-induced Musculoskeletal Stress Markers (MSM) and Subsistence Strategy Changes among Ancient Hudson Bay Eskimos. *International Journal of Osteoarchaeology.* 5: 324-338

Hawkey, DE and Street, SR. 1992. 61st Annual Meeting of the American Association of Physical Anthropologists: Activity - induced stress markers in prehistoric human remains from the eastern Aleutian Islands [abstract]. *American Journal of Physical Anthropology, Supplement.* 89

Hayden, B, Hatch, A, Ullinger, J, Van Gerven, DP and Sheridan, SG. 2004. 73rd Annual Meeting of the American Association of Physical Anthropologists: Musculoskeletal stress markers (MSM) as indicators of kneeling behavior in a Byzantine Jerusalem monastery [abstract]. *American Journal of Physical Anthropology.* 123 (S38): 110-111

Hayes, CW. 1991. Biomechanics of Cortical and Trabecular Bone: Implications for Assessment of Fracture Risk. VC Mow and CW Hayes (ed.) *Basic Orthopaedic Biomechanics.* Raven Press, Ltd.: New York. 93-142

Hayes, CW, Rosenthal, DI, Plata, MJ and Hudson, TM. 1987. Calcific Tendinitis in Unusual Sites Associated with Cortical Bone Erosion. *American Journal of Roentgenology.* 149: 967-970

Hems, T and Tillmann, B. 2000. Tendon entheses of the human masticatory muscles. *Anat Embryol.* 202: 201-208

Henderson, CY. 2002. *Are the presence or absence of post-cranial nonmetric traits linked to occupation and lifestyle?* MSc dissertation. Durham. University of Durham.

Hermann, KGA and Bollow, M. 2004. Magnetic resonance imaging of the axial skeleton in rheumatoid disease. *Best Practice and Research Clinical Rheumatology.* 18 (6): 881–907

Hirschberg, J, Milne, N and Oxnard, CE. 2000. Biomechanics of the tendon/bone interface. *Perspectives in Human Biology.* 5: 55-68

Holst, M. 2005. Artefacts and Environmental Evidence: The Human Bone. CA Spall and NJ Toop (ed.) *Blue Bridge and Fishergate House, York. Report on Excavations: July 2000 to July 2002.* Archaeological Planning Consultancy Ltd.: York, England. http://www.archaeologicalplanningconsultancy.co.uk/mono/001/.

Houtman, PM and Tazelaar, DJ. 1999. Joint and bone involvement in Dutch patients with lyme borreliosis presenting with acrodermatitis chronica atrophicans. *The Netherlands Journal of Medicine.* 54: 5-9

Hoyte, DAN and Enlow, DH. 1966. Wolff's Law and the Problem of Muscle Attachment on Resorptive Surfaces of Bone. *American Journal of Physical Anthropology.* 24: 205-214

Hudson, C, Butler, R and Sikes, D. 1975. Arthritis in the prehistoric Southeastern United States: biological and cultural variables. *American Journal of Physical Anthropology.* 43 (1): 57-62

Hudson-Edwards, KA, Macklin, MG, Finlayson, R and Passmore, DG. 1999. Mediaeval Lead Pollution in the River Ouse at York, England. *Journal of Archaeological Science.* 26: 809-819

Hurov, JR. 1986. Soft-Tissue Bone Interface: How Do Attachments of Muscles, Tendons, and Ligaments Change During Growth? A Light Microscopic Study. *Journal of Morphology.* 189: 313-325

Inamasu, J, Guiot, BH and Sachs, DC. 2006. Ossification of the posterior longitudinal ligament: an update on its biology, epidemiology, and natural history. *Neurosurgery.* 58 (6): 1027-1039

Jankauskas, R. 2003. The Incidence of Diffuse Idiopathic Skeletal Hyperostosis and Social Status Correlations in Lithuanian Skeletal Materials. *International Journal of Osteoarchaeology.* 13: 289-293

Jebaraj, I and Rao, A. 2006. Achilles tendon enthesopathy in ochronosis. *Journal of Postgraduate Medicine.* 52 (1): 47-48

Jennings, J, Inman, J, Ullinger, J, Van Gerven, DP and Sheridan, SG. 2004. 73rd Annual Meeting of the American Association of Physical Anthropologists: Femoral neck activity and kneeling at a Byzantine monastery [abstract]. *American Journal of Physical Anthropology.* 123 (S38): 120-121

Jiang, Y, Zhao, J, van Holsbeeck, MT, Flynn, MJ, Ouyang, X and Genant, HK. 2002. Trabecular microstructure and surface changes in the greater tuberosity in rotator cuff tears. *Skeletal Radiology.* 31: 522-528

Johnson, RC. 1996. Bacteriology. S Baron (ed.) *Medical Microbiology.* University of Texas Medical Branch: Galveston (Texas). http://www.ncbi.nlm.nih.gov/entrez/query.fcgi?cmd=Search&db=books&doptcmdl=GenBookHL&term=lyme+disease+AND+mmed%5Bbook%5D+AND+148385%5Buid%5D&rid=mmed.section.1965#1974

Jordana, X, Galtés, I, Busquets, F, Isidro, A and Malgosa, A. 2006. Clay-Shoveler's Fracture: An Uncommon Diagnosis in Palaeopathology. *International Journal of Osteoarchaeology.* 16 (4): 366-372

Julkunen, H, Heinonen, OP, KNekt, P and Maatela, J. 1975. The epidemiology of hyperostosis of the spine together with its symptoms and related mortality in a general population. *Scandinavian Journal of Rheumatology.* 4: 23-27

Jurmain, RD. 1991. Degenerative Changes in Peripheral Joints as Indicators of Mechanical Stress: Opportunities and Limitations. *International Journal of Osteoarchaeology.* 1: 247-252

Jurmain, RD. 1999. *Stories from the Skeleton: Behavioural Reconstruction in Human Osteology.* Gordon and Breach: Amsterdam.

Jurmain, RD and Kilgore, L. 1995. Skeletal evidence of osteoarthritis: a palaeopathological perspective. *Annals of the Rheumatic Diseases.* 54: 443-450

Kacki, S and Villotte, S. 2006. Maladie hyperostosique et mode de vie: intérêt D'une démarche bio-archéologique. Exemple du cimetière du couvent des s urs grises de beauvais (oise), xve -xviiie siècles. *Bulletins et Mémoires de la Société d'Anthropologie de Paris.* 18 (1-2): 55-64

Karjalainen, A. 1999. *International Statistical Classification of Diseases and Related Health Problems (ICD-10) in Occupational Health.*

Katznelson, L. 2005. Diagnosis and treatment of acromegaly. *Growth Hormone & IGF Research.* 15 (Supplement A): S31-S35

Keats, A. 1999. Spondyloarthropathies. ML Snaith (ed.) *ABC of rheumatology.* British Medical Journal: London.

Keller, JM, Macaulay, W, Nercessian, OA and Jaffe, IA. 2005. New developments in ochronosis: review of the literature. *Rheumatology International.* 25 (2): 81-85

Kennedy, KAR. 1983. Morphological Variations in Ulnar Supinator Crests and Fossae as Identifying Markers of Occupational Stress. *Journal of Forensic Sciences.* 28 (4): 871-876

Kennedy, KAR. 1989. Skeletal Markers of Occupational Stress. MY Iscan and KAR Kennedy (ed.) *Reconstruction of Life from the Skeleton.* Wiley-Liss: New York. 129-160

Kennedy, KAR. 1998. Markers of Occupational Stress: Conspectus and Prognosis of Research. *International Journal of Osteoarchaeology.* 8 (5): 305-310

Khan, MA. 2002. Update on Spondyloathropathies. *Annals of Internal Medicine.* 136: 896-907

Kim, HA, Choi, KW and Song, YW. 1997. Arthropathy in Behçet's disease. *Scandinavian Journal of Rheumatology.* 26 (2): 125-129

Kim, MS, Na, HJ, Han, SW, Jin, JS, Song, UY, Lee, EJ, Song, BK, Hong, SH and Kim, HM. 2003. Forsythia fructus inhibits the mast-cell-mediated allergic inflammatory reactions. *Inflammation.* 27 (3): 129-135

Kiss, C, O'Neill, TW, Mituszova, M, Szilágyi, M, Donáth, J and Poór, GY. 2002. Prevalence of diffuse idiopathic skeletal hyperostosis in Budapest, Hungary. *Rheumatology.* 41: 1335–1336

Knusel, C. 2000. Bone adaptation and its relationship to physical activity in the past. M Cox and S Mays (ed.) *Human Osteology in Archaeology and Forensic Science.* Greenwich Medical Media: London. 381-401

Knüsel, C. 2000. Activity-related skeletal change. V Fiorato, A Boylston and C Knüsel (ed.) *Blood Red Roses: The archaeology of a mass grave from the Battle of Towton AD 1461.* Oxbow Books: Oxford. 103-118

Knusel, CJ. 1993. 62nd Annual Meeting of the American Association of Physical Anthropologists: Activity-Related Skeletal Alterations in Medieval Populations [abstract].

American Journal of Physical Anthropology, Supplement. 16: 127

Knusel, CJ and Boylston, A. 2002. *Little leaguer's elbow (medial epicondylar fractures) in the archaeological record [abstract].* 14th Eurpean Meeting of the Paleopathology Association. Coimbra, Portugal.

Knusel, CJ and Goggel, S. 1993. A Cripple from the Medieval Hospital of Sts James and Mary Magdalen, Chichester. *International Journal of Osteoarchaeology.* 3: 155-165

Knusel, CJ, Roberts, CA and Boylston, A. 1996. When Adam Delved... An Activity-Related Lesion in Three Human Skeletal Populations. *American Journal of Physical Anthropology.* 100: 427-434

Koga, H, Sakou, T, Taketomi, E, Hayashi, K, Numasawa, T, Harata, S, Yone, K, Matsunaga, S, Otterud, B, Inoue, I and Leppert, M. 1998. Genetic mapping of ossification of the posterior longitudinal ligament of the spine. *American Journal of Human Genetics.* 62: 1460-1467

Korkmaz, C. 2005. Hypoparathyroidism simulating ankylosing spondylitis. *Joint Bone Spine.* 72: 89-97

Kovacik, ME, Talarico, L, Ullinger, J and Sheridan, SG. 2004. 73rd Annual Meeting of the American Association of Physical Anthropologists: Non-metric traits of the femur and tibia related to Byzantine monastic prayer [abstract]. *American Journal of Physical Anthropology.* 123 (S38): 127-128

Kozanoglu, E, Guzel, R, Guler-Uysal, F and Goncu, K. 2002. Coexistence of Diffuse Idiopathic Skeletal Hyperostosis and Ankylosing Spondylitis: A case report. *Clinical Rheumatology.* 21: 258-260

Kraemer, EJ and El-Khoury, GY. 2000. Atypical calcific tendinitis with cortical erosions. *Skeletal Radiology.* 29: 690-696

Kremer, P, Gallinet, E, Benmansour, A, Despaux, J, Toussirot, E and Wendling, D. 1996. Sarcoidosis and spondylarthropathy. Three case-reports. *Revue du rhumatisme (English ed.).* 63 (6): 405-411

Krishnamachari, KA. 1086. Skeletal fluorosis in humans: a review of recent progress in the understanding of the disease. *Progress in Food & Nutrition Science.* 10 (3-4): 279-314

Kuettner, KE and Cole, AA. 2005. Cartilage degeneration in different human joints. *Osteoarthritis and Cartilage.* 13: 93-103

Kumai, T and Benjamin, M. 2001. The entheses of the anterior talofibular ligament of the human ankle joint [abstract]. *Journal of Anatomy.* 198: 359

Kumai, T and Benjamin, M. 2002. Heel Spur Formation and the Subcalcaneal Enthesis of the Plantar Fascia. *The Journal of Rheumatology.* 29: 1957-1964

Kumai, T, Takakura, Y, Rufai, A, Milz, S and Benjamin, M. 2002. The functional anatomy of the human anterior talofibular ligament in relation to ankle sprains. *Journal of Anatomy.* 200: 457-465

Kumar, MRV and Rajesekaran, S. 2003. Spontaneous tendon ruptures in alkaptonuria. *The Journal of Bone and Joint Surgery (BR).* 85 (6): 883-886

Lai, P and Lovell, NC. 1992. Skeletal Markers of Occupational Stress in the Fur Trade: a

Case Study from a Hudson's Bay Company Fur Trade Post. *International Journal of Osteoarchaeology.* 2: 221-234

Laloux, L, Voisin, MC, Allain, J, Martin, N, Kerboull, L, Chevalier, X and Claudepierre, P. 2001. Immunohistological study of entheses in spondyloarthropathies: comparison in rheumatoid arthritis and osteoarthritis. *Ann Rheum Dis.* 60: 316-321

Lambert, RG and Becker, EJ. 1989. Diffuse skeletal hyperostosis in idiopathic hypoparathyroidism. *Clinical Radiology.* 40 (2): 212-215

Lanyon, LE. 1987. Functional strain in bone tissue as an objective, and controlling stimulus for adaptinve bone remodelling. *Journal of Biomechanics.* 20 (11): 1083-1093

Larsen, C. 1997. Activity patterns: 2. Structural adaptation. (ed.) *Bioarchaeology: Interpreting Behavior from the Human Skeleton.* Cambridge University Press: Cambridge. 195-225

Larsen, CS. 2000. *Skeletons in Our Closet: Revealing Our Past Through Bioarchaeology.* Princeton University Press: Princeton.

Larsen, CS, Crosby, AW, Griffin, MC, Hutchinson, DL, Ruff, CB, Russel, KF, Schoeninger, MJ, Sering, LE, Simpson, SW, Takács, JL and Teaford, MF. 2002. A Biohistory of Health and Behavior in the Georgia Bight. RH Steckel and JC Rose (ed.) *The Backbone of History: Health and Nutrition in the Western Hemisphere.* Cambridge University Press: Cambridge. 406-439

Larsen, CS and Williams, KD. 2003. 72nd Annual Meeting of the American Association of Physical Anthropologists: History of Behavior and lifestyle in the Western Hemisphere: Osteoarthritis and skeletal robusticity [abstract]. *American Journal of Physical Anthropology.* 120 (S36): 135-136

Laskar, FH and Sargison, KD. 1970. Ochronotic Arthropathy: A Review with Four Case Reports. *The Journal of Bone and Joint Surgery (BR).* 52(B) (4): 653-666

Lawson, JP and Steere, AC. 1985. Lyme Arthritis: Radiologic Findings. *Radiology.* 154: 37-43

Lazenby, RA. 1998. Second Metacarpal Midshaft Geometry in an Historic Cemetery Sample. *American Journal of Physical Anthropology.* 106: 157–167

Lazenby, RA and Pfeiffer, SK. 1993. Effects of a Nineteenth Century Below-knee Amputation and Prosthesis on Femoral Morphology. *International Journal of Osteoarchaeology.* 3: 19-28

Ledger, M, Holtshausen, L-M, Constant, D and Morris, AG. 2000. Biomechanical Beam Analysis of Long Bones From a Late 18th Century Slave Cemetery in Cape Town, South Africa. *American Journal of Physical Anthropology.* 112: 207-216

Lee, S-U and Lang, P. 2000. MR and MR arthrography to identify degenerative and posttraumatic diseases in the shoulder joint. *European Journal of Radiology.* 35: 126-135

Leff, RD. 1993. Lyme Borreliosis (Lyme Disease). KF Kiple (ed.) *The Cambridge World History of Human Disease.* Cambridge University Press: Cambridge. 852-855

Leveringhaus, P. 2003. *Studie unter Mönchen: Lebe Langsam Stirb Alt.* Spiegel Online: http://www.spiegel.de/wissenschaft/mensch/0,1518,266212,00.html

Levey, GS. 1982. Hypothyroidism (Myxedema). R Berkow (ed.) *The Merck Manual of Diagnosis and Therapy.* Merck and Company, Incorporated: Rahway. 1006-1010

Levitz, CL and Iannotti, JP. 1995. Overuse Injuries of the Shoulder. SL Gordon, SJ Blair and LJ Fine (ed.) *Repetitive Motion Disorders of the Upper Extremity.* American Academy of Orthopaedic Surgeons: Rosemont, Illinois. 493-506

Lewis, B. 1994. Treponematosis and Lyme borreliosis connections: Explanation for Tchefuncte disease syndromes? *American Journal of Physical Anthropology.* 93 (4): 455-475

Lieberman, DE, Polk, JD and Demes, B. 2004. Predicting Long Bone Loading from Cross-Sectional Geometry. *American Journal of Physical Anthropology.* 123: 156-171

Liebermann, DE, Devlin, MJ and Pearson, OM. 2000. Articular Area Responses to Mechanical Loading: Effect of Exercise, Age and Skeletal Location. *American Journal of Physical Anthropology.* 116: 266-277

Lin, TW, Cardenas, L and Soslowsky, LJ. 2004. Biomechanics of tendon injury and repair. *Journal of Biomechanics.* 37: 865-877

Linsenmayer, TF. 1991. Collagen. ED Hay (ed.) *Cell Biology of Extracellular Matrix.* Plenum Press: New York.

Lioté, F and Orcel, P. 2000. Osteoarticular disorders of endocrine origin. *Ballière's Clinical Rheumatology.* 14 (2): 251-276

Littleton, J. 1999. Paleopathology of Skeletal Fluorosis. *American Journal of Physical Anthropology.* 109: 465-483

Lodish, H, Baltimore, D, Berk, A, Zipursky, SL, Matsudaira, P and Darnell, J. 1995. *Molecular Cell Biology.* Scientific American Books: New York.

Lories, RJU, Derese, I and Luyten, FP. 2005. Modulation of bone morphogenetic protein signaling inhibits the onset and progression of ankylosing enthesitis. *Journal of Clinical Investigation.* 115: 1571-1579

Lovell, NC and Dublenko, AA. 1999. Further Aspects of Fur Trade Life Depicted in the Skeleton. *International Journal of Osteoarchaeology.* 9: 248-256

Luttmann, A, Jäger, M, Griefahn, B, Caffier, G, Liebers, F and Steinberg, U. 2003. *Protecting Workers' Health Series No. 5: Preventing musculoskeletal disorders in the workplace.* World Health Organization:

Maat, GJR and Mastwijk, RW. 2000. Avulsion Injuries of Vertebral Endplates. *International Journal of Osteoarchaeology.* 10: 142-152

MacGregor, AJ and Keen, RW. 1999. The Genetic of Osteoarthrits. *Arthritis Research Campaign Reports on Rheumatic Diseases.* Series 3 (no 16):

Mader, R. 2002. Manifestations of Diffuse Idiopathic Skeletal Hyperostosis of the Cervical Spine. *Seminars in Arthritis and Rheumatism.* 32: 130-135

Mafart, B. 2005. Description,Significance and Frequency of the Acetabular Crease of the Hip Bone. *International Journal of Osteoarchaeology.* 15: 208-215

Maga, M, Kappelman, J, Ryan, TM and Ketcham, RA. 2006. Preliminary observations on the calcaneal trabecular microarchitecture of extant large-bodied hominoids. *American Journal of Physical Anthropology.* 129 (3): 410-417

Maksymowych, WP. 2000. Ankylosing Spondylitis -At the Interface of Bone and Cartilage [editorial]. *The Journal of Rheumatology.* 27 (10): 2295-2301

Malawista, SE. 2001. Lyme Disease. WJ Koopman (ed.) *Arthritis and Allied Conditions.* Lippincott Williams and Wilkins: Philadelphia. 2629-2648

Malim, T and Hines, J. 1998. *The Anglo-Saxon Cemetery at Edix Hill (Barrington A), Cambridgeshire.*

Mann, GE. 1993. Myositis Ossificans in Medieval London. *International Journal of Osteoarchaeology.* 3: 223-226

Mann, RW and Murphy, SP. 1990. *Regional Atlas of Bone Disease: A Guide to Pathologic and Normal Variation in the human Skeleton.* Charles C. Thomas Publisher: Springfield, Illinois.

Mannoni, A, Selvi, E, Lorenzini, S, Giorgi, M, Airo, P, Cammelli, D, Andreotti, L, Marcolongo, R and Porfirio, B. 2005. Alkaptonuria, Ochronosis, and Ochronotic Arthropathy. *Seminars in Arthritis and Rheumatism.* 33: 239-248

Marchi. 2006. Biomechanical Approach to the Reconstruction of Activity Patterns in Neolithic Western Liguria. *American Journal of Physical Anthropology.* 131 (4): 447-455

Marchi, D, Sparacello, VS, Holt, BM and Formicola, V. 2006. Biomechanical Approach to the Reconstruction of Activity Patterns in Neolithic Western Liguria, Italy. *American Journal of Physical Anthropology.* 131: 447-455

Mariotti, V, Facchini, F and Belcastro, MG. 2004. Enthesopathies - Proposal of a Standardized Scoring Method and Applications. *Collegium Anthropologicum.* 28 (1): 145-159

Mariotti, V, Facchini, F and Belcastro, MG. 2007. The Study of Entheses: Proposal of a Standardised Scoring Method for Twenty-Three Entheses of the Postcranial Skeleton. *Collegium Anthropologicum.* 31 (1): 291-313

Martel-Pelletier, J. 1998. Pathophysiology of osteoarthritis. *Osteoarthritis and Cartilage.* 6: 374-376

Martin, EA. 2000. *Oxford Concise Medical Dictionary.* Oxford University Press: Oxford.

Marzo-Ortega, H, Emery, P and McGonagle, D. 2002. The Concept of Disease Modification in Spondyloarthropathy. *The Journal of Rheumatology.* 29: 1583-1585

Mata, S, Fortin, PR, Fitzcharles, M-A, Starr, MR, Joseph, L, Watts, CS, Gore, B, Rosenberg, E, Chhem, RK and Esdaile, JM. 1997. A Controlled Study of Diffuse Idiopathic Skeletal Hyperostosis: Clinical Features and Functional Status. *Medicine.* 76 (2): 104-117

Mays, S. 1999. A Biomechanical Study of Activity Patterns in a Medieval Human Skeletal Assemblage. *International Journal of Osteoarchaeology.* 9: 68-73

Mays, S. 2001. Effects of Age and Occupation on Cortical Bone in a Group of 18th-19th Century British Men. *American Journal of Physical Anthropology.* 116: 34-44

Mays, S, Steele, J and Ford, M. 1999. Directional Asymmetry in the Human Clavicle. *International Journal of Osteoarchaeology.* 9: 18-28

Mazières, B and Rovensky, J. 2000. Non-inflammatory enthesopathies of the spine a diagnostic approach. *Ballière's Clinical Rheumatology.* 14 (2): 201-217

Mazzocca, AD, Cohen, M, Berkson, E, Nicholson, G, Carofino, BC, Arclero, R and Romeo, AA. 2007. The anatomy of the bicipital tuberosity and distal biceps tendon. *Journal of Shoulder and Elbow Surgery.* 16 (1): 122-127

McCallum, Z and Gerner, B. 2005. Weighty matters--an approach to childhood overweight in general practice. *Australian Family Physician.* 34 (9): 745-748

McDonald, C. 2000. *Epidemiology of Work Related Diseases.* British Medical Journal Books: London.

McGonagle, D, Gibbon, W and Emery, P. 1998. Classification of inflammatory arthritis by enthesitis. *Lancet.* 352 (3): 1137-1140

McGonagle, D, Khan, MA, Marzo-Ortega, H, O'Connor, P, Gibbon, W and Emery, P. 1999. Enthesitis in spondyloarthropathy. *Current Opinion in Rheumatology.* 11: 244-250

McGonagle, D, Marzo-Ortega, H, O'Connor, P, Gibbon, W, Hawkey, P, Henshaw, K and Emery, P. 2002a. Histological assessment of the early enthesitis lesion in spondyloarthropathy. *Ann Rheum Dis.* 61: 534-537

McGonagle, D, Marzo-Ortega, H, O'Connor, P, Gibbon, W, Pease, C, Reece, R and Emery, P. 2002b. The role of biomechanical factors and HLA-B27 in magnetic resonance imaging-determined bone changes in plantar fascia enthesopathy. *Arthritis and Rheumatism.* 46 (2): 489-493

McGonagle, D, Stockwin, L, Isaacs, J and Emery, P. 2001. An Enthesitis Based Model for the Pathogenesis of Spondyloarthropathy. Additive Effects of Microbial Adjuvant and Biomechanical Factors at Disease Sites (editorial). *The Journal of Rheumatology.* 28 (10): 2155-2159

Melton, LJ. 1991. Epidemiology of primary hyperparathyroidism. *Journal of Bone and Mineral Research.* 6 (Supplement 2): S23-S30

Menkes, CJ and Lane, NE. 2003. Are osteophytes good or bad? (Workshop). *OsteoArthritis and Cartilage.* 12 (Supplement): S53-S54

Merbs, CF. 1996. Spondylolysis and Spondylolisthesis: A Cost of Being and Erect Biped or a Clever Adaptation. *Yearbook of Physical Anthropology.* 39: 201-228

Merbs, CF. 2001. Degenerative Spondylolisthesis in Ancient and Historic Skeletons From new Mexico Pueblo Sites. *American Journal of Physical Anthropology.* 116: 285-295

Micheli, LJ and Fehlandt, AF. 1992. Overuse Injuries to Tendons and Apophyses in Children and Adolescents. *Clinics in Sports Medicine.* 11 (4): 713-726

Middleton, J, Arnott, N, Walsh, S and Beresford, J. 1995. Osteoblasts and Osteoclasts in Adult Human Osteophyte Tissue Express the mRNAs for Insulin-like Growth Factors I and II and the Type 1 IGF Receptor. *Bone.* 16 (3): 287-293

Mihmanli, I, Karaarslan, E and Kanberoglu, K. 2001. Inflammation of vertebral bone

associated with acute calcific tendinitis of the longus colli muscle. *Neuroradiology.* 43: 1098-1101

Miles, AEW. 1998. New light on the Acromial Attachment of the Human Coraco-Acromial Ligament. *International Journal of Osteoarchaeology.* 8: 274-279

Milz, S, McNeilly, C, Putz, R, Ralphs, JR and Benjamin, M. 1998. Fibrocartilage in the extensor tendons of the interphalangeal joints of the toes and its functional implications. *Journal of Biomechanics, supplement.* 31: 102

Milz, S, Rufai, A, Buettner, A, Putz, R, Ralphs, JR and Benjamin, M. 2002. Three-dimensional reconstructions of the Achilles tendon insertion in man. *Journal of Anatomy.* 200: 145-152

Milz, S, Valassis, G, Buttner, A, Maier, M, Putz, R, Ralphs, JR and Benjamin, M. 2001. Fibrocartilage in the transverse ligament of the human acetabulum. *Journal of Anatomy.* 198: 223-228

Minagawa, H, Itoi, E, Konno, N, Kido, T, Sano, A, Urayama, M and Sato, K. 1998. Humeral Attachment of the Supraspinatus and Infraspinatus Tendons: An Anatomic Study. *Arthroscopy.* 14 (3): 302-306

Molleson, T. 1994. The Eloquent Bones of Abu Hureyra. *Scientific American.* (August): 70-75

Molleson, T and Cox, M. 1993. *The Spitalfields Project Volume 2. The Anthropology: The Middling Sort.* Council for British Archaeology: York.

Molleson, T and Hodgson, D. 2003. The human remains from Woolley's excavations at Ur. *Iraq.* 65: 91-129

Molnar, P. 2006. Tracing Prehistoric Activities: Musculoskeletal Stress Marker Analysis of a Stone-Age Population on the Island of Gotland in the Baltic Sea. *American Journal of Physical Anthropology.* 129: 12-23

Molnar, P. 2008. Patterns of Physical Activity and Material Culture on Gotland, Sweden, During the Middle Neolithic. *International Journal of Osteoarchaeology.* online:

Mondragón, M and Pearson, OM. 2003. 72nd Annual Meeting of the American Association of Physical Anthropologists:Occupational activity level in relation to bone strength [abstract]. *American Journal of Physical Anthropology.* 120 (S36): 153

Moreno, AC, Gonzalez, ML, Duffin, M, Lopez-Longo, FJ, Carreno, L and Forrester, DM. 1996. Simultaneous occurrence of diffuse idiopathic skeletal hyperostosis and ankylosing spondylitis. *Revue du rhumatisme (English ed.).* 63 (4): 292-295

Morfin, LM, McCaa, R, Storey, R and Del Angel, A. 2002. Health and Nutrition in Pre-Hispanic Mesoamerica. RH Steckel and JC Rose (ed.) *The Backbone of History: Health and Nutrition in the Western Hemisphere.* Cambridge University Press: Cambridge. 307-338

Morgan, H, Damron, T, Cohen, H and Allen, M. 2001. Pseudotumour deltoideus: a previously undescribed anatomic variant at the deltoid insertion site. *Skeletal Radiology.* 30: 512-518

Morgan, SJ, Furry, K, Parekh, AA, Agudelo, KF and Smith, WR. 2006. The Deltoid Muscle: An Anatomic Description of the Deltoid Insertion to the Proximal Humerus. *Journal of Orthopaedic Trauma.* 20: 19-21

Moriggl, B, Jax, P, Milz, S, Buttner, A and Benjamin, M. 2001. Fibrocartilage at the entheses of the suprascapular (superior transverse scapular) ligament of man - a ligament spanning two regions of a single bone. *Journal of Anatomy.* 199: 539-545

Mucci, R. 1987. 56th Annual Meeting of the American Association of Physical Anthropologists: Modeling bone remodeling: beam analysis and observed remodeling [abstract]. *American Journal of Physical Anthropology.* 72 (S2): 235

Mukherjee, S, Rogers, S, Mayeux, R and Mukherjee, DP. 1996. *A Study of Achilles Tendon Rupture.* Proceedings of the fifteenth Southern Biomedical Engineering Conference.

Mulhern, DM. 1998. 67th Annual Meeting of the American Association of Physical Anthropologists: Bone remodelling in a Medieval Nubian population: A comparison of the rib and femur [abstract]. *American Journal of Physical Anthropology, Supplement.* 26: 167

Neri, R and Lancellotti, L. 2002. *The analysis of the fractures of the lower limb in a skeleton of an adult carpenter of the nineteenth century [abstract].* 14th European Meeting of the Paleopathology Association. Coimbra, Portugal.

Neri, R and Lancellotti, L. 2004. Fractures of the Lower Limbs and their Secondary Skeletal Adaptations: a 20th Century Example of Pre-Modern Healing. *International Journal of Osteoarchaeology.* 14: 60-66

Niepel, GA and Sitaj. 1979. Enthesopathy. *Clinics in Rheumatic Diseases.* 5 (3): 857-872

Nishida, K, Doi, T, Matsuo, M, Ishiwari, Y, Tsujigiwa, H, Yoshida, A, Shibahara, M and Inoue, H. 2001. Involvement of nitric oxide in chondrocyte cell death in chondro-osteophyte formation. *Osteoarthritis and Cartilage.* 9: 232–237

Niyibizi, C, Visconti, CS, Gibson, G and Kavalkovich, K. 1996. Identification and Immunolocalization of Type X Collagen at the Ligament-Bone Interface. *Biochemical and Biophysical Research Communications.* 222: 584-589

Nystrom, KC and Buikstra, JE. 2004. Trauma-Induced Changes in Diaphyseal Cross Sectional Geometry in Two Elites From Copan, Honduras. *American Journal of Physical Anthropology.* 128: 791–800

Oakberg, K, Levy, T and Smith, P. 2000. A Method for Skeletal Arsenic Analysis, Applied to the Chalcolithic Copper Smelting Site of Shiqmim, Israel. *Journal of Archaeological Science.* 27: 895–901

Oates, J, Molleson, T and Soltysiak, A. 2008. Equids and an acrobat: closure rituals at Tell Brak. *Antiquity.* 82: 390-400

Ogata, S and Uhthoff, HK. 1990. Acromial Enthesopathy and Rotator Cuff Tear: A Radiologic and Histologic Postmortem Investigation of the Coracoacromial Arch. *Clinical Orthopaedics and Related Research.* 254: 39-48

O'Neill, MC and Ruff, CB. 2003. 72nd Annual Meeting of the American Association of Physical Anthropologists: Radiographic reconstruction of human long bone cross-sectional geometric propoerties: A test of two non-invasive techniques [abstract]. *American Journal of Physical Anthropology.* 120 (S36): 161-162

Oostveen, JC and van de Laar, MA. 2000. Magnetic resonance imaging in rheumatic disorders of the spine and sacroiliac joints. *Seminars in Arthritis and Rheumatism.* 30 (1): 52-

Ortner, DJ. 2003a. Erosive Arthropathies, Enthesopathies, and Miscellaneous Pathological Conditions of Joints. DJ Ortner (ed.) *Identification of Pathological Conditions in Human Skeletal Remains.* Academic Press: San Diego.

Ortner, DJ. 2003b. *Identification of Pathological Conditions in Human Skeletal Remains.* Academic Press: San Diego.

Ortner, DJ. 2003c. Infectious Diseases: Treponematosis and Other Bacterial Infectious Diseases. DJ Ortner (ed.) *Identification of Pathological Conditions in Human Skeletal Remains.* Academic Press: San Diego. 273-323

Ortner, DJ. 2003d. Metabolic Disorders. DJ Ortner (ed.) *Identification of Pathological Conditions in Human Skeletal Remains.* Academic Press: San Diego.

Panjabi, MM and White, AA. 1978. Appendix: Glossary. AA White and MM Panjabi (ed.) *Clinical Biomechanics of the Spine.* J.B. Lippincott Company: Philadelphia. 455-515

Papathanasiou, A. 2005. Health Status of the Neolithic Population of Alepotrypa Cave, Greece. *American Journal of Physical Anthropology.* 126 (4): 377-390

Pattekar, MA. 2003. *Myositis Ossificans*. eMedicine.com, Inc.: http://www.emedicine.com/ped/topic1538.htm

Peng, B, Hou, S, Shi, Q and Jia, L. 2000. Experimental study on mechanism of vertebral osteophyte formation. *Chinese Journal of Traumatology.* 3 (4): 202-205

Peterson, J. 1998. The Natufian Hunting Conundrum: Spears, Atlatls, or Bows? Musculoskeletal and Armature Evidence. *International Journal of Osteoarchaeology.* 8: 378-389

Pinsolle, V and Vandermeersch, B. 2002. La rhizarthrose d'hier et d'aujourd'hui. Comparison epidemiologique a partir d'une population ancienne. *Ann Chir Plast Esthet.* 47: 57-61

Pitt, MJ. 1988. Rickets and Osteomalacia. D Resnick and G Niwayama (ed.) *Diagnosis of Bone and Joint Disorders.* W.B. Saunders Company: Philadelphia. 2086-2126

Platzer, W. 1978. *Color Atlas and Textbook of Human Anatomy: Volume 1: Locomotor System.* Georg Thieme Publishers: Stuttgart.

Pollock, RG, Flatow, EL, Bigliani, LU, Kelkar, R and Mow, VC. 1995. Shoulder Biomechanics and Repetitive Motion. SL Gordon, SJ Blair and LJ Fine (ed.) *Repetitive Motion Disorders of the Upper Extremity.* American Academy of Orthopaedic Surgeons: Rosemont, Illinois. 145-160

Porac, C and Coren, S. 1981. *Lateral Preferences and Human Behavior.* Springer-Verlag: New York.

Porter, AMW. 1999a. The Prediction of Physique from the Skeleton. *International Journal of Osteoarchaeology.* 9: 102-115

Porter, R. 1999b. *The Greatest Benefit to Mankind: A Medical History of Humanity from Antiquity to the Present.* Fontana Press: London.

Putz-Anderson, V, Bernard, BP, Burt, SE, Cole, LL, Fairfield-Estill, C, Fine, LJ, Grant, KA,

Gjessing, C, Jenkins, L, Hurrell, JJ, Nelson, N. Pfirman, D, Roberts, R, Stetson, D. Haring-Sweeney, M and Tanaka, S. 1997. *Musculoskeletal Disorders and Workplace Factors: A Critical Review of Epidemiologic Evidence for Work-Related Musculoskeletal Disorders of the Neck, Upper Extremity, and Low Back.* U.S. Department of Health and Human Services. Public Health Service, Centers for Disease Control and Prevention, National Institute for Occupational Safety and Health: Cincinatti, Ohio.

Pyatt, FB and Grattan, JP. 2001. Some consequences of ancient mining activities on the health of ancient and modern human populations. *Journal of Public Health Medicine.* 23 (3): 235-236

Rabey, K. 2006. 75th Annual Meeting of the American Association of Physical Anthropologists: Morphological study of the upper limb articulations and muscular insertion in humans [abstract]. *American Journal of Physical Anthropology.* 129 (S42):

Radin, EL. 1993. Mechanically Induced Perarticular and Neuromuscular Problems. V Wright and EL Radin (ed.) *Mechanics of Human Joints.* Marcel Dekker, Incorporated.: New York. 355-370

Raman, R, Dinopoulos, H and Giannoudis, PV. 2004. Management of pyogenic sacroilitis: an update. *Current Orthopaedics.* 18: 321-325

Ramazzini, B. 1983. *Diseases of Workers.* The Classics of Medicine Library: New York.

Ramos, M and Lopez de Castro, JA. 2002. HLA-B27 and the pathogenesis of spondyloarthropathy. *Tissue Antigens.* 60: 191-205

Rasing, LAJ and van Kampen, A. 2000. A rare case of enthesopathy of the bicipital tuberositas of the radius. *Arch Orthop Trauma Surg.* 120: 601-602

Reddy, DR, Srikanth, RD and Misra, M. 1998. Fluorosis. *Surgical Neurology.* 49: 635-636

Rehmus, W and Kimball, AB. 2005. *POEMS syndrome*. eMedicine: http://www.emedicine.com/derm/topic771.htm

Reinhard, K and Wall, N. 2002. *Identifying equestrian skeletal markers [abstract].* 14th European Meeting of the Paleopathology Association. Coimbra, Portugal.

Remme, JHF, Feenstra, P, Lever, PR, Medici, AC, Morel, CM, Noma, M, Ramaiah, KD, Richards, F, Seketeli, A, Schmunis, G, van Brakel, WH and Vassall, A. 2006. Tropical Diseases Targeted for Elimination: Chagas Disease, Lymphatic Filariasis, Onchocerciasis, and Leprosy. DT Jamison, JG Breman, AR Measham, G Alleyne, M Claeson, DB Evans, P Jha, A Mills and P Musgrove (ed.) *Disease Control Priorities in Developing Countries.* The World Bank Group: Washington D.C.

Resnick, D. 1985. Degenerative Diseases of the Vertebral Column. *Radiology.* 156: 3-14

Resnick, D. 1988a. Alkaptonuria. D Resnick and G Niwayama (ed.) *Diagnosis of Bone and Joint Disorders.* W.B. Saunders Company: Philadelphia. 1787-1803

Resnick, D. 1988b. Pituitary Disorders. D Resnick and G Niwayama (ed.) *Diagnosis of Bone and Joint Disorders.* W.B. Saunders Company: Philadelphia. 2172-2198

Resnick, D. 1988c. Plasma Cell Dyscrasias and Dysgammaglobulinemias. D Resnick and G Niwayama (ed.) *Diagnosis of Bone and Joint Disorders.* W.B. Saunders Company: Philadelphia. 2358-2403

Resnick, D. 1988d. Thyroid Disorders. D Resnick and G Niwayama (ed.) *Diagnosis of Bone and Joint Disorders.* W.B. Saunders Company: Philadelphia. 2199-2218

Resnick, D. 1995a. Calcification and Ossification of the Posterior Spinal Ligaments and Tissues. D Resnick (ed.) *Diagnosis of Bone and Joint Diseases.* W.B. Saunders Company: Philadelphia.

Resnick, D. 1995b. Calcium Hydroxyapatite Crystal Deposition Disease. D Resnick (ed.) *Diagnosis of Bone and Joint Disorders.* W.B. Saunders Company: Philadelphia. 1615-1648

Resnick, D. 1995c. Disorders Due to Medications and Other Chemical Agents. D Resnick (ed.) *Diagnosis of Bone and Joint Disorders.* W.B. Saunders Company: Philadelphia. 3321-3330 Fluorine

Resnick, D, Goergen, T and Niwayama, G. 1995. Physical Injury: Concepts and Terminology. D Resnick (ed.) *Diagnosis of Bone and Joint Disorders.* W.B. Saunders Company: Philadelphia. 2561-2692

Resnick, D and Niwayama, G. 1983. Entheses and Enthesopathy: Anatomical, Pathological, and Radiological Correlation. *Diagnostic Radiology.* 146: 1-9

Resnick, D and Niwayama, G. 1988. Osteomyelitis, Septic Arthritis, and Soft Tissue Infection: The Organisms. D Resnick and G Niwayama (ed.) *Diagnosis of Bone and Joint Disorders.* W.B. Saunders Company: Philadelphia. 2647-2754

Resnick, D and Niwayama, G. 1995a. Degenerative Disease of Extraspinal Locations. D Resnick (ed.) *Diagnosis of Bone and Joint Disorders.* W.B. Saunders Company: Philadelphia. 1263-1371

Resnick, D and Niwayama, G. 1995b. Diffuse Idiopathic Skeletal Hyperostosis (DISH): Ankylosing Hyperostosis of Forestier and Rotes-Querol. D Resnick (ed.) *Diagnosis of Bone and Joint Disorders.* W.B. Saunders Company: Philadelphia. 1463-1495

Resnick, D and Niwayama, G. 1995c. Rheumatoid Arthritis. D Resnick (ed.) *Diagnosis of Bone and Joint Disorders.* W B Saunders Company: Philadelphia. 866-970

Resnick, D and Niwayama, G. 1995d. Rheumatoid Arthritis and the Seronegative Spondyloarthropathies: Radiographic and Pathologic Concepts. D Resnick (ed.) *Diagnosis of Bone and Joint Disorders.* W B Saunders Company: Philadelphia. 807-865

Resnick, D and Niwayama, G. 1995e. Soft Tissues. D Resnick (ed.) *Diagnosis of Bone and Joint Disorders.* W.B. Saunders Company: Philadelphia. 4491-4622

Resnick, D, Shaul, SR and Robins, JM. 1975. Diffuse Idiopathic Skeletal Hyperostosis (DISH): Forestier's Disease with Extraspinal Manifestations. *Radiology.* 115: 513-524

Rhodes, JA. 2006. Adaptations to Humeral Torsion in Medieval Britain. *American Journal of Physical Anthropology.* 130: 160–166

Rhodes, JA and Knüsel, CJ. 2006. Activity-Related Skeletal Change in Medieval Humeri: Cross-Sectional and Architectural Alterations. *American Journal of Physical Anthropology.* 128: 536–546

Riddle, DL, Pulisic, M, Pidcoe, P and Johnson, RE. 2003. Risk Factors for Plantar Fasciitis: A Matched Case-Control Study. *The Journal of Bone and Joint Surgery A.* 85 (5): 872-877

Robb, JE. 1998. The Interpretation of Skeletal Muscle Sites: A Statistical Approach. *International Journal of Osteoarchaeology.* 8: 363-377

Roberts, C. 2002. *The antiquity of leprosy in Britain: the skeletal evidence.* The Past and Present of Leprosy: Archaeological, historical, palaeopathological and clinical approaches. International Congress on the Evolution and Palaeoepidemiology of the Infectious Diseases 3 (ICEPID). University of Bradford, 26th-31st July 1999.

Roberts, C and Connell, B. 2004. Guidance on recording palaeopathology. M Brickley and JI McKinley (ed.) *Guidelines to the Standards for Recording Human Remains.* British Association For Biological Anthropology and Osteoarchaeology
Institute of Field Archaeologists: Southampton. 34-39

Roberts, C and Cox, M. 2003. *Health and Disease in Britain: From Prehistory to the Present Day.* Sutton Publishing: Stroud.

Roberts, C and Manchester, K. 2005. *The Archaeology of Disease.* Sutton Publishing: Stroud.

Rodrigues-Carvalho, C, Souza, S, Salles, S and Salles, A. 2002. *Occupational stress markers in prehistoric coastal populations from Rio De Janerio State, Brazil: First results [abstract].* 14th European Meeting of the Paleopathology Association. Coimbra, Portugal.

Roger, B and Grenier, P. 1997. MRI of plantar fasciitis. *European Radiology.* 7: 1430-1435

Rogers, J, Shepstone, L and Dieppe, P. 1997. Bone formers: osteophyte and enthesophyte formation are positively associated. *Annals of the Rheumatic Diseases.* 56: 85-90

Rogers, J and Waldron, T. 1995. *A Field Guide to Joint Disease in Archaeology.* John Wiley & Sons: Chichester.

Rogers, J and Waldron, T. 2001. DISH and the Monastic Way of Life. *International Journal of Osteoarchaeology.* 11: 357-365

Rogers, JM and Dieppe, PA. 1993. Ridges and grooves on the bony surfaces of osteoarthritic joints. *Osteoarthritis and Cartilage.* 1: 167-170

Ronchese, F. 1948. *Occupational Marks and Other Physical Signs: A Guide to Personal Identification.* Grune & Stratton: New York.

Rosenstock, L, Cullen, M and Fingerhut, M. 2006. Occupational Health. DT Jamison, JG Breman, AR Measham, G Alleyne, M Claeson, DB Evans, P Jha, A Mills and P Musgrove (ed.) *Disease Control Priorities in Developing Countries.* Oxford University Press: New York. 1127-1146

Rothschild, BM and Woods, RJ. 1991. Spondyloarthropathy: erosive arthritis in representative defleshed bones. *American Journal of Physical Anthropology.* 85: 125-134

Rufai, A, Ralphs, JR and Benjamin, M. 1995. Structure and Histopathology of the Insertional Region of the Human Achilles Tendon. *Journal of Orthopaedic Research.* 13: 585-593

Ruff, C. 1992. Biomechanical Analyses of Archaeological Human Skeletal Samples. SR Saunders and MA Katzenberg (ed.) *Skeletal Biology of Past Peoples: Research Methods.* Wiley-Liss: New york. 37-58

Ruff, C. 1994. Biomechanical Analysis of Northern and Southern Plains Femora: Behavioral

Implications. DW Owsley and RL Jantz (ed.) *Skeletal Biology of the Great Plains: Migration, Warfare, Health, and Subsistence.* Smithsonian Institution Press: Washington. 235-245

Ruff, CB, Holt, B and Trinkaus, E. 2006. Who's Afraid of the Big Bad Wolff?: "Wolff's Law" and Bone Functional Adaptation. *American Journal of Physical Anthropology.* 129: 484–498

Ruff, CB, Larsen, CS and Hayes, CW. 2005. Structural changes in the femur with the transition to agriculture on the Georgia coast. *American Journal of Physical Anthropology.* 64 (2): 125-136

Ruff, CB, Scott, WW and Liu, AY-C. 1991. Articular and Diaphseal Remodeling of the Proximal Femur With Changes in body Mass in Adults. *American Journal of Physical Anthropology.* 86: 397-413

Ryan, TM and van Rietbergen, B. 2005. Mechanical significance of femoral head trabecular bone structure in Loris and Galago evaluated using micromechanical finite element models. *American Journal of Physical Anthropology.* 126 (1): 82-96

Rybicki, EF, Simonen, FA and Weis, EB. 1972. On the mathematical analysis of stress in the human femur. *Journal of Biomechanics.* 5: 203-215

Sadat-Ali, M. 1998. Plantar Fasciitis/Calcaneal Spur among Security Forces Personnel. *Military Medicine.* 163 (1): 56-57

Sahin, B and Wilhelmi, BJ. 2003. *Hand, Anatomy.* eMedicine: www.emedicine.com

Sahin, G, Milcan, A, Bagis, S, Köktürk, A, Pata, C and Erdogan, C. 2001. A case of ochronosis: upper extremity involvement. *Rheumatology International.* 21: 78-80

Sailer, R, Sladek, V, Berner, M and Estl, M. 2003. 72nd Annual Meeting of the American Association of Physical Anthropologists: Computer tomography and calculation of bone biomechanics in cross-sections of long bones [abstract]. *American Journal of Physical Anthropology.* 120 (S36): 182

Sainburg, RL. 2002. Evidence for a dynamic-dominance hypothesis of handedness. *Experimental Brain Research.* 142: 241-258

Sakamoto, K and Kozuki, K. 2002. Calcific tendinitis at the biceps brachii insertion of a child: A case report. *Journal of Shoulder and Elbow Surgery.* 11: 88-91

Saraux, A, Devauchelle, V, Jousse, S and Goff, P. 2002. Spondylarthropathies tropicales. *Revue du Rhumatisme.* 69: 809-813

Sartoris, DJ, Schreiman, JS, Kerr, R, Resnik, CS and Resnick, D. 1986. Sternocostoclavicular hyperostosis: a review and report of 11 cases. *Radiology.* 158 (1): 125-128

Saunders, SR, Herring, A, Sawchuk, L, Boyce, G, Hoppa, R and Klepp, S. 2002. The Health of the Middle Class: The St. Thomas' Anglican Church Cemetery Project. RH Steckel and JC Rose (ed.) *The Backbone of History: Health and Nutrition in the Western Hemisphere.* Cambridge University Press: Cambridge. 130-161

Savas, S, Çetin, M, Akdogan, M and Heybeli, N. 2001. Endemic fluorosis in Turkish patients: relationship with knee osteoarthritis. *Rheumatology International.* 21: 30-35

Saylan, T, Mat, C, Fresko, I and Melikoglu, M. 1999. Behçet's Disease in the Middle East.

Clinics in Dermatology. 17: 209-223

Scarr, AJT. 1967. *Metrology and precision engineering.* McGraw-Hill: London.

Scheuer, L and Black, S. 2000a. Development and Ageing of the Juvenile Skeleton. M Cox and S Mays (ed.) *Human Osteology in Archaeology and Forensic Science.* Greenwich Medical Media: London. 9-21

Scheuer, L and Black, S. 2000b. *Developmental Juvenile Osteology.* Elsevier Academic Press: Amsterdam.

Schwartz, EE, Lantieri, R and Teplick, JG. 1977. Erosion of the Inferior Aspect of the Clavicle in Secondary Hyperparathyroidism. *American Journal of Roentgenology.* 129: 291-295

Sciulli, PW and Oberly, J. 2002. Native Americans in Eastern North America: The Southern Great Lakes and Upper Ohio Valley. RH Steckel and JC Rose (ed.) *The Backbone of History: Health and Nutrition in the Western Hemisphere.* Cambridge University Press: Cambridge. 440-480

Sencan, D, Elden, H, Nacitarhan, V, Sencan, M and Kaptanoglu, E. 2005. The prevalence of diffuse idiopathic skeletal hyperostosis in patients with diabetes mellitus. *Rheumatology International.* 25 (7): 518-21

Shakoor, N and Moisio, K. 2004. A biomechanical approach to musculoskeletal disease. *Best Practice and Research Clinical Rheumatology.* 18 (2): 173-186

Silva, C, Cardoso, F and Tavares, T. 2002. *An occupational marker of human activity. A case report from Arrentela (Portugal) [abstract].* 14th European Meeting of the Paleopathology Association. Coimbra, Portugal.

Sluiter, JK, Rest, KM and Frings-Dresen, MHW. 2001. Criteria document for evaluating the work-relatedness of upper-extremity musculoskeletal disorders. *Scandinavian Journal of Work, Environment and Health.* 27 (Supplement 1): 1-102

Smith, CB. 1982. Behçet's Syndrome. R Berkow (ed.) *The Merck Manual of Diagnosis and Therapy.* Merck and Company, Incorporated: Rahway, New York. 1195-1196

Smith, R, O'Connell, S and Palmer, S. 2000. Lyme Disease Surveillance in England and Wales, 1986–1998. *Emerging Infectious Diseases.* 6 (4): 404-407

Sokoloff, L. 1983. Aging and Degenerative Diseases Affecting Cartilage. BK Hall (ed.) *Cartilage, Vol. 3: Biomedical Aspects.* Academic Press: 109-141

Solano, MC. 2006. 75th Annual Meeting of the American Association of Physical Anthropologists: Variation in postcranial robusticity in the Albany County Almshouse [abstract]. *American Journal of Physical Anthropology.* 129 (S42): 168-169

Sparacello, VS and Marchi, D. 2008. Mobility and subsistence economy: A diachronic comparison between two groups settled in the same geographical area (Liguria, Italy). *American Journal of Physical Anthropology.* 136 (4): 485-495

Srsen, S, Müller, CR, Fregin, A and Srsnova, K. 2002. Alkaptonuria in Slovakia: thirty-two years of research on phenotype and genotype. *Molecular Genetics and Metabolism.* 75: 353-359

Stafford, L and Yousse, PP. 2002. Spondyloarthropathies: an overview. *Internal Medicine Journal.* 32: 40-46

Steckel, RH, Larsen, CS, Sciulli, PW and Walker, PL. 2006. *The Global History of Health. Data Collection Codebook.*

Steckel, RH and Rose, JC. 2002. *The Backbone of History: Health and Nutrition in the Western Hemisphere.* Cambridge University Press: Cambridge.

Steele, J. 2000. Skeletal Indicators of Handedness. M Cox and S Mays (ed.) *Human Osteology in Archaeology and Forensic Science.* Greenwich Medical Media: London. 307-23

Steele, J and Mays, S. 1995. *New Findings on the Frequency of Left- and Right- Handedness in Mediaeval Britain.* http://www.soton.ac.uk/%7Etjms/handed.html

Steen, SL and Lane, RW. 1998. Evaluation of Habitual Activites among Two Eskimo Populations Based on Musculoskeletal Stress Markers. *International Journal of Osteoarchaeology.* 8: 341-353

Stenn, FF, Milgram, JW, Lee, SL, Weigrand, RJ and Veis, A. 1977. Biochemical identification of homogentisic acid pigment in an ochronotic Egyptian mummy. *Science.* 197 (4303): 566-568

Stevens, A and Lowe, JS. 1997. *Human Histology.* Mosby: London.

Sticht, G. 1998. Fluorine. HG Seiler and H Sigel (ed.) *Handbook on toxicity of inorganic compounds.* Marcel Dekker: New York.

Stirland, A. 1998. Musculoskeletal evidence for activity: problems of evaluation. *International Journal of Osteoarchaeology.* 8: 354-362

Stirland, AJ. 2000. *Raising the Dead: The Skeleton Crew of Henry VIII's Great Ship, Mary Rose.* John Wiley and Sons Ltd.: Chichester.

Stirland, AJ and Waldron, T. 1997. Evidence for Activity Related Markers in the Vertebrae of the Crew of the *Mary Rose*. *Journal of Archaeological Sciences.* 24: 329-335

Stock, JT and Shaw, CN. 2007. Which measures of diaphyseal robusticity are robust? A comparison of external methods of quantifying the strength of long bone diaphyses to cross-sectional geometric properties. *American Journal of Physical Anthropology.* 134 (3): 412-423

Stone, RJ and Stone, JA. 2000. *Atlas of Skeletal Muscles.* McGraw-Hill: Boston.

Stuart-MacAdam, P, Glencross, B and Kricun, M. 1998. Traumatic Bowing Deformities in Tubular Bones. *International Journal of Osteoarchaeology.* 8: 252-262

Summerton, N. 1995. Lyme disease in the eighteenth century. *British Medical Journal.* 311 (1478):

Terranova, CJ, Null, C, Shujaa, KJ and Medford, EG. 2000. 69th Annual Meeting of the American Association of Physical Anthropologists: Musculoskeletal indicators of work stress in enslaved Africans in Colonial New York: functional anatomy of the axial and appendicular skeleton [abstract]. *American Journal of Physical Anthropology, Supplement.* 301

Thomopoulos, S, Hattersley, G, Rosen, V, Mertens, M, Galatz, L, Williams, GR and Soslowsky, LJ. 2002. The localized expression of extracellular matrix components in healing

tendon insertion sites:an in situ hybridization study. *Journal of Orthopaedic Research.* 20: 454-463

Thomopoulos, S, Williams, GR, Gimbel, JA, Favata, M and Soslowsky, LJ. 2003. Variation of biomechanical, structural, and compositional properties along the tendon to bone insertion site. *Journal of Orthopaedic Research.* 21: 413-419

Thurston, AJ. 2002. Bone spurs: mechanisms of production of different shapes based on observations in Dupuytren's diathesis. *ANZ Journal of Surgery.* 72: 290-293

Toyne, JM. 2003. 73rd Annual Meeting of the American Association of Physical Anthropologists: Musculoskeletal Stress Markers (MSM) and weaving activities at a prehistoric coastal site in Peru [abstract]. *American Journal of Physical Anthropology.* 123 (S38): 211

Trinkaus, E. 1978. Bilateral Asymmetry of Human Skeletal Non-metric Traits. *American Journal of Physical Anthropology.* 49: 315-318

Ubelaker, DH. 1979. Skeletal Evidence for Kneeling in Prehistoric Ecuador. *American Journal of Physical Anthropology.* 51: 679-686

Ubelaker, DH and Newson, LA. 2002. Patterns of Health and Nutrition in Prehistoric and Historic Ecuador. RH Steckel and JC Rose (ed.) *The Backbone of History: Health and Nutrition in the Western Hemisphere.* Cambridge University Press: Cambridge. 343-375

Uhthoff, HK and Sarkar, K. 1991. Pathology of rotator cuff tendons. MS Watson (ed.) *Surgical Disorders of the Shoulder.* Churchill Livingstone: Edinburgh. 259-270

Ullinger, J, Sheridan, SG and de Vries, B. 2004. 73rd Annual Meeting of the American Association of Physical Anthropologists: "Fall on your knees": Squatting facets in Byzantine monasticism [abstract]. *American Journal of Physical Anthropology.* 123 (S38): 198

Uppal, SS, Abraham, M, Chowdhury, RI, Kumari, R, Pathan, EM and Rashed, AA. 2005. Ankylosing spondylitis and undifferentiated spondyloarthritis in Kuwait: a comparison between Arabs and South Asians. *Clinical Rheumatology.* Online first, 21st Oct. 2005:

van den Berg, WB. 1999. Osteophyte formation in osteoarthritis. *Osteoarthritis and Cartilage.* 7: 333

Velemínský, P, Dobisková, M, Stránská, P, Likovský, J, Zikán, V, Stloukal, M, Zítková, P, Žaloudková, M, Fialová, L and Polácek, L. 2005. 74th Annual Meeting of the American Association of Physical Anthropologists: Locomotory apparatus and health status of the early Medieval population in Great Moravia (the Czech Republic) [abstract]. *American Journal of Physical Anthropology.* 126 (S40): 212-213

Vidal, P. 2000. A paleoepidemiologic study of diffuse idiopathic skeletal hyperostosis. *Joint Bone Spine.* 67 (3): 210-214

Villotte, S. 2006. Connaissances Médicales Actuelles, Cotation des Enthésopathies: Nouvelle Méthode. *Bulletins et Mémoires de la Société d'Anthropologie de Paris.* 18 (1-2):

von Cramon-Taubadel, N, Frazier, BC and Lahr, MM. 2007. The Problem of Assessing Landmark Error in Geometric Morphometrics: Theory, Methods, and Modifications. *American Journal of Physical Anthropology.* 134 (1): 24-35

Waggett, AD, Ralphs, JR, Kwan, APL, Woodnutt, D and Benjamin, M. 1998.

Characterization of Collagens and Proteoglycans at the Insertion of the Human Achilles Tendon. *Matrix Biology.* 16: 457-470

Waldron, HA. 1993. The health of the adults. T Molleson and M Cox (ed.) *The Spitalfields Project: The Middling Sort.* Council for British Archaeology: York.

Waldron, T. 1991. Variations in the Rates of Spondylolysis in Early Populations. *International Journal of Osteoarchaeology.* 1: 63-65

Waldron, T and Rogers, J. 1990. An Epidemiologic Study of Sacroiliac Fusion in Some Human Skeletal Remains. *American Journal of Physical Anthropology.* 83: 123-127

Waldron, T and Rogers, J. 1991. Inter-observer Variation in Coding Osteoarthritis in Human Skeletal Remains. *International Journal of Osteoarchaeology.* 1: 49-56

Wedel, V and Rankin-Hill, L. 2004. 73rd Annual Meeting of the American Association of Physical Anthropologists: Evidence of biomechanical stress in a Middle Mississippian skeletal population [abstract]. *American Journal of Physical Anthropology.* 123 (S38): 205

Weiler, A, Scheffler, S and Apreleva, M. 2006. Healing of Ligament and Tendon to Bone. WR Walsh (ed.) *Repair and Regeneration of Ligaments, Tendons and Joint Capsule.* Humana Press, Inc.: Totowa, New Jersey. 201-231

Weinfeld, RM, Olson, RN, Maki, DD and Griffiths, HJ. 1997. The prevalence of diffuse idiopathic skeletal hyperostosis (DISH) in two large American Midwest metropolitan hospital populations. *Skeletal Radiology.* 26: 222-225

Weintraub, W. 2003. *Tendon and Ligament Healing: A New Approach to Sports and Overuse Injury.* Paradigm Publications: Brookline, Massachussetts.

Weiss, E. 2005. Humeral Cross-Sectional Morphology From 18th Century Quebec Prisoners of War: Limits to Activity Reconstruction. *American Journal of Physical Anthropology.* 126: 311–317

Weiss, E and Jurmain, RD. 2007. Osteoarthritis revisited: a contemporary review of aetiology. *International Journal of Osteoarchaeology.* 17 (5): 437-450

Wells, C, Denston, B and Hawkes, SC. 2003. The Inhumations and Cremations. SC Hawkes and G Grainger (ed.) *The Anglo-Saxon Cemetary at Worthy Park, Kingsworthy, near Winchester, Hampshire. Monograph No. 59.* Oxford University School of Archaeology: Oxford. 153-189

WHO. 2000. *Air Quality Guidelines. Chapter 6.5 Fluorides. 2nd edition.* World Health Organisation (Regional Office for Europe): http://www.who.dk/document/aiq/6_5fluorides.pdf

WHO. 2003a. *Fluoride.* World Health Organisation: http://www.who.int/docstore/water_sanitation_health/GDWQ/draftchemicals/fluoride2003.pdf

WHO. 2003b. *Water-related Diseases: Fluorosis.* World Health Organisation: http://www.who.int/water_sanitation_health/diseases/fluorosis/en/print.html

WHO. ? *Sources of Chemicals in the Environment.* World Health Organisation: http://www.who.int/pcs/training_material/hazardous_chemicals/section_1.htm

Wilczak, CA and Kennedy, KAR. 1998. Mostly MOS: technical aspects of identification of skeletal markers of occupational stress. K Reichs (ed.) *Forensic Osteology: Advances in the Identification of Human Remains.* C.C. Thomas Publisher Ltd.: Springfield, Illinois. 461-490

Williams, JA. 1994. DW Owsley and RL Jantz (ed.) *Skeletal Biology of the Great Plains:Migration, Warfare, Health, and Subsistence.* Smithsonian Institution Press: Washington.

Wolf, WB. 1999. Calcific Tendinitis of the Shoulder: Diagnosis and Simple, Effective Treatment. *The Physician and Sports Medicine.* 27 (9): (online)

Woo, SLY, Maynard, J, Butler, D, Lyon, R, Torzilli, P, Akeson, W, Cooper, RR and Oakes, B. 1988. Ligament, Tendon, and Joint Capsule Insertions to Bone. SLY Woo and JA Buckwalter (ed.) *Injury and Repair of the Musculoskeletal Soft Tissues.* Amercan Academy of Orthopaedic Surgeons: Park Ridge, Illinois. 133-166

Woo, SLY and Young, EP. 1991. Structure and Function of Tendons and Ligaments. VC Mow and WC Hayes (ed.) *Basic Orthopaedic Biomechanics.* Raven Press Ltd.: New York.

Woodhead-Galloway, J. 1980. *Collagen: the Anatomy of a Protein (The Institute of Biology's Studies In Biology no 117).* Edward Arnold Publishers Ltd.: London.

Wren, TAL, Scott, AY, Beaupre, GS and Carter, DR. 2001. Influence of bone mineral density, age, and strain rate on the failure mode of human Achilles tendons. *Clinical Biomechanics.* 16: 529-534

Yoshizawa, T, Takizawa, F, Iizawa, F, Ishibashi, O, Kawashima, H, Matsuda, A, Endo, N and Kawashima, H. 2004. Homeobox Protein Msx2 Acts as a Molecular Defense Mechanism for Preventing Ossification in Ligament Fibroblasts. *Molecular and Cellular Biology.* 24 (8): 3460-3472

Yu, X and White, KE. 2005. FGF23 and disorders of phosphate homeostasis. *Cytokine & Growth Factor Reviews.* 16: 221–232

Yurtkuran, M, Yurtkuran, M, Alp, A, Sivrioglu, K, Dilek, K, Tamgac, F, Alper, E, Tunali, S, Saricaoglu, H and Nasircilar, A. 2006. Hand involvement in Behçet's disease. *Joint Bone Spine.* In press:

Zabecki, M. 2006. 75th Annual Meeting of the American Association of Physical Anthropologists: Workloads and activity patterns of three Egyptian populations [abstract]. *American Journal of Physical Anthropology.* 129 (S42): 191-192

Zabecki, M, O'Neill, MC and Ruff, CB. 2004. 74th Annual Meeting of the American Association of Physical Anthropologists: Relative bone strength in the upper and lower limbs of a Predynastic Egyptian population [abstract]. *American Journal of Physical Anthropology.* 126 (S40): 214-215

Zannoni, VG, Lomtevas, N and Goldfinger, S. 1969. Oxidation of homogentisic acid to ochronotic pigment in connective tissue. *Biochimica et Biophysica Acta.* 177 (1): 94-105

Zatkova, A, de Bernabe, DB, Polakova, H, Zvarik, M, Ferakova, E, Bosak, V, Ferak, V, Kadasi, L and de Cordoba, SR. 2000. High frequency of alkaptonuria in Slovakia: evidence for the appearance of multiple mutations in HGO involving different mutational hot spots. *American Journal of Human Genetics.* 68 (5): 1333–1339

Zumwalt, AC. 2004. *A new method to quantify the 3D morphology of bone surfaces, with*

application to muscle enthesis rugosity. American Association of Physical Anthropologists. Tampa, Florida.

Zumwalt, AC. 2005. A New Method for Quantifying the Complexity of Muscle Attachment Sites. *The Anatomical Record (Part B).* 286B: 21-28

Zumwalt, AC. 2006. The effect of endurance exercise on the morphology of muscle attachment sites. *The Journal of Experimental Biology.* 209: 444-454